Heat sources of the groundwater in the Zara-Zarqa Ma'in-Jiza area, Central Jordan

By

Ali Khalaf Al Sawarieh
From Madaba, Jordan

A thesis for the degree of Doctor of Natural Sciences submitted to the
Faculty of Civil Engineering, Geosciences and Environmental Sciences

University of Karlsruhe, Germany

ABSTRACT

The study area is located in the central part of Jordan, south of Amman. It consists of two sub-catchments: Wadi Waleh and Wadi Zarqa Ma'in. It extends from Zara hot springs at the eastern shore of the Dead Sea through Zarqa Ma'in thermal springs to Jiza region in the east, with a total area of about 2300 km^2.

A sequence of more than 1000m of sedimentary rocks is well exposed in the study area ranging in age from Cambrian to Recent. This sequence was subdivided into two major aquifer systems (upper and lower) separated by one major aquitard. Groundwater in both aquifers flows towards the Dead Sea in the west through out the investigated area.

The study area contains two geothermal manifestations: first, Zara-Zarqa Ma'in hot springs, receiving their water from the Lower Cretaceous and older sandstones with temperatures ranging from 30 to 63°C; second, the thermal wells field of the Madaba-Jiza region, where many wells discharge thermal water (30 to 46°C) from the upper aquifer, despite that this aquifer is a major source for cold fresh water in Jordan. This is most probably due to the presence of many faults of different trends and types in the area, which strongly suggest that the two aquifer systems are hydraulically connected, especially in the eastern parts. This might allow the thermal water from the lower aquifer to flow up via faults (conduits) to the upper aquifer raising the water temperature in the vicinity of these faults.

A total of 49 chemical analyses were used to classify the water types in the upper and lower aquifers in the study area. All samples were analyzed in the Water Authority Labs, Amman. Of these samples, 24 samples were also analyzed for stable isotopes in the same labs. The chemical analysis shows that the groundwater in the upper aquifer system is of bicarbonate type, whereas, it is of chloride type in the lower aquifer system. The isotope content indicates that water in both aquifers is of meteoric origin.

The results of the chemical and isotope analyses interpretation (the location of the thermal water samples in the Cl-SO4-HCO3, Na-K-Mg, Schoeller and Durov diagrams, the positive relationships between Cl and the other elements, d^{18}O and d^{2}H relation, the negative relationship between d^{18}O and Cl, the absence of the negative relation between d^{18}O and the temperature, the positive relations of temperature versus Cl and temperature versus F and the disagreement among all the geothermometers used in estimating the

I

reservoir temperature) strongly suggest mixing between bicarbonate water of the upper aquifer and the chloride thermal water of the lower aquifer.

Cation (Na-K and K/Mg) and silica (quartz and chalcedony) geothermometers were used to estimate the reservoir temperatures. The results show disagreement between all geothermometers estimations, which suggest that the water is a mixture of hot thermal water and cold water of shallower depth.. Therefore, to take account of the effect of mixing of different waters, the Enthalpy-silica diagram is used for better temperature estimations, it shows that the maximum reservoir temperature in Zara-Zarqa Ma'in is about 105°C. It also shows that the reservoir temperature for the thermal wells ranges from 65 to 105°C depending on the mixing ratio from the lower aquifer.

In the course of this study the GeoSys/RockFlow scientific modeling software was used in two applications: first, to model (2D) the water flow and heat transport along a vertical cross section and the simulation results show the clear up-coning effect of warm water at the fault i.e. higher temperatures along the vertical fracture. The second application represents the first attempt to use the software in order to model (3D) the groundwater flow and heat transport based on GIS data. The prepared hydrogeological conceptual model of the study area is converted to shape files (GIS Project) using the ArcGIS software. All required data for modeling, such as aquifer geometry, boundary conditions, material properties, well positions and pumping rates etc. are kept in the GIS Project. These data are directly imported to GeoSys for modeling purposes. In the steady state, the simulation results of water flow are quite similar to the water heads measured in 1985 in the area. In the transient state, well data (locations and pumping rates) are included in the hydro-system model and the flow simulation gave good results. The flow model was not calibrated, therefore, the simulation results form a solid base for further improvement of the model using the GIS Project of this study.

Dedication

To my parents, sisters and brothers for their

love and continuous support

To my lovely wife "Randa" for her efforts, moral

support and unlimited encouragement

To my children "Zaid, Farah and Yazan" for the

understanding during my absence

with my love to them all

Ali

ACKNOWLEDGEMENTS

TABLE OF CONTENTS   **Page**

LIST OF FIGURES **Page**

LIST OF TABLES   **Page**

LIST OF PHOTOS

1.INTRODUCTION

1.1 Location of the Study Area

The study area is located in the central part of Jordan (Figure-1.1) and belongs mainly to Wadi Mujib groundwater catchment (Figure-1.2). The Mujib catchment has two major sub-catchments: Wadi Mujib and Wadi Waleh/Heidan with total catchment area of about 6.600 km^2.

The study area consists of Wadi Waleh sub-catchment and Zara-Zarqa Ma'in thermal springs area, which belongs to a small catchment that lies to the north west of Wadi Waleh sub-catchment, known as Wadi Zarqa Ma'in sub-catchment. Figure-1.2 shows the irregular shape of the whole study area with total area of about 2300km^2, enclosed between coordinates 200000–280000 E and 90000–145000 N (PG).

The study area possesses a good roads system, with the main Desert, Kings and Dead Sea Shore Highways running north-south through the area, in addition to many other roads and tracks.

Three of the main topographic units of Jordan are present in the study area: the Rift area in the west, the Highlands in the middle and the Plateau in the east. Therefore, different weather conditions prevail in the area, due to the high differences in elevation (-400 to about 1000m asl).

In the study area intensive agricultural activities have developed in recent decades. In the highlands agriculture is supported by rainfall with the major crops of wheat, barely, tobacco, olive and grapes. Vegetables are mainly grown by irrigation in Zara–Zarqa Ma'in area and in the eastern parts of the study area.

The main international airport of Jordan (Queen Alia International Airport) is located in the Jiza region within the study area. In addition, many industrial activities have been established there during the last twenty years.
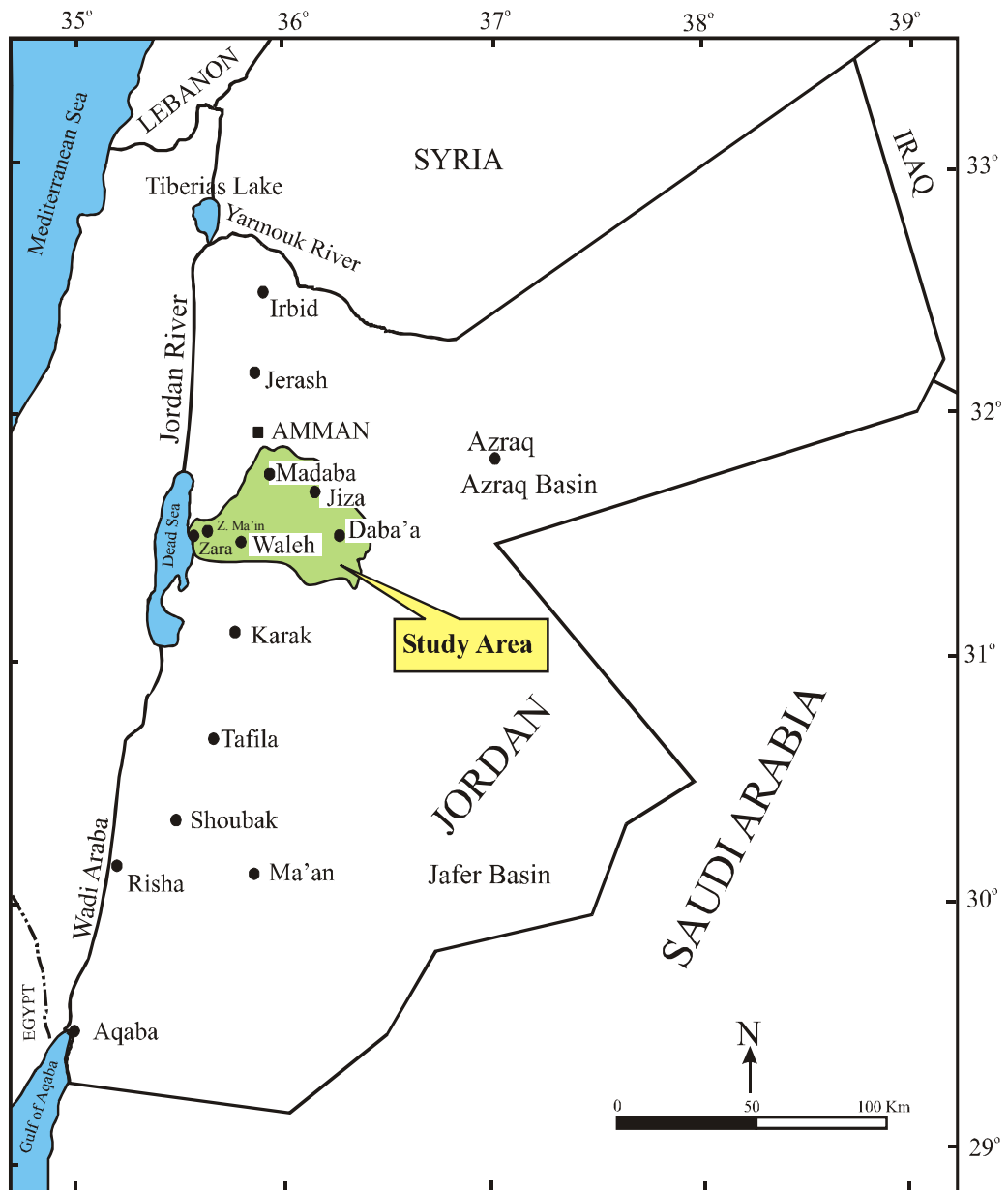
Figure -1.1: Location map of the study area
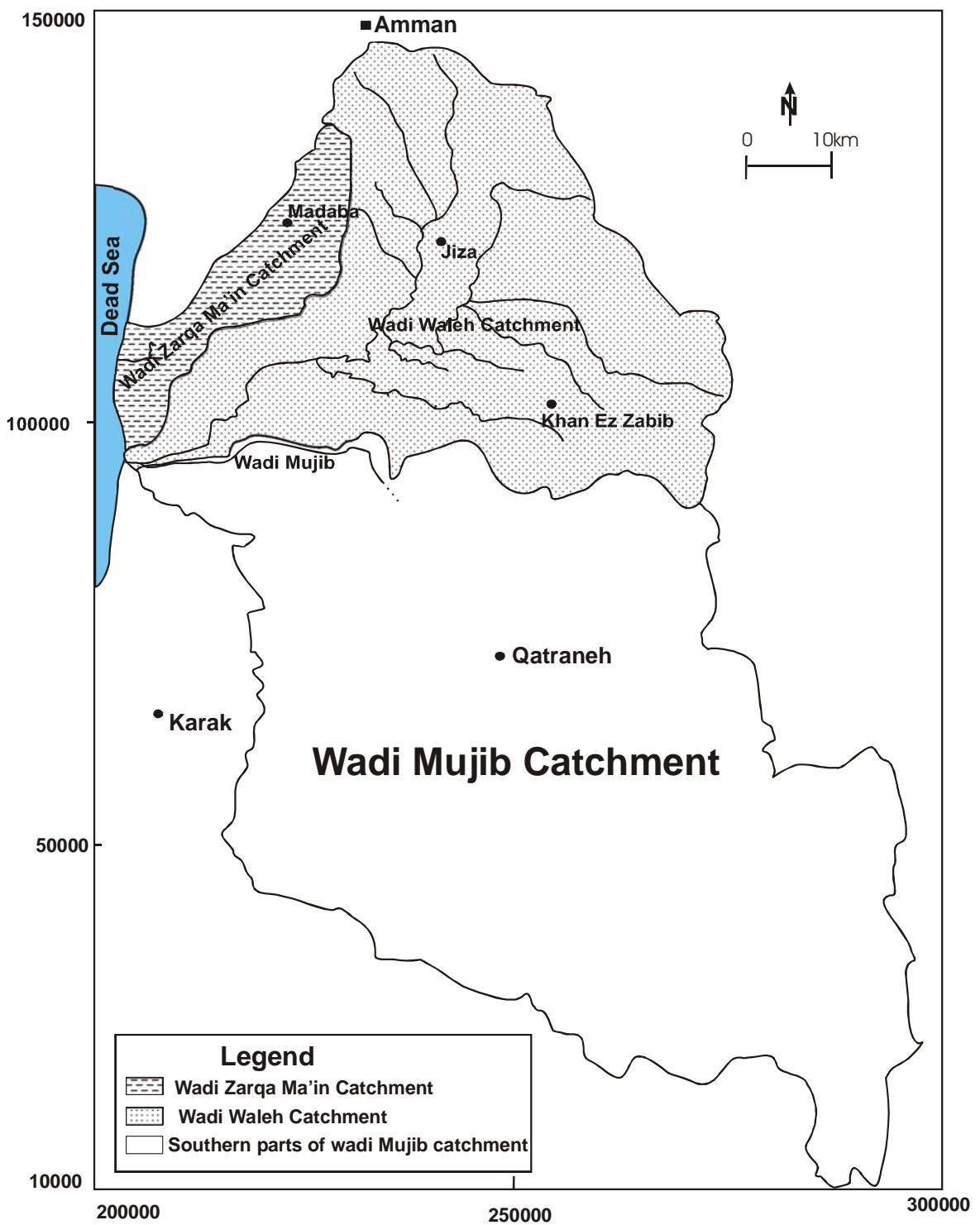
Figure -1.2: Wadi Mujib groundwater catchment including the study area

1.2 Geothermal Problem

The geothermal activity in Jordan is expressed entirely in form of thermal springs. Other geothermal phenomena such as fumarolic activity and boiling mud pools or altered ground are not found. Therefore, there is no physical evidence from surface manifestations of the existence of high temperatures at shallow depths.

The location of nearly all thermal springs and anomalously hot thermal wells (Mukheibeh, North Shuneh, and TDS-1) is dictated by their proximity to the Dead Sea Rift. Photo-1.1 shows the North Shuneh thermal well.

Generally, they are distributed along a distance of about 200km on the eastern side of the Rift, extending from Yarmouk River in the north to Tafileh in the south with temperatures ranging from 30 to $63^{o}C$ (Figure-1.3). Photo-1.2 shows the swimming pool of Al Himmeh thermal springs at Yarmouk River. The thermal water of these sources discharges from the lower aquifer complex (Kurnub sandstone and sandstones of older ages) except for Mukheibeh well field and Jiza thermal wells which discharge from the upper aquifer complex (B_2/A_7). The Zara–Zarqa Ma'in hot springs are considered as the major geothermal manifestation in Jordan. Most of the geothermal investigations in Jordan were concentrated on this hot thermal system due to its high temperatures and flow rates.

Away from the Rift, about 30km east of Zara–Zarqa Ma'in hot springs, many wells were drilled to the upper aquifer (<350m depth) in the last three decades, mainly by the private sector for agricultural purposes. Most of these wells discharge thermal water with temperatures up to $46^{o}C$, despite that the upper aquifer is known as a major source for fresh cold water in Central Jordan. This might be due to the presence of many faults, of different trends and types, affecting the study area especially in the eastern parts (Jiza region) where the hottest thermal wells are located close to some of these faults. This strongly suggests that the two-aquifer systems are hydraulically connected by faults, where the thermal water from the lower aquifer flows upwards to the upper aquifer raising the water temperature in the vicinity of these faults.

The thermal wells anomaly in Madaba-Jiza region is the main target of this study, aiming to:

1- Build up a conceptual hydrogeological model for the areas from Zara–Zarqa Ma'in in the west through Madaba to Jiza region in the east.

4
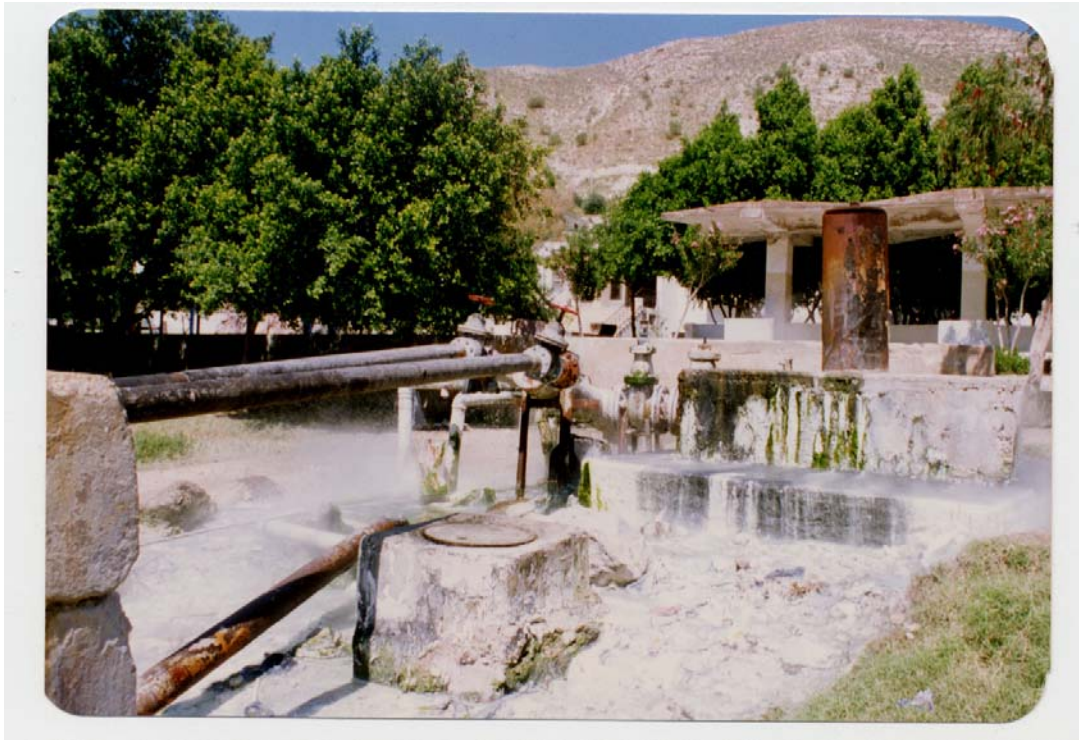
Photo-1.1: North Shuneh thermal well.

Photo-1.2: The swimming pool of Al Himmeh thermal springs

5

2- Study the groundwater chemistry and isotopes content of both aquifers as well as their water origin.

3- Determine the heat source of the thermal wells discharging from the upper aquifer and the maximum reservoir temperature of the lower aquifer.

4- Assess the mixing process between the two aquifers in the area and locate the main up-flow zones.

5- Use the GeoSys/RockFlow scientific software to develop a GIS based 3D numerical model for groundwater flow and heat transport in the study area.
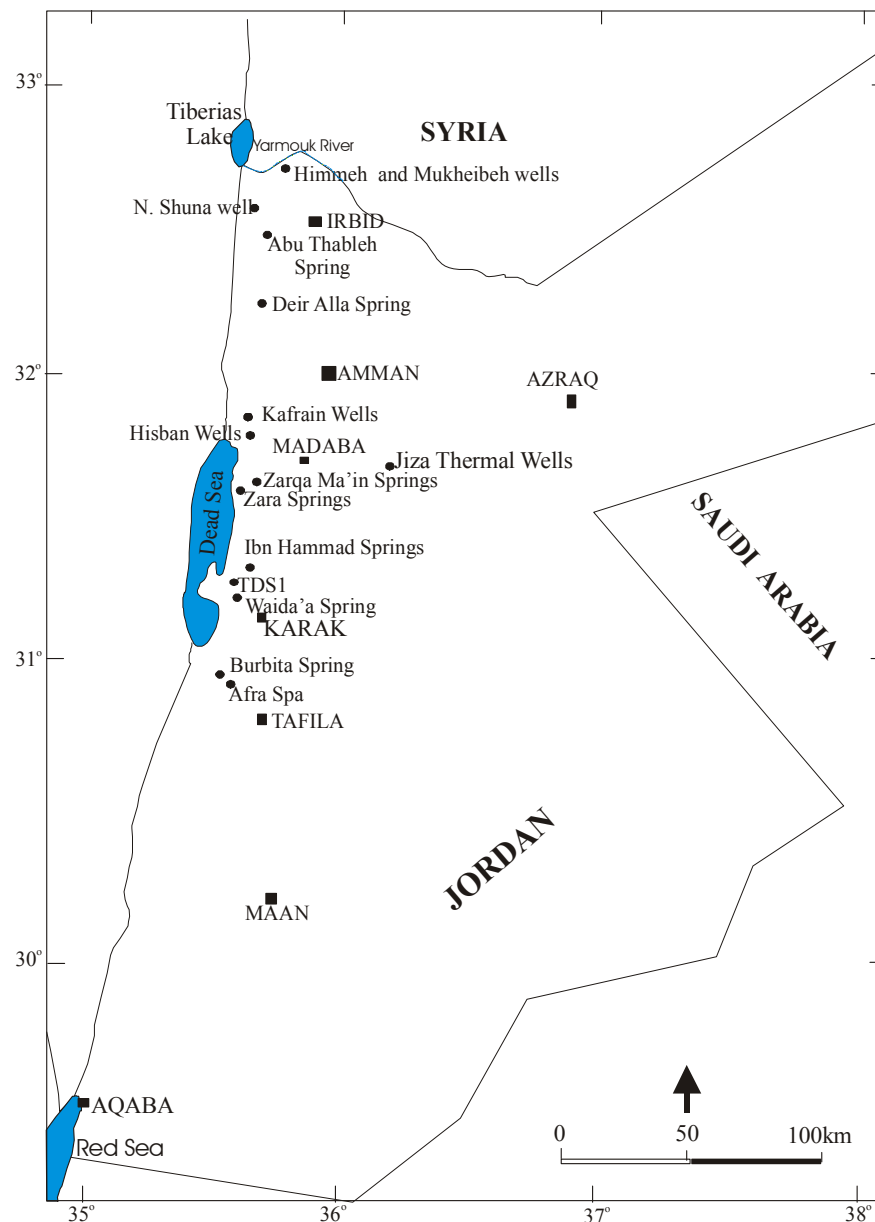
Figure-1.3: Thermal resources distribution in Jordan

2. GEOLOGICAL SETTING

2.1 Overview on the Geology of Jordan

Jordan is located in the northern western part of the Arabian Peninsula. It consists of three elongated distinctive topographic provinces trending in a general north-south direction. The Rift Floor Province forms the western part of the country. It extends from the Gulf of Aqaba in the south through Wadi Araba and Dead Sea to Lake Tiberias in the north. The floor elevation of the Rift rises from sea level at Aqaba at Red Sea shore to about 240m above sea level (asl) at Risha area in Wadi Araba, and falls to a round 750m below sea level (bsl) at the bottom of the northern part of the Dead Sea. Then, to the north of the Dead Sea, it rises gradually to about 210m bsl at the shores of Lake Tiberius (Salameh and Bannayan, 1993). The highlands province located east of the Rift and extends from the Yarmouk River in the north to Aqaba in the south with width ranging from 30 to 50km. The highlands rise in elevation to more than 1000m asl in the northern Jordan and to more than 1200m asl in Shoubak in the southern part. These elevations drop sharply to the Rift in the west, but gradually towards the Plateau in the east. The Plateau province developed at the eastern toes of the highlands with land surface ranging from 1000m asl in the south to 700m asl in the northeast. Two main basins are located in this province: Jafer Basin in the south and Azraq Basin in the northeast. Azraq Basin forms the deepest part of the plateau with an elevation of 500m asl (Figure-1.1).

The dominant structural feature of Jordan is the north-south trending Dead Sea Rift. It forms an active part of the African-Syrian Rift, which extends for about 6000km, from east Africa through the Red Sea, Wadi Araba, Dead Sea, Jordan Valley to south Turkey. Long time before the formation of the Dead Sea Rift, the movement of the African plate including the Arabian plate to the north caused the formation of the Syrian Arc Fold Belt, which was named by Krenkel (1924). The Syrian Arc formed in two stages: the first in the Turonian-Maestrichtian and the second in the Oligocene (Burdon, 1959; Bandel and Mikbel, 1985; Abed, 1989, 2000). It extends in S shape, from Sinai through Palestine, Jordan to Syria. Examples of the Syrian Arc Fold Belt structures in Jordan are Wadi Shuaib and Amman- Hallabat structures.

After that, in the Miocene the Arabian plate separated from the African plate and continued its movement to the north causing the creation of the Transverse Fault System in the Miocene-Pliocene. This system accompanied by a group of tensional faults trending NW-SE and dextral shears trending E-W and compressional structures trending NE-SW.

Then the Dead Sea Rift was created. It trends nearly N-S and extends from Gulf of Aqaba to south Turkey with total length of 1100km. It consists of two faults: The southern fault, Risha or Wadi Araba Fault and the northern fault, Jordan Valley Fault. Wadi Araba Fault starts from Gulf of Aqaba to Risha area in the middle of Wadi Araba and to Dead Sea basin along its eastern shore and ends at its northern eastern corner. The Jordan Valley Fault starts in the southern western part of the Dead Sea and continue to the north along its western shore to the east of the Tiberias lake. Two theories were used to explain the formation of the Dead Sea Rift: vertical movement (Graben tectonics) and horizontal movement (Plate tectonics). Detailed investigations have proved the horizontal movement theory, where the Arabian plate has been continuously moving to the north (Quennell, 1956; Freund et al. 1970; Abed, 1982; Girdler, 1983 and many others).

The left-lateral strike slip displacement along this transform boundary was estimated in Jordan at about 107km by Quennell (1956). In former litretureit was assumed that the movement has taken place in two stages: the first (62km) which should have started in Eocene (Girdler, 1983) or started in the Mid-Miocene time, before 15-17 million years, (Garfunkel et al. 1981) and the second stage (45km) started in the Pleistocene (5 million years) and still going on (Quennell,1956; Abed 1982). Results from the Midyan peninsula (Bayer et al. 1988; Purser and Hoetzl, 1988) and from Ocean spreading in the Gulf of Aden (Gass, 1979) document a more or less continuous movement since about 12 million years.

As a result of major structures (Syrian Arc, Transverse Fault System and Dead Sea Rift) and the continuous northward movement of the Arabian plate, faults of different trends and ages have developed (Figure-2.1). The different trends are due to different stress fields resulting from the different tectonic movements in different ages. The main fault trends are N-S sinistral strike-slip faults, E-W dextral strike-slip faults, NW-SE tensional faults and NE-SW compressional faults.

The crossing of the fault systems acted locally as conduits for the Neogene-Pleistocene basaltic intrusions and flows. Several of the E-W faults are traceable for tens of kilometers from the Rift inside the country. Examples of these faults; Siwaqa Fault, traceable for about 150km (Masri, 2002) and the Zarqa Ma'in fault, traceable for about 50km (Abu Ajameih, 1980). The offset along these faults generally decreases eastward where they are associated with or merge into monoclinal flexures.

Sedimentary rocks cover almost the whole area of Jordan with a thickness of more than 5000m in Azraq Basin. The Precambrian basement rocks are only exposed in the south-west of the country (Aqaba region).   The basement rocks deepen northwards and northeastwards. The simplified geological map of Jordan, produced by the Geological Mapping Division/ Natural Resources Authority (NRA), is shown in figure-2.2.

According to Bender (1974b) the sedimentation began in Late Pre-Cambrian with the deposition of the Saramuj Conglomerates. During the Cambro-Ordovician, the Salib Sandstone, Burj Dolomite Shale, Umm Ishrin, Disi and Umm Sahm sandstones (Ram Group) were deposited through out Jordan and northwest Saudi Arabia. Then Khrayim Group (silty sandstone series) of Ordovician-Silurian age were deposited during the major marine transgression, which occurred from Lower to Middle Ordovician up to lower Devonian. In north Jordan, alteration of transgressions and regressions during Triassic and Jurassic resulted in the deposition of Zarqa complex. From Cretaceous to Eocene the whole country was covered by an extensive marine transgression and caused the deposition of the Kurnub, Ajlun and Belqa groups.   In the Upper Eocene, the sea regressed and a period of erosion began which lasted to the present day.   This period has been characterized by volcanic activity resulting in the extensive basalt flows mainly in northeast Jordan and extended to Syria and Saudi Arabia, and by localized lacustrine and fluviatile deposits in the Azraq and Jafer basins as well as the Rift Valley. Table-2.1 shows the lithological sequence in Jordan.
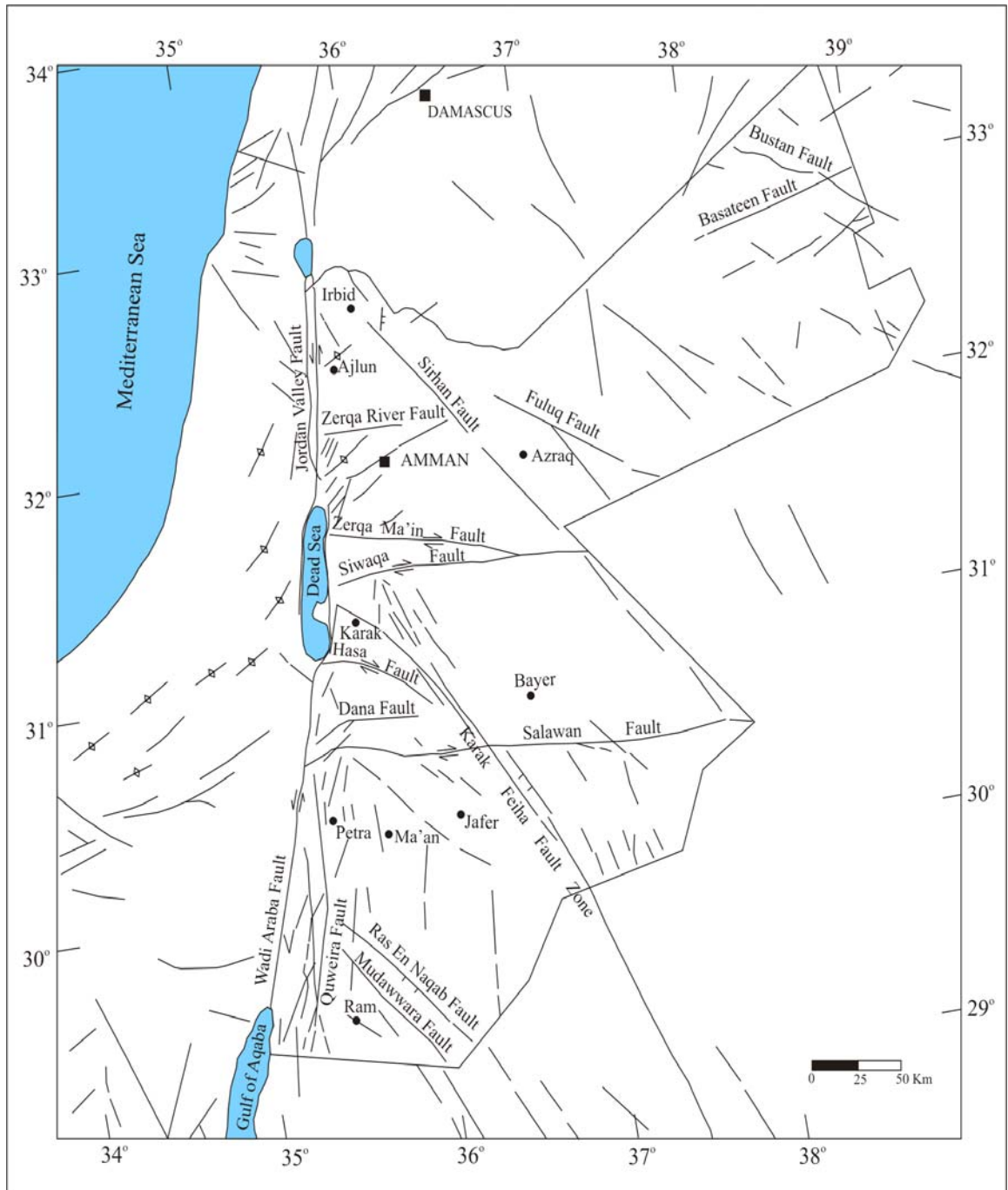
Figure-2.1: The structural map of Jordan (after Diabat, 2004).
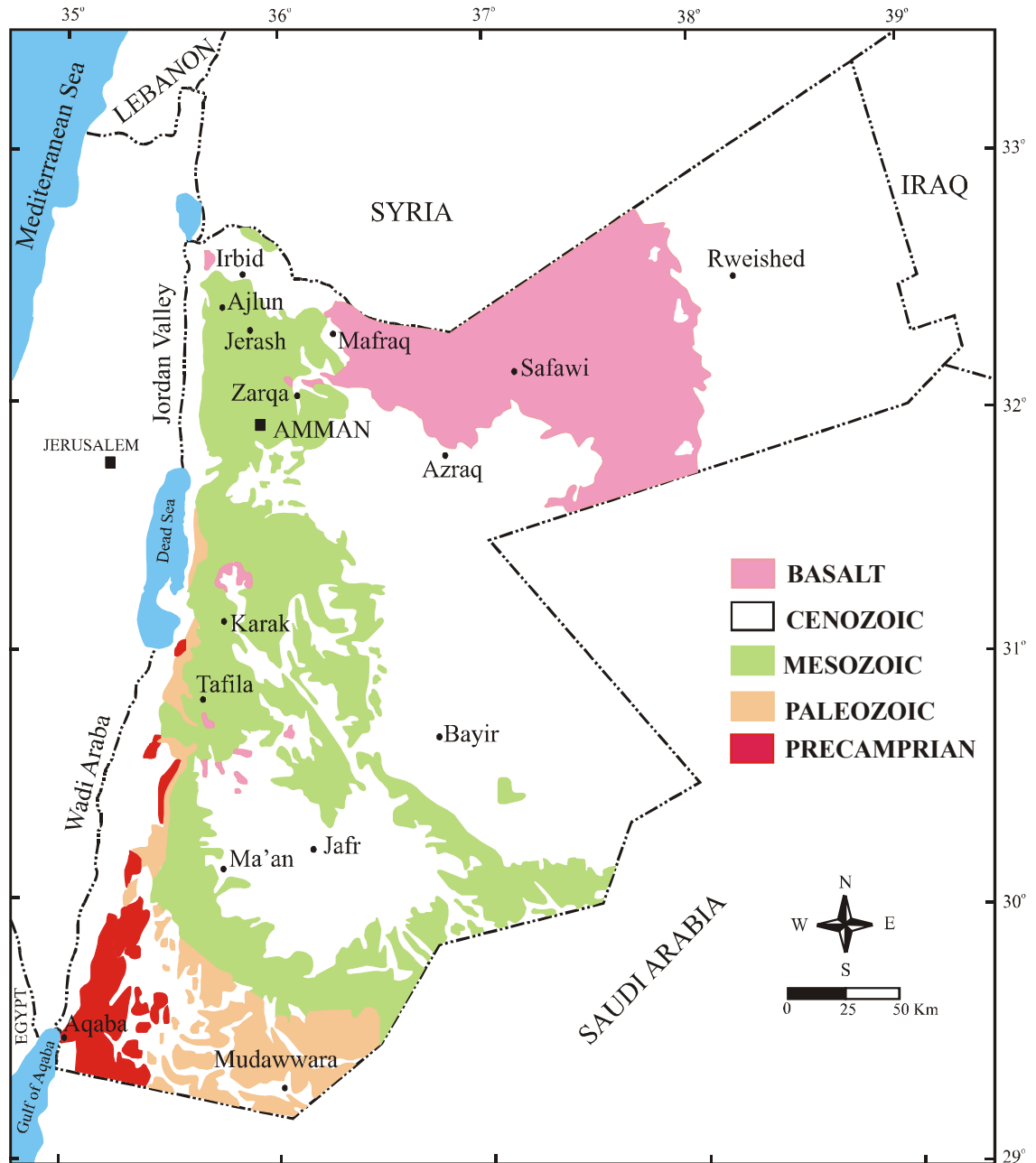
Figure-2.2: A simplified geological map of Jordan (NRA open files).

TABLE- 2.1: Lithological sequence in Jordan (compiled from NRA open files)

Period	Age	Group	Formation	Lithology
Quaternary	Holocene (Recent)		Fan, Talus, Terrace, River	Sand, Clay, Gravel
	Pleistocene	Jordan Valley	Lisan	Marl, Clay, Gypsum, Sand, Gravel
Tertiary	Pliocene		Undifferentiated	Conglomerate, marl
	Miocene			
	Oligocene			
	Eocene	Belqa	Wadi Shallala (B5)	Sandstone
	Paleocene		Umm Rijam (B4)	Chert, limestone
Upper Cretaceous	Maestrichtion		Muwaqqar (B3)	Chalk, Marl
	Companion		Al Hasa (B2a) Amman (B2b)	Phosphate Silicified Limestone
	Santonian		W. Ghudran (B1)	Chalk, Chalky marl
	Turonian	Ajlun	Wadi Es Sir (A7)	Limestone
	Cenomanian		Shueib (A5-6)	Marly Limestone
			Hummar (A4)	Dolomitic Limestone
			Fuheis (A3)	Marl
			Na'ur (A1-2)	Marly Limestone
Lower Cretaceous	Albian	Kurnub	Kurnub Sandstone	White Sandstone, dol.
	Aptian			Varicolored Sandstone
	Neocomian			Lst., shale, marl, dol.
Permo-Triassic		Zarqa	Dardur	Sandstone, marl,shale
			Ma'in	Sandstone, siltst.,clay
			Umm Irna	Sandstone, siltst. shale
Silurian		Khryim	Khushsha	Sandstone, shale
			Mudwwara	Sandstone, shale, mud
Ordovician			Dubaydib	Sandstone, shale
			Hiswah Sandstone	Mudstone, sandstone
		Ram	Umm Sahm	Sandstone
			Disi	Sandstone
Cambrian			Umm Ishrin	Sandstone, siltstone
			Burj dolomite	Shale, dol., sandstone
			Salib	Sandstone, siltstone
Pre-Cambrian		Safi	Saramuj Conglomerate	Conglomerates

2.2 Lithological setting of the study area.

A sequence of more than 1000m of sedimentary rocks is well exposed in the study area ranging in age from Cambrian to Recent. This sequence is subdivided into many geological formations, as described in the detailed geological maps (1:50,000) produced by the Geological Mapping Division in NRA like; Ma'in, Madaba and Khan Ez Zabib Sheets. These geological formations are described below:

2.2.1 Paleozoic Ram Sandstone Group

The name was used first by Quennell (1951) and Burdon (1959) for siliclastics of assumed Ordovician to Permian age. Bender (1974) showed that these and the overlying silicates in the southern desert are all of Early Paleozoic age. The Ram Group includes all the dominantly fluvio-clastic sediments below the first distinctive siltstone-mudstone horizon with microfossils. Two formations of the group exposed in the study area, these are:

2.2.1.1 Burj Dolomite – Shale Formation (BDS).

The Burj Formation is the oldest geological formation (Lower Cambrian) cropping out in the study area. Quennell (1951) defined the formation, and its name was taken from the ruins of El Burj in the lower course of Wadi El Hasa.

The formation is subdivided into three members, in ascending order, Tayan siltstone, Numaryi dolomite, and Hanneh siltstone with a total thickness of up to 130m (Bender, 1968b)

Only the upper two members are exposed in the study area, where a succession of 75 m is exposed near Wadi Zarqa Ma'in on the main road along the Dead Sea Shore (Shawabkeh, 1998).

This succession is composed of gray finely laminated carbonate, fine grained quartz arenite with burrows and ripple cross-lamination, overlain by intercalated green to gray cross-laminated siltstone, fine grained sandstone and shelly grain stone, passing upward to oolitic packstone and cross-bedded trilobite. The base of Umm Ishrin Formation easily marks the top of this formation.

2.2.1.2 Umm Ishrin Sandstone Formation (IN)

The formation name was first used by Lloyd (1969) and is taken from the type locality, Jabel Umm Ishrin in the southern deserts of Jordan. The Umm Ishrin Formation is exposed in the western part of the study area along the Dead Sea escarpment as steep rugged cliffs. The total thickness of this formation at Zarqa Ma'in area is about 123m measured in well GTZ–3D in Zarqa Ma'in area (Andrews, 1992). But, it has a thickness of 300 to 330m to the south of the study area in Karak area (Powell, 1988).

Umm Ishrin Formation consists of yellow-brown and mauve red medium to course grained massive weathered sandstone with scattered quartz granules pebbles, intercalated with thin beds of siltstone and mudstone. It ranges in age from Middle to Upper Cambrian.

2.2.2   Zarqa Ma'in Group (Permo–Triassic)

Triassic sediments unconformably overlie the Cambrian sandstones in Wadi Zarqa Ma'in. The outcrops are restricted to the cliffs adjacent to the Dead Sea with a maximum thickness of about 170m.

Bandel and Khoury (1981) subdivided the Triassic strata in Jordan into nine formations. Only three formations are exposed in the study area;

2.2.2.1 Umm Irna Sandstone Formation (UI)

The outcrop of this formation is at Wadi Himara at the western northern corner of the study area. The measured section of the formation ranges from 60 to 85m (Bandel and Khoury, 1981).

It consists of six fining upward cycles. Each cycle (except the lower most one) starts with an errosively based, course to fine grained sandstone overlain by maroon siltstone and shale. The lower most cycle consists mainly of silt and clay and contains abundant plant fragments.

2.2.2.2 Ma'in Sandstone Formation (MN)

The formation is well exposed at Zarqa Ma'in area along the Dead Sea Shore and in the deep wadis. Bandel and Khoury (1981) subdivided the formation into two members: Nimra, and Himara. The measured sections range from 35 to 55m. It consists of alternation of thinly bedded of sandstone, siltstone and clay. Burrows are present in the lower part. The upper part is composed of cross-bedded sandstone with carbonates.

2.2.2.3 Dardur Sandstone Formation

The formation is only exposed at the western northern corner of the study area between Wadi Zarqa Ma'in and Wadi Himara along the Dead Sea Shore. Bandel and Khoury (1981) named the formation after Wadi Dardur where the type section is exposed. The formation consists of cream, yellowish, black and dark green laminated marl and shale, dolomitic limestone with cross-bedded sandstone and dolomitic sandstone. The maximum-recorded thickness of the formation is 57m as measured in Wadi Dardur (Shawabkeh, 1998).

2.2.3 Kurnub Sandstone Group (Lower Cretaceous)

The Kurnub Sandstone Group crops out along the eastern side of the Dead Sea. It overlies unconformably the Triassic sediments in Wadi Zarqa Ma'in, while it overlies conformably the Jurassic sediments in north Jordan. To the south of Wadi Mujib the group unconformably overlies the pen-planed Paleozoic sandstone (Disi sandstone).

The group name was first used for the sandstones exposed at Kurnub, near Beersheba in an unpublished report. Quennell (1959) used the term, Kurnub sandstone, and correlated this formation with the equivalent sandstone in Jordan. Bender (1968b) subdivided the Lower Cretaceous sandstone into two parts: upper and lower.

The lower part is massive white sandstone, medium to course grained, with planar to tangential cross-bedding and abundant quartz pebbles. Several silty intercalations (up to 5m) occur in the lower portion of this part.

The upper part is varicolored sandstone and composed of alternating thin-bedded fine clastic and thick to thin, medium to course grained sandstone. Intercalations of red and green clay and siltstone with gypsum lamina near the top occur in this part. The dominant

feature of this part is the violish and reddish colors that form a marked contrast with the overlying greenish marls and ochre limestone of the Cenomanian, Upper Cretaceous.

The maximum thickness of the Kurnub Group, in the study area, was given by Shawabkeh (1998) as 220m in the measured section from Wadi Abu Khusheiba. In well GTZ–2D in Zarqa Ma'in area, the Kurnub Group recorded a thickness of 219m.

2.2.4 Ajlun Group (Upper Cretaceous).

Throughout most of Jordan, the Ajlun Group (Cenomanian-Turonian) overlies disconformably the Kurnub sandstone. The group consists of a thick sequence of predominantly carbonate rocks overlain by the chalk, chert and phosphate of the Belqa Group. Quennell (1951) first named the Cenomanian to Turonian carbonate sequence as the Ajlun Series. Wolfart (1959) subdivided the group into seven lithostratigraphic formations (A_1-A_7). Masri (1963) established five formations (Na'ur, Fuheis, Hummar, Shueib and Wadi Es Sir) in the group based on mapping in the Amman-Zarqa area. Some of these formations are equivalent to Wolfart's subdivisions, but A_1 and A_2 were combined as one formation called Na'ur and A_5 with A_6 as Shueib Formation. All the group subdivisions are well exposed in the study area:

2.2.4.1 Na'ur Formation (A_{1-2})

The Na'ur Formation forms the basal unit of Ajlun Group and it crops out in the deep wadis at the western part of the study area. It consists of shelly limestone, dolomite limestone, dolomite and marl. The lower part is characterized by yellow marl overlying the reddish sandy shale, fine sandstone glauconite of the transition zone (Juhra member) with the underlying Kurnub sandstone. The thickness of Na'ur formation in Mukawir is 145m (Powell, 1989), in addition to 55m the thickness of the Juhra member (Shawabkeh, 1998).

2.2.4.2 Fuheis Formation (A_3)

The formation is composed mainly of marl and marly limestone, nodular limestone, reddish and greenish shale and gypsum. It forms a gentle slope at outcrops between two distinctive cliffs; the upper cliff of Na'ur Formation and the main cliff of the overlying Hummar Formation. The thickness of the formation is about 65m (Shawabkeh, 1998).

2.2.4.3 Hummar Formation (A$_4$)

The formation crops out in the western part of the study area. It is characterized by a thick hard cliff. In Wadi Abu Khusheiba (Mukawir) the formation exhibits a vertical cliff with step like morphology.

The Hummar Formation consists mainly of gray limestone, dolomitic limestone and dolomite. Sub-horizontal burrows are common in the formation, consisting of inter-bedded shelly wakestone. The upper part is rich in oysters, rudest and corals. The thickness of the formation is about 40m (Shawabkeh, 1998). It is highly fractured and forms an important local aquifer in north Jordan.

2.2.4.4 Shueib Formation (A$_{5-6}$)

The Shueib Formation crops out in the western parts of the study area. It exhibits distinctive, yellow, to yellow-gray gentle slope forming saddles between the underlying main cliff of the Hummar Formation and the overlying steep slopes of the thick bedded of the Wadi Es Sir Formation. It is made up of yellow, gray and green marls alternating with thin and thick-bedded marly limestone. The formation has a thickness of 70m as measured in Wadi Abu Khusheiba to the south of Wadi Zarqa Ma'in (Powell, 1989).

2.2.4.5 Wadi Es Sir Formation (A$_7$)

The formation is widely exposed in the study area. It is mainly composed of well-bedded massive limestone. However, dolomitic limestone, calcareous siltstone and marl are also present. Beds of gypsum are locally present near the base, and beds of chert nodules are common in the middle and upper parts. Micrite is the most common limestone texture, but shelly and oolitic wakestone and packstone types also occur.

The formation shows a wide variation in thickness, 250m at Ajlun district in north Jordan and 80m southwest of Madaba. In Wadi Abu Khusheiba the thickness of the formation is 105m as given by Powell (1989).

Wadi Es Sir Formation forms the lower part of the main aquifer system for fresh water through out Jordan.

2.2.4.6 Khureij Limestone Formation

The formation crops out at Zarqa Ma'in and Wadi Abu Khusheiba areas, the thicknesses are 26m and 16m respectively (Shawabkeh, 1998). It is made up of yellow-buff marls, calcareous siltstone and dolomitic marl with local oyster coquina at the top.

2.2.5 Belqa Group

The Belqa Group comprises a predominantly pelagic sequence of sediments including chalk, marl, chert, phosphate, coquina, limestone, and siliclastic sand overlaying the Ajlun Group. It ranges in age from Cenomanian to Eocene.

Quennell (1951) first established the name. Wolfart (1959) subdivided the group to five units (B_1-B_5). Parker (1970) named the units as Wadi Umm Ghudran, Amman, Muwaqqar, Umm Rijam and Wadi Shallalah formations.

2.2.5.1 Wadi Umm Ghudran Formation (B_1)

The formation is well exposed in Wadi Waleh and Wadi Zarqa Ma'in. At the southern part of Wadi Zarqa Ma'in, it is subdivided into three members: Mujib, Tafileh and Dhiban Chalk with maximum thickness of 86m. Only one member is exposed in the northern part of the Wadi with a maximum thickness of 25m.

The formation, litho-logically consists mainly of cream to white chalk with the presence of gray chert, gray microcrystalline limestone concretions with phosphatic chert. It ranges in age from Cenomanian to Campanian (Powell, 1989).

2.2.5.2 Amman Silicified Limestone (B_{2a})

The formation is widely exposed within the study area, in the highland and the deep tributaries of Wadi Waleh. It is of Campanian age and composed predominantly of pale to dark gray and brown thin to thick bedded chert intercalated with subsidiary gray microcrystalline limestone, bioturbated chalky laminate, marl and oyster-coqunial limestone. Phosphate is common towards the top of the formation and is usually concentrated in a thin layers on top of individual chert beds. The thickness of the formation ranges from 60 to 100m at the western parts of the study area, and decreases towards the eastern parts till it reaches less than 50m.

18

2.2.5.3 Al Hasa Phosphorite Formation (B₂ᵦ)

This formation starts to crop out in areas east of Madaba city as small isolated hills surrounded by areas of thicker soil. It ranges in thickness from 55–67m in the middle part of the study area (Al Hunjul, 1991c). It has been subdivided into three members: Bahiya Coquina, Sulttani Phosphorite and Qatraneh Phosphorite.

The formation lithology is heterogeneous and made up of alternative beds of phosphatic chert, phosphatic limestone, phosphate, chalky limestone, micritic limestone, marl, cross-bedded oyster banks and reworked broken shells.

2.2.5.4 Muwaqqar Chalk Marl Formation (B₃)

The formation crops out at the eastern third of the study area. It consists of marl, chalky limestone, micritic limestone and chert. The formation is subdivided into two parts: a lower part of thick beds of white to light gray chert, white chalk with light gray layers and large limestone concretions which reach up to 2m in diameter. And an upper part consisting of chalky limestone, chalk and micrite limestone inter-bedded with dark gray to brownish chert. The oil shale (Bitumen) is found at the bottom of the lower part. Thin beds of gypsum are found in the middle part of the formation.

The measured outcrop thickness of the formation ranges from 70 to 100m and in wells from 180 to 270m (Al Hunjul, 1991c; Jaser, 1986).

2.2.5.5 Umm Rijam Formation (B4)

The formation crops out in Wadi El Thamad in a graben structure (Al Hunjul, 1995) at the middle of the study area while it is widely exposed in the eastern parts of the study area. It forms the topographic divide at Massttarat El Falij Mountains between the Mujib and Azraq basins.

Pebbles of limestone and few dark brown cherts characterize the surface of the formation. It consists litho-logically of a sequence of thin-bedded brown chert, chalk, and chalky limestone. The formation has a thickness of about 80m in the study area increasing eastwards of the study area to 130m (Jaser, 1986).

2.2.6 Basalts

No basaltic flows are found in the eastern part of the study area, where the thermal wells are located. To the south of the study area, basalt sheets are found in the area south of Wadi Mujib, with an eruption center at Jabel Shihan.

At Zarqa Ma'in area the basalt flows form a resistant cap on the southern rim of the Wadi Zarqa Ma'in and form the lip of the 100m high waterfall, about 2km upstream from the principal area of thermal springs. All of the lavas appear to represent intra-canyon flows that were channeled westward, within earlier courses of the wadi (Duffield et al. 1987).

Three lava flows are exposed in the south wall of Wadi Zarqa Ma'in down stream of the waterfall and upstream of the thermal springs. The lava is underlain by Cretaceous limestone. Stream gravels are present between the limestone and the lowest lava flow.

Duffield and others (1987) reported, according to K-Ar aging, that the age of the basalts at Zarqa Ma'in area ranges from 0.6 to 3.4 million years. While, it is as old as 6.1 million years in the areas south of Wadi Mujib.

2.2.7   Superficial deposits

Various superficial deposits are found in the study area. The main deposits are; fluvitile gravel, calcrete and travertine.

2.2.7.1 Fluvitile Gravel

Pleistocene gravel, which consists of course grained sand and gravel with rounded pebbles and boulders, is found as plateau gravels up to 10m thick and on wadi flanks. This kind of deposits is very wide spread in Wadi Zarqa Ma'in and along the eastern shore of the Dead Sea. Limestone, sandstone, chert and basalt are the main constituents of this gravel. It consists of chert, limestone, phosphatic chert, phosphatic limestone and marble in the eastern part of the study area, where it occurs in relatively high areas above the present day erosional surface, and is dissected by recent wadis.

2.2.7.2 Travertine

This is a carbonate rock resulting from the precipitation of limestone from thermal waters and it is found to overlie the fluvitile gravels in the Zarqa Ma'in area. Normally, it occurs on the lower slopes of the thermal springs courses. Two types of travertine occur: A younger soft, creamy colored travertine, slightly manganiferous occurs in the vicinity of the hot springs. An older, dark colored and thick travertine forms layers of varying thicknesses down streams of the hot springs locations. It is hard, filled with cavities and highly manganiferous and looks like basalts.

In the eastern part of the study area where the thermal wells are located, no travertine deposits were found except at the top of Rujum (Mountain) Qial. At the southern border of the study area (Siwaqa area) a large amounts of travertine deposits are found indicating the presence of thermal water in the past. Bender (1974) stated that the travertine is of Pleistocene age.

2.2.7.3 Holocene and Resent Sediments

These sediments comprise recent alluvial deposits in channels and associated flood plains of ephemeral streams. In the eastern part of the study area it consists of clay, sand, and sorted and unsorted pebbles and boulders. In Wadi Zarqa Ma'in, it is mainly basalt scree from denudation and physical weathering of the basalt flows.

Recent sediment in the highland part of the study area is the lime crust (Calcrete). This develops as surface cementation of carbonaceous material in areas of high seasonal rainfall.

2.3 Structural setting of the study area

The main structural element governing the morphology, hydrology and hydrogeology of Jordan is the Rift fault zone, which trends nearly N-S and extends southwards beyond the Gulf of Aqaba into the Red Sea and northwards through Lebanon into Turkey (Figure-2.1). Away from the Dead Sea Rift, the geological units generally dip very gently, up to three degrees, to the east-northeast. Whereas, adjacent to the main faults local disturbances have occurred. Along the slopes bordering the Dead Sea the area is highly block faulted, resulting in random strikes and dips of the tilted blocks.

The area shows flat undulations and is intersected by a network of numerous fault trends of different behavior and displacement. The dominated structures in the area are the E-W, NE-SW, NW-SE and N-S faults associated with faulted blocks as horsts, grabens and tilted blocks.

2.3.1 Faults

The study area is dissected by numerous faults with several trends, which probably originated in the Precambrian and early Paleozoic due to different strain pattern. The faults were covered by Paleozoic and Cretaceous sediments. The different trends are due to different stress fields resulting from the different tectonic movements in different ages, from the Late Cretaceous to Tertiary and Quaternary. The main fault trends are E-W dextral strike-slip faults, NW-SE tensional faults and NE-SW compressional faults (Diabat and Masri, 2002):

2.3.1.1 E–W Trending Faults

The E-W trending faults were originated first as normal faults during the creation of the Transverse Fault System in Miocene then they reactivated as strike-slip faults during the creation of the Dead Sea Rift in Mid Miocene-Pleistocene.

This fault trend dissected the study area into four regional blocks, trending E-W. The faults; Zarqa Ma'in, Daba'a and Siwaqa are the major faults of this trend.
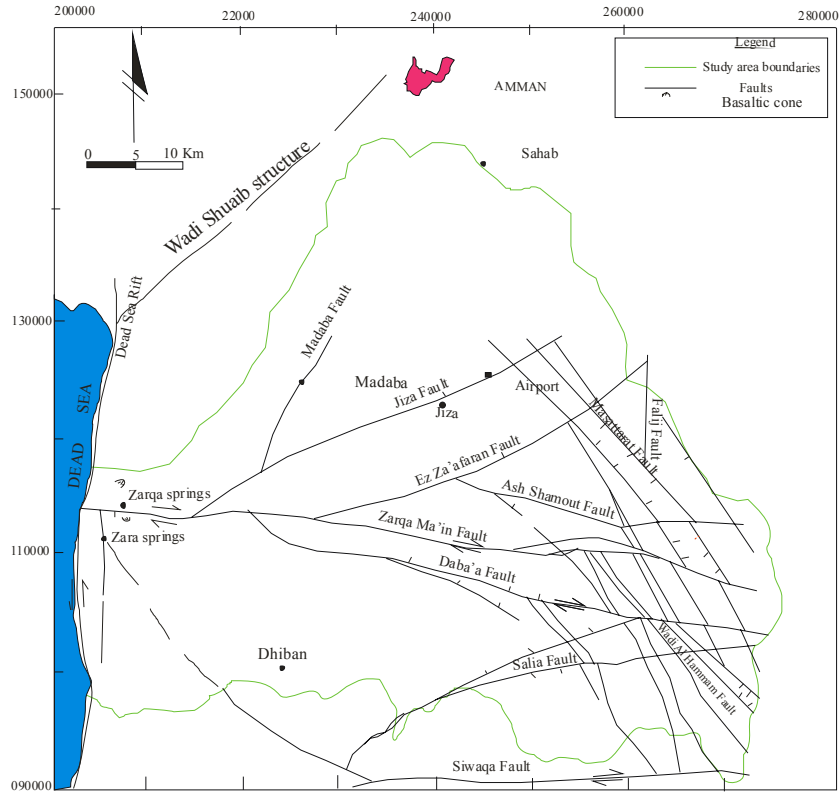
Figure-2.3: Major faults in the study area (modified from Diabat and Masri, 2002).

2.3.1.1.1 Zarqa Ma'in Fault

This is the most important structural feature in the study area. The fault strikes E-W and it can be traced eastwards for a distance of 50km from the Dead Sea. The fault originated as normal fault and was reactivated during later stages as dextral shear. This is evidenced from the presence of the horizontal slickenside on the fault plane, the variation of down throw on both sides of the fault, and the presence of the compressional and tensional structures on the left and right bands of the fault, respectively (Diabat and Masri, 2002). The maximum down throw is about 400m at the eastern part of the study area, just west of the Desert Highway, where Umm Rijam Formation (B_4) is faulted against Wadi Umm Ghudran Formation (B_1), Photo-2.1.

Photo-2.1: Zarqa Ma'in Fault (red line) and one of the thermal wells

In Wadi Zarqa Ma'in, the down faulted Na'ur Formation (A_{1-2}) at the southern side stands against the Kurnub Sandstone at the northern side of the wadi, where all the thermal springs are located as typical fault contact springs.   Volcanic activities took place during the Neogene age and intruded along the fault system and formed the volcanic cone of Hammamat Umm Hasan, which stands opposite to Hammam El Amir thermal spring as a high peak.

2.3.1.1.2   Daba'a Fault.

This fault branches from Zarqa Ma'in Fault with WNW - ESE direction and extends for more than 75km in the study area with a down throw of about 50m towards NNE. It could be of dextral strike-slip nature accompanied by transtensional and transpressional structures (Diabat and Masri, 2002).

2.3.1.1.3   Siwaqa Fault

Siwaqa Fault is a distinctive structural feature located to the south of the study area and it can be considered as the southern boundary for the study area. It trends E-W and crosses Jordan from the Dead Sea in the west to Sirhan Graben at the Saudi Borders in the east. The fault is of dextral shear type and the vertical movement changes several times from north to south, especially in the western areas, while in the eastern areas the down throw is mainly to the south.

2.3.1.2 NE-SW Trending Faults

2.3.1.2.1 Salia Faulted – Folded Belt

This is a complicated structure, which extends from Siwaqa Fault in the west to Rujum Qial, just east of the Desert Highway, to Daba'a Fault. The regional apparent vertical throw is less than 100m due to south (Diabat and Masri, 2002).

2.3.1.2.2 Ez Za'afaran Fault

Ez Za'afaran Fault branches from Zarqa Ma'in Fault and extends to about 30 km in the study area. It started as normal fault with vertical displacement of more than 150m in areas near the Desert Highway (Al Hunjul, 1995). The fault was then reactivated to a dextral strike-slip nature and demonstrates transpressional structures and elongated compressional hills parallel to the fault.

2.3.1.2.3 Jiza and Madaba Faults

The Jiza Fault branches from Zarqa Ma'in Fault. It extends from south Madaba city through Jiza town to Queen Alia International Airport. Over most of it extension it is covered by superficial deposits.

The Madaba Fault passes east of Madaba City under thick soil cover. Both faults are commenced from land sat images and some regional geophysical studies.

2.3.1.3 NW–SE and sub parallel faults

This fault trend is the oldest, probably it dates back to the Precambrian, but was reactivated as a result of the Syrian Arc Belt creation in the Turonian age. The faults of this trend were crossed and reactivated by E-W faults of the transverse fault system (Miocene), such as Zarqa Ma'in, Daba'a and Siwaqa faults. They are sub-parallel and dominate the eastern part of the study area, where the thermal wells are located. These faults are mainly located between Siwaqa and Zarqa Ma'in faults and are closely spaced with a variable downthrown in amount (few tens of meters) and direction. The faults of this trend are

25

normal and have extensional nature (Diabat and Masri, 2002). The main faults of this type are Wadi Al Hammam and Masattarat faults. Masattarat Fault has a vertical downthrown of less than 50m to the east.

In the course of the geothermal project of NRA during 2002, some faults and lineaments within the study area were studied using the Controlled Source Audio-Magnetotelluric (CSAMT) method. Figure-2.4, shows the method results across major lineament trending NW-SE parallel to Masattarat Fault at the coordinates 119000N and 256000E.
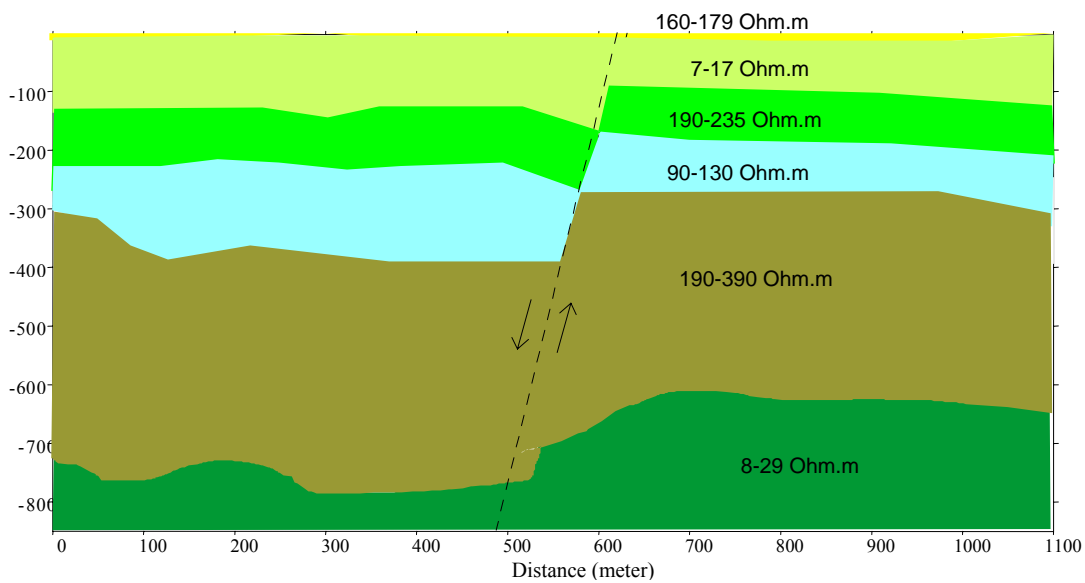
Figure-2.4: CSAMT result across the NW-SE lineament.

2.3.2 Folds

The folding in the study area is of three types: gentle folding associated with regional compression, folding occurring adjacent to the faults and directly associated with drag during faulting and folding in interference structures caused by the interaction of E-W and NW-SE faulting influences. Dips across the fault blocks which are presumed to be away from edge structures, are predictably moderate, with most beds-strikes aligned sub-parallel to the major fault trends. These structural features are illustrating that the faulting and folding are in any case closely associated and have generated in response to the same stress system (Diabat and Masri, 2002).

A major folding feature in Zarqa Ma'in area is the Wadi Zarqa Ma'in syncline, which plunges westwards. The axis is approximately along the wadi and parallel to the Zarqa Ma'in Fault. The syncline can be traced to a point one-kilometer north-east of Muleih village in the southern part of the study area.

There are several prominent domal structures, which form also topographic heights scattering through out the study area.

2.3.3   Paleostress Analysis

In 2002, Diabat and Masri in the course of the geothermal project studied the structures in the eastern part of the study area. They measured about 435 fault-slip data distributed in 24 stations along the major faults (Figure-2.5).

The paleostress analyses indicate two main stress fields in the study area since the upper Cretaceous: the older one is the Syrian Arc Stress Field (SAS) and formed the Syrian Arc System that occurred in Turonian age. It is characterized by E to ESE – W to WNW compression, and corresponding to N to NNE – S to SSW extension. While the younger stress field, Dead Sea Stress Field (DSS), is responsible for the Dead Sea Rift that is still active since the Middle Miocene. It is characterized by N to NNW-S to SSE compression and corresponding to E to ENE–W to WSW extension. The DSS stress field is the one affecting the recent movement in the study area. This can be seen from the interpretation of the paleostress, the NW–SE trend faults such as Wadi Al Hammam, Massttarat and Daba'a faults demonstrates an extensional regime that may allow water mixing between the upper and lower aquifers in the area.
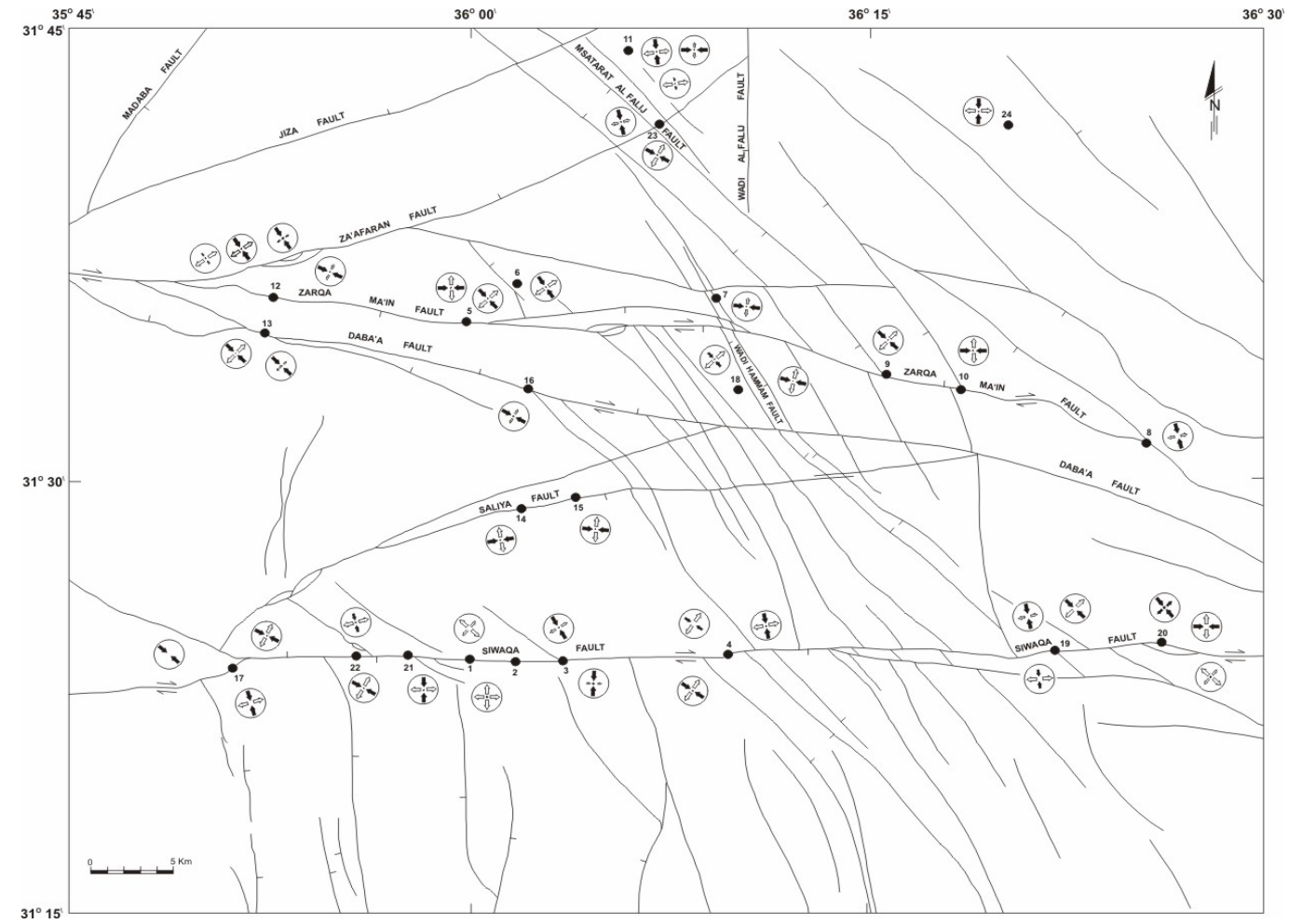
Figure2.5: The paleostress analyses and the field measurements stations (Diabat and Masri, 2002)

3. HYDROGEOLOGY

3.1 General Hydrology of Jordan

3.1.1 Climatic Conditions

Jordan has an area of about 90,000km^2 and its relief is extremely of diverse nature. The western part consists of the world deepest rift; the Jordan Valley, Wadi Araba and the Dead Sea (410m bsl). Eastwards, the highlands range in elevation from about 1000m in the north to around 1200m in the south (Shoubak Mountains). East of the highlands comes the plateau with desert basins (about 500m asl) of restricted drainage. This sharp variation in topography within a small country leads to major differences in its climate. Therefore, the highlands have a semi-arid Mediterranean climate, characterized by cold, wet winter and moderate, dry summer. The plateau (desert) has arid Mediterranean climate, with dry cold winter and hot summer. But the climate in the Jordan Valley and the Dead Sea can be classified as arid climate with hot summer and warm winter.

Along the highlands, temperatures in winter reach a few degrees below zero at night, while in summer as high as 30°C at noon but with relative humidity of 15-30 %, which makes the heat more acceptable.

Temperatures in the Jordan Valley, Wadi Araba and the Dead Sea can rise in summer to 45°C with an annual average of 24°C (Salameh, 1996). In the winter season the temperatures during the day are around 20°C, during the night the temperature can fall down to a few degrees above zero.

On the plateau the temperatures can reach more than 40°C during summer days and drop in the winter nights to a few degrees below zero. Figure-3.1 shows the temperature seasonal distribution in three meteorological stations: Shoubak in the highland, Ghor Es Safi in the Jordan Valley and Ma'an in the plateau (Water Authority of Jordan (WAJ) open files.

Prevailing winds light to moderate (73% occur with a speed less than 10km/h) blow from northwest during summer and from southwest during winter. Hot dust-laden winds blow from the east and south, the Khamasin, occur sometimes during winter and spring.

The mean annual sunshine duration ranges from 8.3 to 9.4 hr in the Jordan Valley, from 8.5 to 9.5 hr in the highlands and from 8.6 to 9.6 in the plateau (The Jordan Climatological Data Handbook,1988).
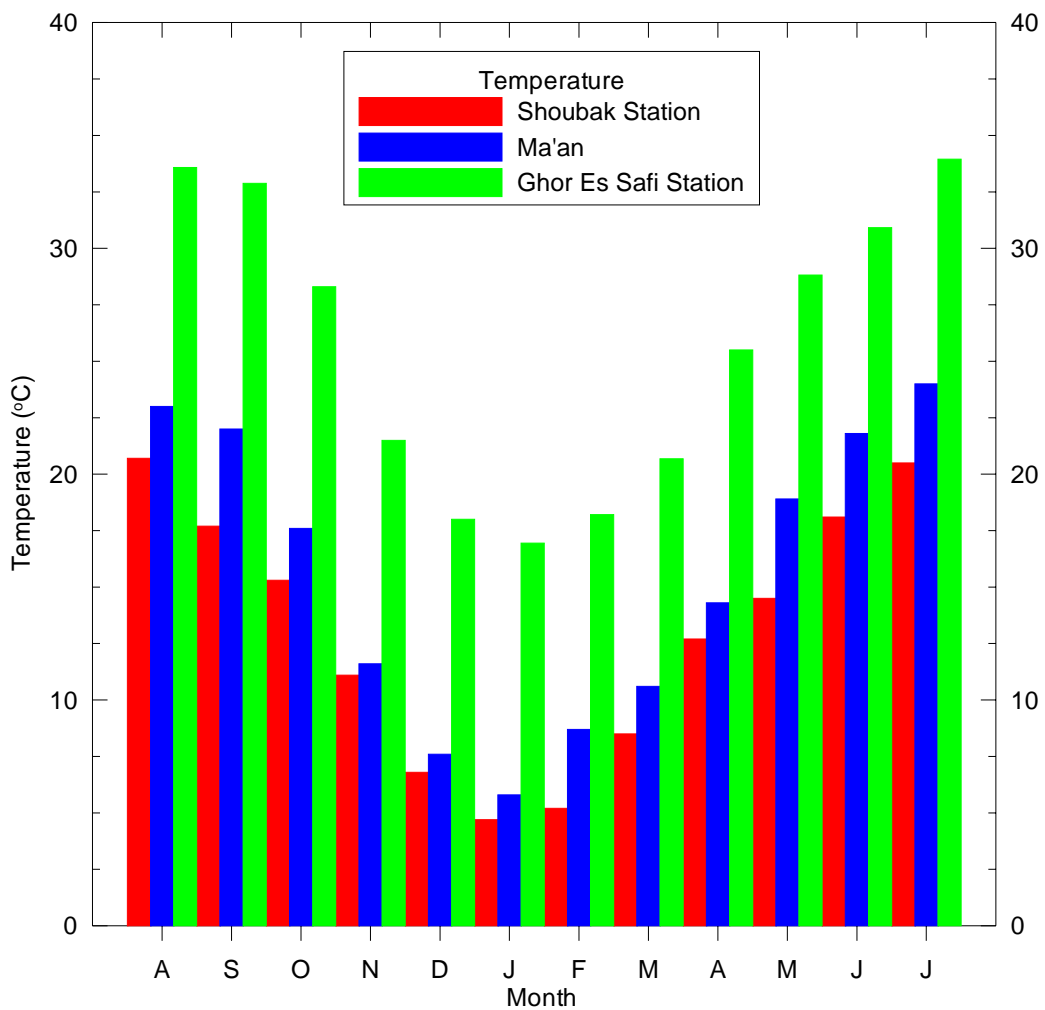
Figure-3.1: Monthly temperature variations between the highlands (Shoubak), the Jordan Valley (Ghor Es Safi) and the deserts (Ma'an)

3.1.2 Precipitation

Precipitation in Jordan is produced by Eastern Europe and Western Mediterranean cold fronts drawn by the Eastern Mediterranean low pressure, so called Cyprus Low. Precipitation falls normally in the form of rainfall, snowfall occurs generally once or twice a year. The distribution of the rainfall reflects the topographic effect of the highlands. The high rainfall zones coincide with the high mountain range east of the Jordan Rift. The rainfall within the highland decreases gradually from north to south. In the north, Ajlun heights receive the highest long-term annual average of 600mm, while Shoubak Mountains in the south receive 300 mm/y as long-term average. To the east of the highlands and more strongly to the west, rainfall decreases rapidly. The rainfall long-term annual average distribution in Jordan is shown in figure-3.2.

The rainy season extends from October to April. But the maximum amount of rain falls usually during January and February. Figure-3.3 shows the monthly average rainfall in three stations: Karak in the highlands, Ghor Es Safi in the Jordan valley and Qatraneh in the plateau (data from WAJ open files). It can be seen from the figure, how the rainfall decreases rapidly from highlands towards the east and the west.

About 80% of the Jordan's area receives an annual average rainfall of less than 100mm, 12.5% between 100-200mm, 3.8% between 200-300mm, 1.8% between 300-500mm and only 1.3% receives more than 500mm/y. Figure-3.4 shows the annual average rainfall percentages distribution. The average amount of water falling all over Jordan territories is 7200 MCM/y (Salameh, 1996).

The potential evaporation is highly affected by the prevailing climatic conditions namely high temperatures. It ranges from about 1600 mm/y in the extreme northern western edge of the country to more than 4000 mm/y in the Aqaba and Azraq areas.
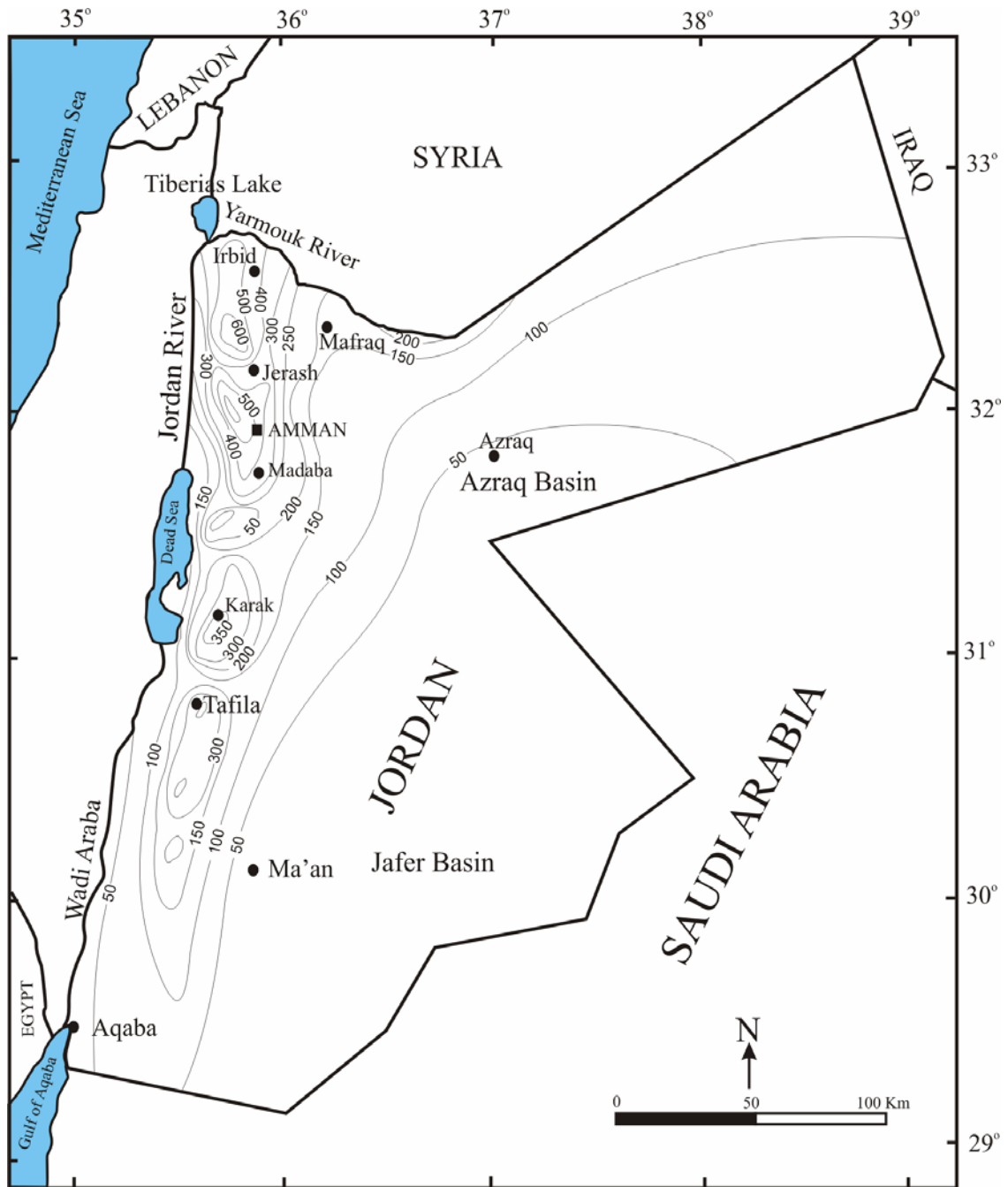
Figure-3.2: Rainfall long-term (1938-1988) average distribution (after WAJ open files)
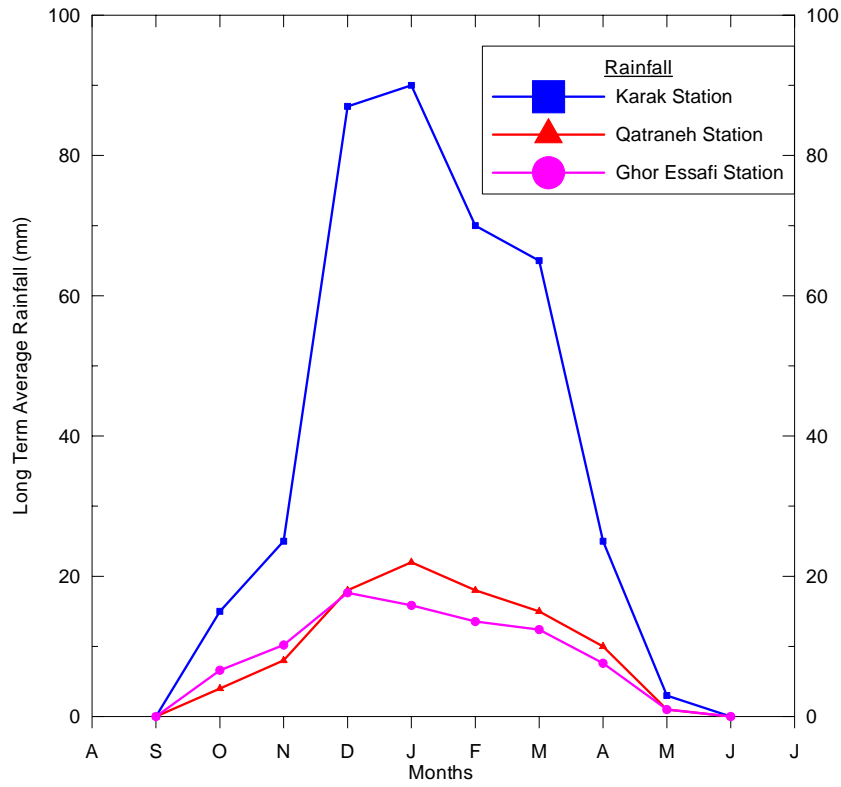
Figure-3.3: The differences in monthly average rainfall between Karak station in the highlands, Ghor Es Safi in the Jordan Valley and Qatraneh station in the Plateau
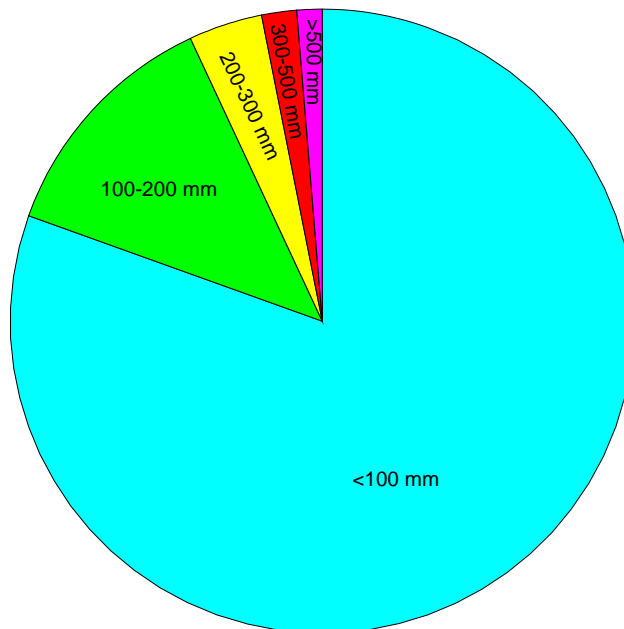
Figure-3.4: The annual average rainfall percentages distribution over Jordan territories (data from Salameh, 1996)

3.1.3 Surface Water Resources

Surface water in Jordan is distributed in fifteen basins as permanent and flood flows (Figure-3.5). The Yarmouk River Basin is the major contributor; it contributes 40% of the total surface water in Jordan including the water from the Syrian part of the basin.

Other major basins include Zarka, Mujib, Dead Sea, Hasa, Wadi Araba and side wadis of Jordan River. Table-3.1 shows the total flow and the area of the main surface water basins.

TABLE-3.1: Main surface water basins in Jordan (after Belbeisi, 1992 and Salameh, 1996).

Basin	Total flow[1] MCM/Y	Total flow[2] MCM/Y	Area[2] (Km^2)
Yarmouk	285	360	6790
Jordan Valley	21.7	-	-
N. Jordan River side wadis	49.98	28 (Wadi Arab) 10 (Wadi Ziglab)	267 106
S. Jordan River side wadis	30.34	5.71 (Wadi Shueib) 6.4 (Wadi Kafrain)	180 189
Zarka River	59.18	64.88	4025
Dead Sea	61.15	30 (W. Zarqa Ma'in) 18 (Wadi Karak) 30 (Wadis in between)	272 190 972
Mujib	83.64	83	6596
Hasa	36.44	34	2520
N. Wadi Araba	18.2	26	2938
S. Wadi Araba	5.6	1	1278
Southern Desert	2.2	1.5 (W. Yutum)	4400
Azraq	27.4	27	11600
Sirhan	10	-	15155
Hammad	13	10	19270
Jafer	11.29	15	12200

(1) M. Belbeisi, 1992. (2) E. Salameh, 1996

Several Dams and irrigation projects have been established on some of those sources, in order to use water before it drains into the Dead Sea. Table-3.2 shows the names and the capacity of the constructed dams in Jordan.

TABLE- 3.2: Dams in Jordan (after Salameh, 1996 and Abed, 2000)

Dam name	Total capacity (MCM)	Location
King Talal	89	Zarka River
Wadi Al Arab	20	Wadi Al Arab
Sharhabeel (Ziglab)	4.3	Wadi Ziglab
Shueib	2.3	Wadi Shueib
Kafrain	7.5	Wadi Al Kafrain
Al Waleh	9.3	Wadi Al Waleh
Al Mujib	35	Wadi Al Mujib
Tanoor	16.8	Wadi Al Hasa
Al Karameh	55	Wadi Al Mallaheh
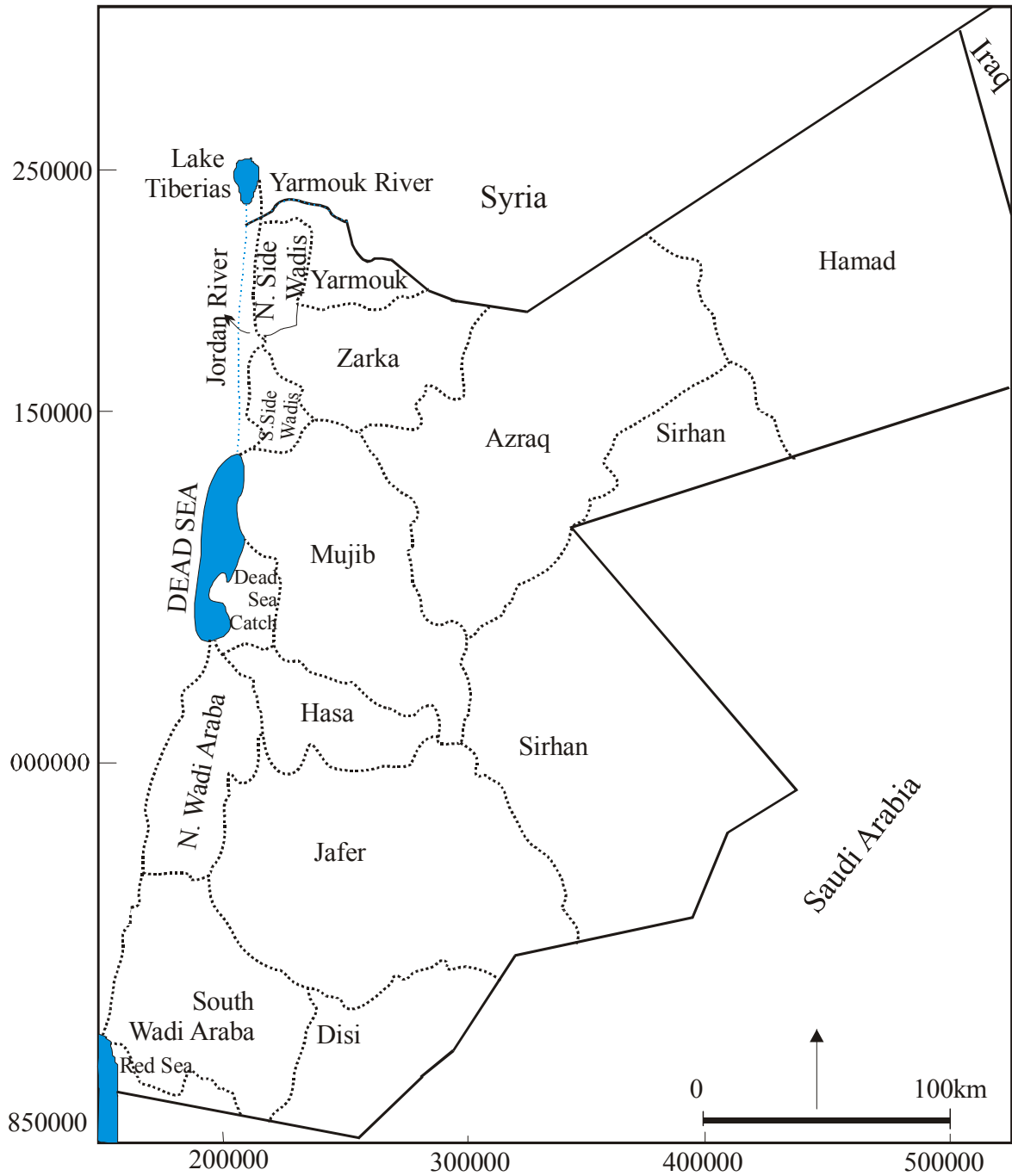
Figure-3.5: Surface water basins in Jordan (after WAJ open files)

3.1.4 Groundwater Resources

3.1.4.1 Groundwater Aquifers

Ground water aquifers of Jordan are subdivided into three main complexes:

1- Deep Sandstone Aquifer Complex

This complex consists of two aquifers: the Disi Sandstone Aquifer and the Kurnub/Zarqa Aquifer.

The Disi Aquifer (Paleozoic) is the oldest and the deepest water bearing sediments in Jordan. It crops out only in the southern part of the country, forming the fresh water aquifer of the Upper Wadi Yutum, Qa' Disi- Muddawara region. It underlies most of the areas in Jordan. But a large part of it is likely to contain mineralized groundwater.

The Kurnub/Zarka Aquifer (Jurassic-Lower Cretaceous) is also a sandstone aquifer extending over much of the country and overlying the Disi aquifer. It crops out along the lower Zarka River basin and along the escarpment of the Dead Sea, Wadi Araba and Disi region. Fairly good yields have been obtained from the aquifer, but direct recharge is limited due to its small outcrop area. The groundwater in this aquifer apart from the recharge areas is highly mineralized.

These two aquifers are separated by Khreim Group, which often acts locally as an aquitard. But on a large scale, they are interconnected through the Khreim Group and are considered as a single basal aquifer and hydraulic complex (Salameh and Bannayan, 1993).

2- Amman – Wadi Es Sir Aquifer Complex (B_2/A_7)

B_2/A_7 aquifer of the Upper Cretaceous age is the most important aquifer system in Jordan. It is composed mainly of limestone and hydraulically separated from the underlying sandstone aquifer by marls and marly limestone of the A_{1-2}, A_3, A_4 and A_{5-6} formations. The B_2/A_7 crops out in the western highlands where it has the highest groundwater recharge rates in the country. To the east, the aquifer is confined by thick marl layers of Upper Cretaceous and Lower Tertiary age. After infiltration, the groundwater flows partly to the western escarpment within the faulted blocks and mainly to the east forming a groundwater divide lying 20-30km to the east of the Dead Sea escarpment. The easterly-directed groundwater infiltrates through the aquitard (A_{1-6}) down to the deep sandstone aquifer complex (Salameh and Udluft, 1985).

37

3- Shallow Aquifers Complex

This complex consists of two main aquifers:

The Basalt aquifer consists of the basalts extended from the Syrian Jabel Druz area southwards to the Azraq and Wadi Dhuleil region. Recharge to this aquifer is taking place in the elevated area of Jabel Druz. The groundwater flows radially from Jabel Druz to all directions and its quality is quite good.

The sedimentary rocks and alluvial deposits of the Tertiary and Quaternary form local aquifers. They are distributed all over the country, but are concentrated in the eastern deserts, Wadi Araba, Jordan Valley, Jafer Basin and the Yarmouk River area (Salameh and Bannayan, 1993).

3.1.4.2 The Groundwater basins

Groundwater is the main water resource in many parts of Jordan, and it is the only source in others. Jordan's groundwater comprises both renewable and non-renewable resources, distributed among twelve basins (Figure-3.6).

Studies on Jordanian aquifers have concluded that the total safe yield for the renewable resources is 275 MCM/y (Table-3.3). The non-renewable resources are found mainly in the Disi sandstone aquifer, which may have a safe yield of 125 MCM/y for 50 years.

TABLE- 3.3: Groundwater resources in Jordan and their safe yields (Belbeisi, 1992).

Basin or well field	Safe yield (MCM/y)
Yarmouk Basin	40
Jordan River side wadis (N. Jordan Valley)	15
Jordan River Valley	21
Zarka River Basin	87.5
Dead Sea, including Mujib Basin	57
North wadi Araba	3.5
South Wadi Araba	5.5
Azraq	24
Jafer Basin	9.0
Sirhan Basin	5.0
Hammad Basin	8.0
Total Renewable	**275.5**
Disi- Muddawara	125
Jafer	18
Total non-renewable	**143**
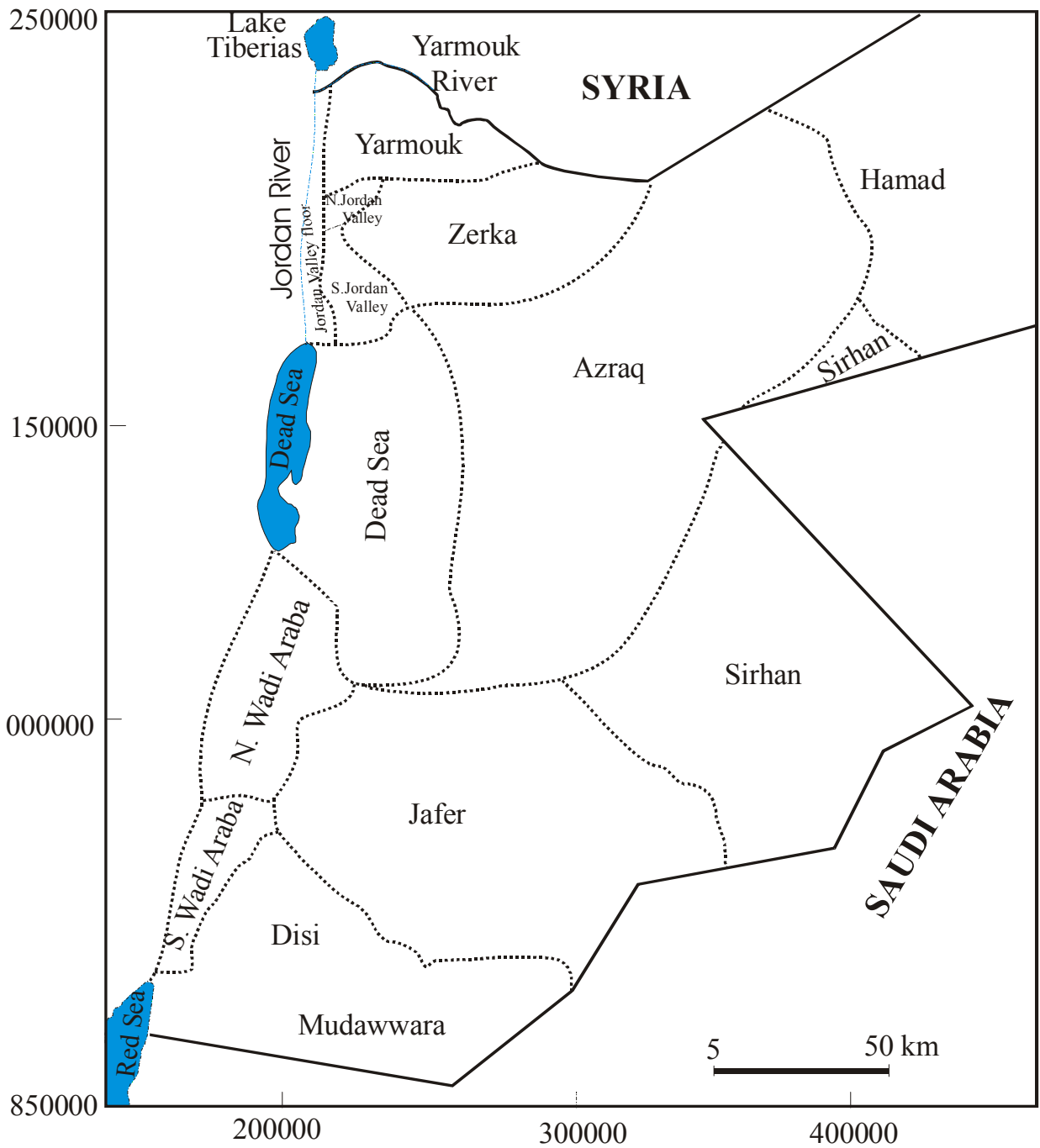
Figure-3.6: Groundwater basins in Jordan (after WAJ open files)

3.2 Hydrology of the study area

3.2.1 Topography

The study area extends from Amman in the north to Wadi Mujib in the south. The Dead Sea forms the western boundary, while the surface water divide between Mujib and Azraq basins is the eastern border of the area.

The three main topographic features of Jordan are found in the study area. The highlands along the Dead Sea escarpment, the area to the west of the escarpment, which is characterized by steep slopes and the elevation sharply, decreases down to 410m bsl at the Dead Sea coast. To the east of the highlands most of the study area belongs to the eastern highlands toes and the plateau feature is found only in the far eastern parts of the study area.

Wadi Waleh/Heidan and Wadi Zarqa Ma'in are the main wadis running throughout the study area, roughly in east-west direction. Figure-3.7 shows the study area and the main wadis.
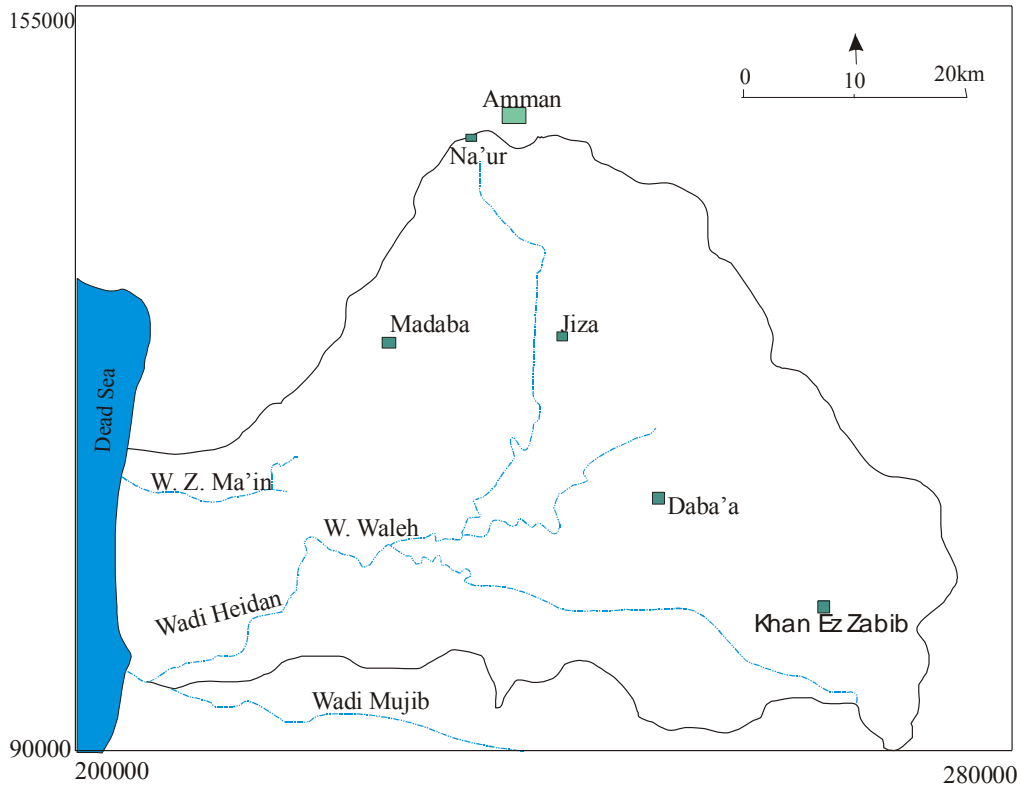
Figure-3.7: The study area and its main wadis

3.2.2 Climate

The study area lies within the Mediterranean bioclimatic region and its climate is characterized as semi-arid to arid. An essential feature of this climate is receiving rainfall during the cool winter season (October–April) and having very marked drought summer.

The study area experiences a marked annual and diurnal variation in temperature. The monthly and annual air temperature for the meteorological stations show that January is the coldest month and August is the hottest. The highlands enjoy a climate considerably cooler than that of the Dead Sea coast and the eastern parts of the study area. The mean annual temperature for the highlands is 16°C, and it is 22°C in the lower parts of the study area including the Dead Sea coast. Figure-3.8 (A,B) shows the seasonal and regional temperature variations within the study area (data from WAJ open files). Part (A) shows that the mean monthly temperature in Madaba station is higher than that in Jiza station in winter season while it is lower in the summer season. This is because Jiza is located in the Plateau and Madaba in the Highlands. It can be seen from part (B) that the mean monthly temperature increase from the north (Na'ur) to the south (Wadi Waleh) within the study area.

West to north-west winds prevail in winter seasons and east, north-east prevail in summer season with speed of 3-7km/h. The relative humidity ranges from 39% in June to 80% during January (Jeries, 1986).

High evaporation rates due to high temperatures prevailing in most parts of the study area. Salameh (1996) computed the actual evaporation in 1980 as 80% of the rainfall in the highlands and up to 97% in the eastern parts of Jordan. The potential evaporation in the highlands is around 1600mm/y. It increases eastwards to about 2000mm/y (Daba'a town) and westwards to 2500mm/y along the Dead Sea coast (Salameh, 1996).

41
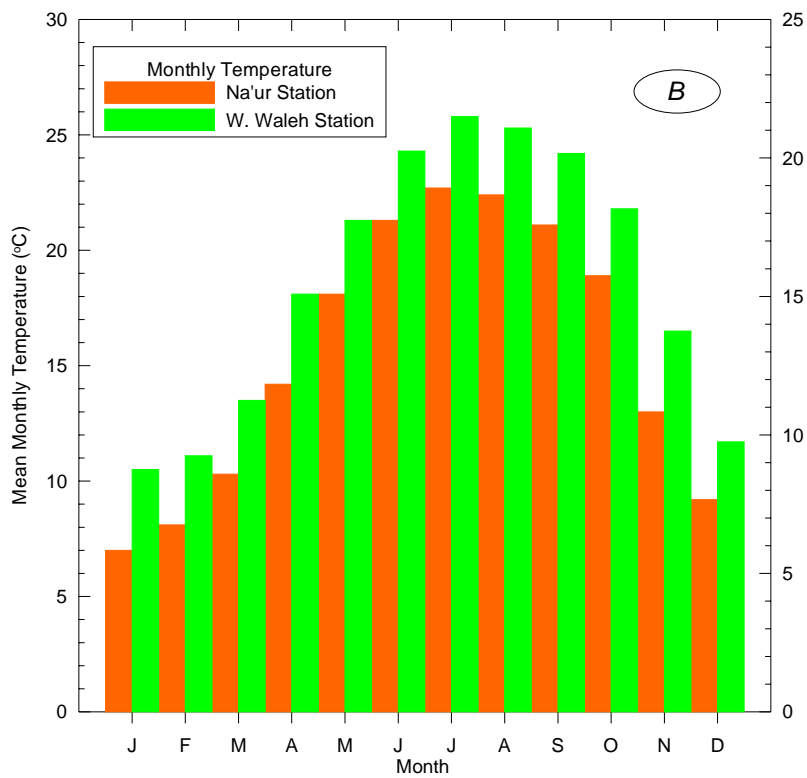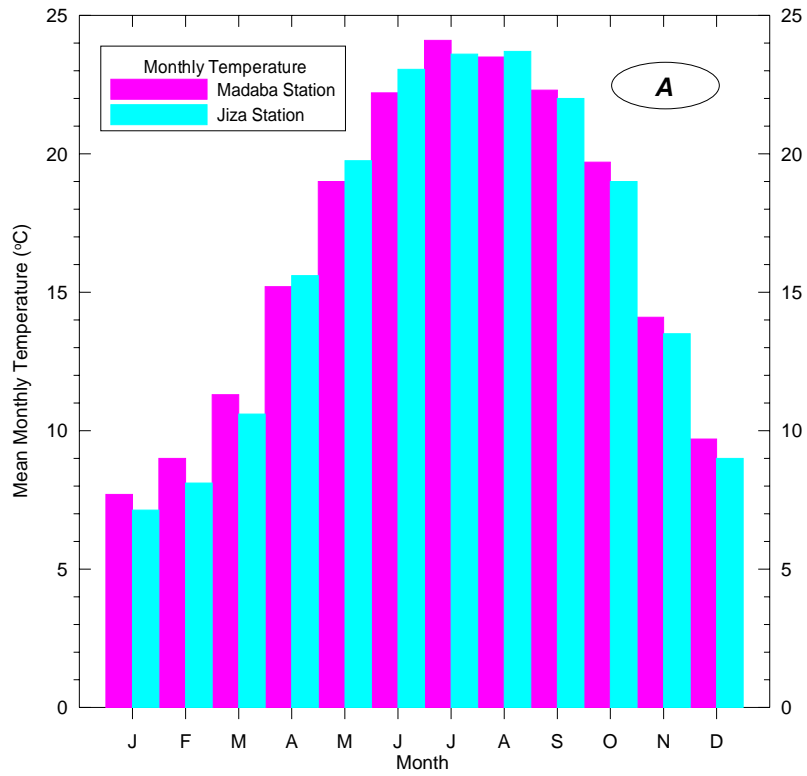
Figure-3.8 (A, B): Seasonal and regional variation in temperature within the study area.

3.2.3 Rainfall

Several rainfall stations are located in the study area, the location, type and altitude of the main ones are shown in table-3.4.

TABLE-3.4: Main Rainfall stations in the study area (WAJ open files).

Station Name	Coordinates (PG)		Altitude (m)	Station Type
	East	North		
Sahab	245000	142500	830	Daily
Madaba	225500	125000	785	Recorder
Wadi Waleh	223000	107500	450	Daily
Dhiban	224000	100800	745	Recorder
Um El Rasas	237500	101000	750	Daily
Daba'a	250500	111600	750	Daily
Jiza	242000	125000	715	Daily
Na'ur	228500	142500	910	Daily
Ma'in	219900	120800	880	Daily

The marked difference in elevations within the study area results in considerable variations in amount and distribution of rainfall.

The rainfall long-term average distribution over the study area is shown in figure-3.9. It can be seen from the figure that rainfall decreases rapidly to the west and to the east-southeast. The highest average rainfall (400 mm/y) is seen in the extreme northwestern edge of the study area, near Amman. Decreasing to less than 150 mm/y in the southeastern areas (Khan Ez Zabib area), as well as in the western part along the Dead Sea coast. Figure- 3.10 (a, b) shows the rainfall decrease from west (Madaba) to the east (Jiza) and from north (Jiza) to southeast (Khan Ez Zabib).

Most of the study area receives less than 200 mm/y as long-term average rainfall. The average all over Wadi Waleh sub-catchment is about 189 mm/y (Khdeir, 1997), while it is higher than that in Wadi Zarqa Ma'in sub-catchment.
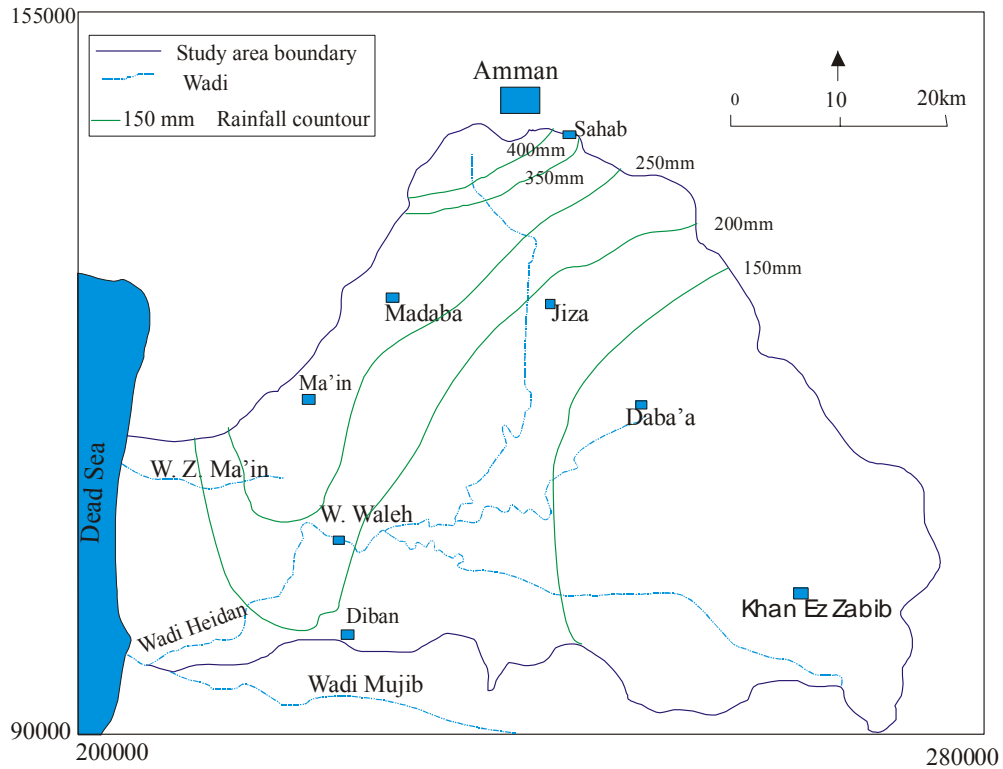
Figure-3.9: The long term average rainfall distribution in the study area
(after WAJ open files).
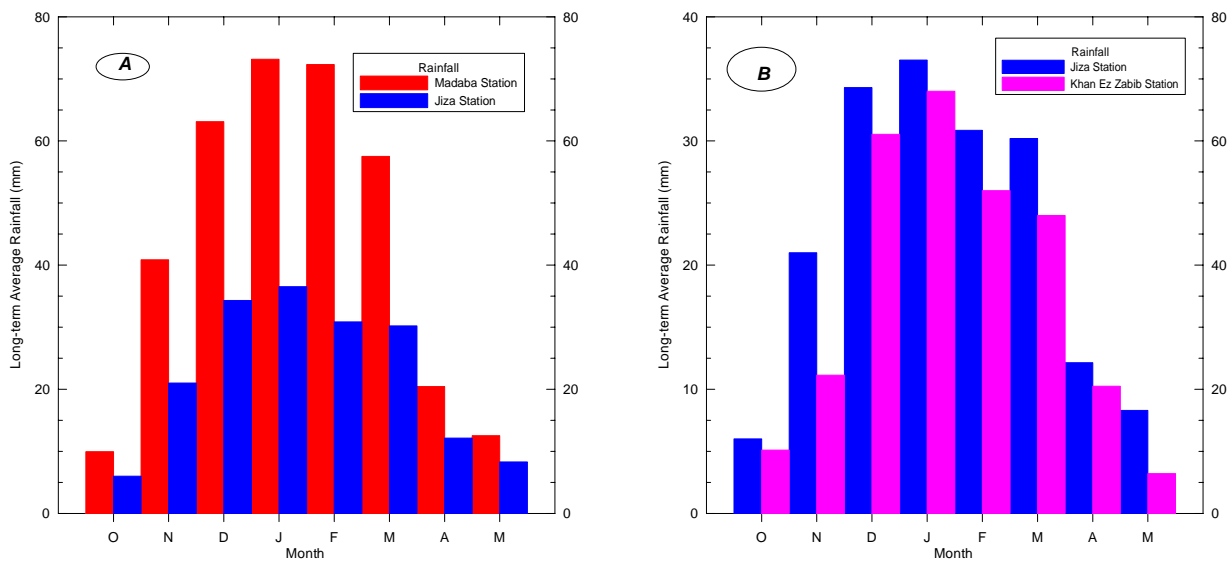
Figure-3.10: Rainfall decrease from west to east (A) Madaba-west, Jiza-east; and from
north to south (B) Jiza-north, Khan Ez Zabib-south (data from WAJ open files).

3.2.4 Stream discharge

The study area drains westwards to the Dead Sea via two major wadis; Wadi Zarqa Ma'in and Wadi Waleh and their numerous tributaries. The tributaries are dry except for a short period after rainfall. Perennial base flow is seen only on the lowest sections down stream of Wadi Waleh/Heidan and on the lowest parts of Wadi Zarqa Ma'in from a short distance east of the Zarqa Ma'in thermal springs.

The base flow in the two wadis is derived from a number of springs and seepages. These two westwards trending wadis have cut down to intersect zones of saturated aquifers underlying the highlands and perennial flow is maintained by spring discharges. The lower part of Wadi Waleh/Heidan drains base flow with an annual groundwater flow of 23 MCM/y. The occurrences of the base flow in Wadi Waleh/Heidan is mainly dependent on the upper aquifer (B_2/A_7), it discharges about 80% of the total base flow while the rest is supported by outflows from the lower aquifer. The discharge of Wadi Waleh/Heidan in the rainy season referred to as the flood flow is estimated at 29 MCM/y (Khdeir, 1997). Part of the base flow along Wadi Waleh/Heidan is used in irrigation before it joints the base flow of Wadi Mujib into the Dead Sea.

There are more than 100 springs and many seepages along the lower reaches of Wadi Zarqa Ma'in. Most of these are thermal water discharge outlets with temperatures ranging from 30 to $63^{o}C$. The total discharge of Wadi Zarqa Ma'in into the Dead Sea amounts to 23 MCM/y; only 3 MCM/y of which are flood flows. The lower aquifer system, mainly the Kurnub Group, is supporting the base flow along this wadi. Part of the base flow in the wadi has been used in bathing and irrigation before it reaches the Dead Sea. Recently, about 15 MCM/Y is planned to be treated and used for drinking purposes.

3.3 Hydrogeology of the study area

The study area consists of two sub-catchments; Wadi Waleh, which forms the northern third (2030 km^2) of the Wadi Mujib groundwater catchment and Wadi Zarqa Ma'in to the north west of Wadi Waleh sub-catchment with an area of 272 km^2 (Figure-1.1).

The Paleozoic, Mesozoic and Cenozoic sedimentary rocks with some basic intrusions underlie the area. The Mesozoic sequence especially Cretaceous carbonate sedimentary rocks are dominant in the study area with a thickness of about 1000m.

The Middle to Lower and the pre-Cretaceous sedimentary and intrusive rocks crop out along the valley slopes in the lower reaches of Wadi Waleh and Wadi Zarqa Ma'in.

The Tertiary carbonate rocks are found in the eastern parts of the area. Pleistocene basalt flows associated with plugs, cones and vents are present in the lower reaches of Wadi Zarqa Ma'in.

The Paleozoic to Cenozoic sedimentary rocks in the basin generally have the structure of monoclinal flexure at low angles, disturbed by faults. The major trending E-W fault is the Siwaqa fault zone just at the border of the southern edge of the study area. It bisects the groundwater in Wadi Mujib catchment into two parts; the southern and northern part that is of interest of this present study. Within the study area Zarqa Ma'in fault zone is the major E-W trending fault.

3.3.1 Aquifers

The Mesozoic sediments in Jordan form a sequence of aquifers and aquitards (Table- 3.5). Four aquifer units (B$_2$/A$_7$, A$_4$, A$_{1-2}$ and Kurnub Group) have been recognized. Among them, the Amman-Wadi Es Sir (B$_2$/A$_7$), which has regional and economic importance. It extends throughout much of the entire country and varies considerably in lithology, depth of occurrence and hydraulic properties. The Kurnub sandstone group and the sandstone of older ages (Zarqa, Ram and Disi groups), form the deepest aquifer system in Jordan. The other two aquifers; A$_4$ and A$_{1-2}$ are considered as important local aquifers in North Jordan. Therefore, the Mesozoic sequence in the study area is grouped into two major aquifers; the Upper Aquifer (B$_2$/A$_7$) and the Lower Aquifer (the sandstone of the Kurnub and older ages), and one major aquitard (A$_{1-6}$), which separates these two major aquifers.

TABLE-3.5: Aquifers and aquitards within the Lithological section in the study area

Age	Group	Formation	Hydrogeology
Tertiary	Belqa 350m	B4: Umm Rijam	AQUITARD
Upper Cretaceous		B3: Muwaqqar Chalk-Marl	
		B2b: Al Hasa Phosphorite	UPPER AQUIFER
		B2a: Amman Silicified Limestone	
		B1:Wadi Umm Ghudran	
	Ajlun 500m	A7: Wadi es Sir	
		A5-A6: Shueib	AQUITARD
		A4: Hummar	
		A3: Fuheis	
		A1-2 Na'ur	
Lower Cretaceous	Kurnub 220m	K: Kurnub	LOWER AQUIFER
Permo-Triassic	Zarqa 170m	Dardur Sandstone	
		Ma'in Sandstone	
		Umm Irna Sandstone	
Middle to upper Cambrian	Ram 250 m	Umm Ishrin Sandstone	
Lower Cambrian		Burj Dolomite-shale	

Based on the geological maps, well records and the hydraulic model of Central Jordan (Salameh and Udluft, 1985) a hydrogeological cross-section was constructed in E-W direction within the study area (Figure-3.11). The figure shows the two main aquifer complexes and their potentiometric surfaces.
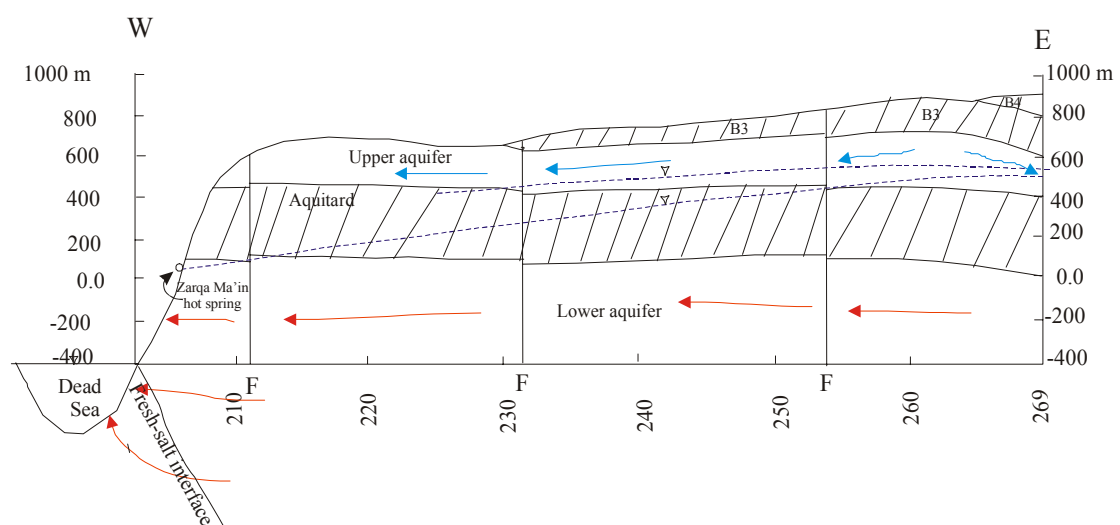
Figure-3.11: The conceptual hydrogeological model of the study area

3.31.1 The Upper Aquifer System (B$_2$/A$_7$)

This is the most important and extensive aquifer system in the study area. It is composed of Wadi Es Sir Formation (A$_7$), including Khureij Limestone Formation of the Ajlun Group of Turonian age and Wadi Ghudran and Amman formations (B$_1$ and B$_2$) of the Belqa Group of Campanian age.

The B$_2$/A$_7$ materials are limestones, chert-limestones and marl intercalations. The upper part contains phosphatic limestone and silicified phosphate. The middle part (B$_1$) consists of marl and chalky marl and acts as a minor aquitard within the system. But due to its limited lateral extend the B$_2$ and the A$_7$ are hydraulically connected.

The aquifer crops out in the highlands in the western part of the area, where rainfall is relatively high. Despite of that, it is unsaturated due to the lowering of the potentiometric surface by the Rift and the major wadis deeply intersecting the area. The aquifer thickness ranges from 170 to 327m.

The aquifer is overlain by Muwaqqar Chalk Formation (B$_3$) and Umm Rijam Limestone Formation (B$_4$) in the eastern parts of the study area and underlain by thick impervious marl to marly limestone layers of the Shueib Formation (A$_{5-6}$) allover the study area.

3.3.1.1.1 Recharge and discharge of the aquifer

Most of the recharge enters the (B$_2$/A$_7$) aquifer in the structurally high outcrop areas along the western highlands, where rainfall is relatively high, and where the aquifer crops out at the west flank of the mountains blocks of Amman, Madaba and Ma'in.

Khdeir (1997) computed the average rainfall as 144.8 MCM/y for the 5 years period, 1980-1985, within the Wadi Waleh sub-catchment. About 11% of this amount of rainfall (18.3 MCM/y) enters the aquifer as an average direct recharge. Also, he computed for the same period, 2.2 MCM/y as indirect recharge and 7.3 MCM/y as lateral recharge into the area from the adjacent high recharge mounds. Therefore, the total annual recharge to the aquifer sums up to 27.66 MCM/y.

Rimawi (2004) computed the average rainfall as 357 MCM/y for the 28 years period, (1975-2003), within the Wadi Waleh sub-catchment. About 6% of this amount of rainfall (21.5 MCM/y) enters the aquifer as an average direct recharge.

In addition, the relation between the thermal boreholes and some of the faults in the area suggest strongly an upward flow of the thermal water from the lower aquifer to the upper one via these faults, which means addition flows into the aquifer to be added to the calculated amounts mentioned above.

The main outflows from the aquifer are manifested in the form of springs. Most of the large springs that discharge regional flows within Wadi Waleh sub-catchment are located in the lower reaches of the Wadi Waleh/Heidan. The major group of springs with annual average flow discharge of 15 MCM/y is located in the wadi where ground elevation is about 350m asl, 5km westwards from Waleh bridge, where the Kings Highway crosses the wadi. Further to the west at the confluence with Wadi Mujib the base flow increases to 23 MCM/y.

The total recharge (direct and indirect) to the (B_2/A_7) aquifer, in Zarqa Ma'in sub-catchment, was given by Abu Ajameih (1980) as 6 MCM/y. Only 0.7 MCM/y appear as base flow of springs in the upper reaches of wadi Zarqa Ma'in and the rest leaks downward into the lower aquifer. The discharged base flow mix with the thermal water discharges from the lower sandstone aquifer, further downstream.

About 300 wells were drilled in the study area, mostly by the private sector for agricultural purposes. Others were drilled by the government for domestic uses, as well fields; Qastel, Waleh, Heidan,…etc. The pumping from all wells during the last five years averaged about 35.6 MCM/y. The pumping quantities from each well during the years 1999-2003 are given in appendix-1.

3.3.1.1.2 Aquifer Hydraulic properties

The hydraulic properties of any aquifer are the main factors governing the amount of water in storage, the rate at which water moves through the aquifer, and the rate and the areal extent of water level declines caused by groundwater abstraction. The essential hydraulic

features for aquifer assessment include; the saturated thickness, storage capacity and transmissivity. These have been estimated from rock fabric, borehole drilling, geophysical and pumping test data. A data set of about 300 wells (Appendex-2) spread through out the study area is used to describe the hydraulic properties of the B_2/A_7 aquifer. The source of these data is the data base of the Water and Irrigation Ministry.

The hydraulic conductivity values were obtained from a few pumping test (Table-3.6). The majority was obtained from the specific capacities values. Specific capacities ($m^3/h/m$) were transformed to transmissivities (m^2/d). The hydraulic conductivity values gained by dividing the transmissivities by the saturated thickness taped in the wells and expressed in m/s (WAJ open files and Khdeir, 1997).

The data set shows that the aquifer has hydraulic conductivity values ranging from 1 E -3 to 1 E -7 m/s with an average of 2.7 E –5 m/s. The wide range in the hydraulic conductivity values is related to karst features, including enlarged joints, sinkholes, caves and solution breccias that developed in and around the fault zones. The transmissivities values differ widely from one well to another and this is due to the wide range in permeability rather than the variation of the saturated thickness. Transmissivity varies from very low values, as low as 2 m^2/d to very high values (51000 m^2/d). But, the majority of the values are less than 120 m^2/d.

TABLE-3.6: Pumping test data in the study area (after Khdeir, 1997).

Well name	Coordinates E N	Durat-ion (hrs)	Saturation thickness (m)	Specific capacity ($m^3/h/m$)	Trans-draw down (m^2/d)	Transmi-sivity recovery (m^2/d)	Hydr-aulic conduc. (m/d)
Pumping tests carried out by Parker 1970							
PP80	232830 111160	3.25	89	4.72	43.4	-	1.4 E-4
PP85	238380 108460	48	121	0.48	15	12.9	3.3 e-5
S70	249800 104060	34	48	11.04	210	608	2.4 E-3
Pumping tests carried out by JICA, 1987							
T1	233910 104560	72	167	7.2	-	189	3.1 E-4
T2	251450 96690	72	93	0.8	-	24	7.2 E-5
Pumping tests, WAJ open files							
Q11	239250 130700	-	43	43.5	1368	1477	9.2 E-3
Q12	238950 125850	-	150	0.63	264	-	4.9 E-4
Q14	239000 131500	-	135	55.8	1557	-	3.2 E-3
ER1	241100 121950	-	141	81	4660	-	9.2 E-3
W5	220810 107700	-	193	4.6	46	-	6.7 E-5
W13	224930 106990	-	129	35	684	-	1.5 E-3

3.3.1.1.3 Groundwater Flow in the aquifer

The groundwater flow pattern in the upper aquifer system within the study area is strongly governed by several features. The most important are; the recharge mounds, the geological structural setting, the presence of Wadi Waleh/Heidan, Wadi Zarqa Ma'in and the Dead Sea, being the final base level for all flows. From the recharge mound (Amman-Madaba), where the high hydraulic heads are found, the major part of the groundwater flows southwards to Jiza region then southwestwards along the main drainage system of Wadi Waleh/Heidan, where the major outflows from the aquifer occur as spring discharge in the lower reaches of the wadi. There is a direct hydraulic connection between the base flow in the wadi and the aquifer in the area between elevations of 250–450m asl.

Other part of the groundwater in this mound flows directly southwestwards along the main drainage of Wadi Zarqa Ma'in. Also, some groundwater flows from this mound to the east towards Azraq Basin.

The Siwaqa Fault at the southern boundary of the study area is known as a barrier preventing the groundwater flow from the southern part of Mujib basin to the study area (northern part). But it seems that it allows some flow from Karak mound into Khan Ez Zabib area in the southern eastern part of the study area. This explains the presence of a small potentiometric high in that area.

Based on water level measurements in the area before the start of the heavy pumping; before 1985, a water level contour map was constructed (Figure-3.12). It can be seen from the map that the groundwater flows from the recharge areas, Amman-Madaba, towards south-southeast, to Jiza areas. A small groundwater flow comes from Karak recharge mound into Khan Ez Zabib area in the southern eastern part of the study area and flows mainly northwestward and partly to the east towards Azraq basin. Within the study area the groundwater flows from the two recharge mounds, join together and flow westwards along Wadi Waleh. Similar flow pattern in the area was mentioned by Jeries (1986). In Wadi Zarqa Ma'in sub-catchment, the figure shows that the groundwater flows from north to southwest towards Wadi Zarqa Ma'in.

As it appears from the different directions of groundwater flow, there are two groundwater divides: the first, in the western part and separate the Wadi Zarqa Ma'in sub-catchment from the Wadi Waleh sub-catchment. It is more or less the same as the topographic divide between the two wadis. The second lies in the eastern part and runs nearly north-south, to the west of the topographic divide with a considerable distance.

Water table measurements in the observation wells, spread through the area, were conducted in October 2003 and used in constructing a water level contour map (Figure 3.13). The map shows that the groundwater level has been lowered at least by 20m after almost 20 years of pumping. In the southeastern parts, where the wells are concentrated, the water level declined by up to 40 meters.
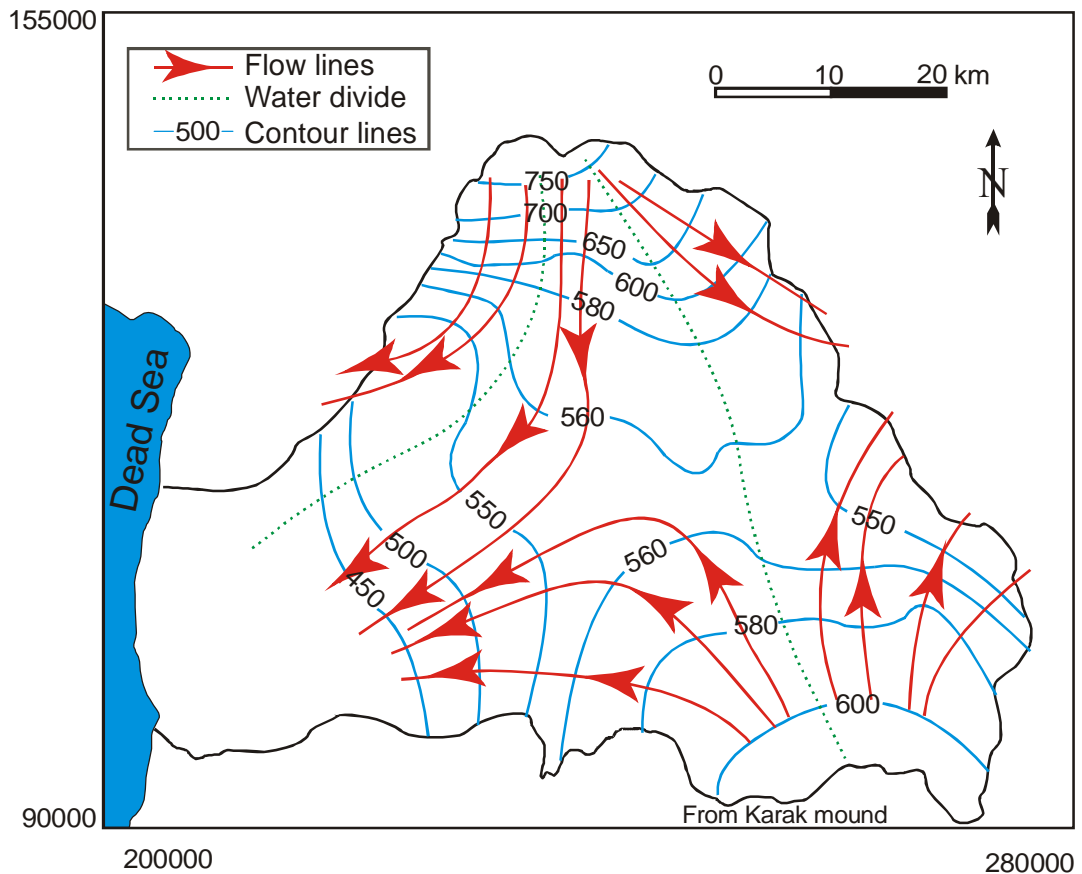
Figure-3.12: Water level contour map based on water level measurements in 1985
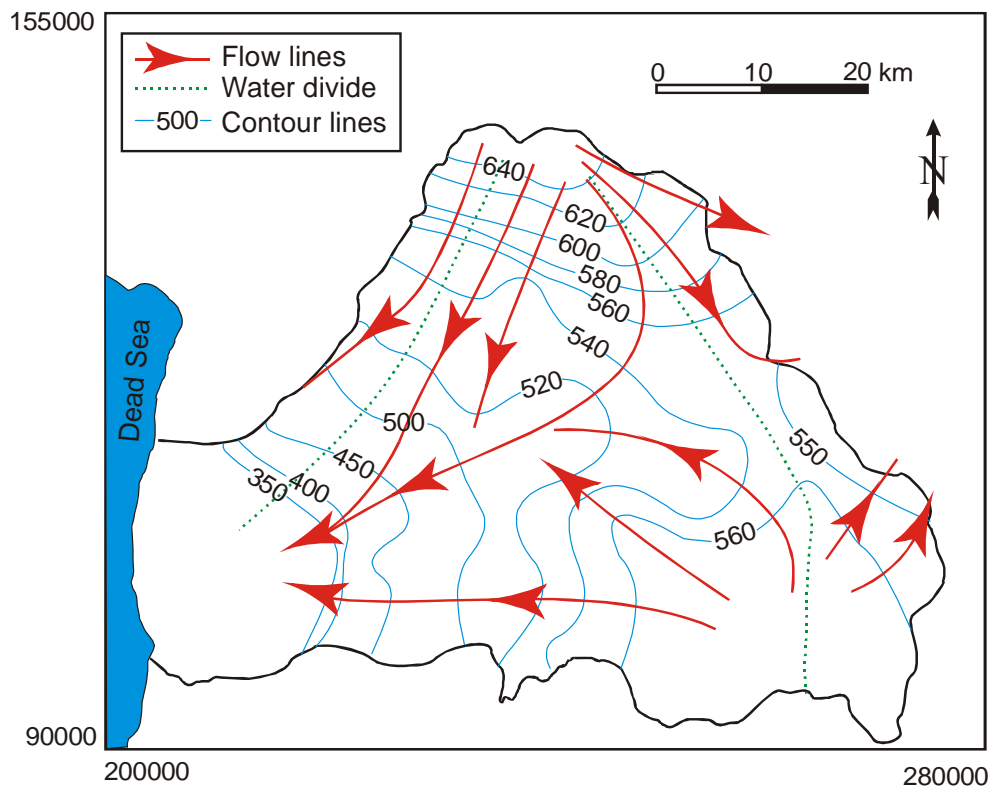
Figure-3.13: Water level contour map based on water level measurements in 2003

3.3.1.2 The Lower Sandstone Aquifer

The aquifer system includes the Kurnub Group sandstone and the Lower Zarqa sandy shale and sandstones together with the underlying Cambrian sandstone. It crops out along the Dead Sea Shore and in the lower reaches of Wadi Zarqa Ma'in and Wadi Waleh/Heidan. The thickness of this aquifer system is more than 600m in Wadi Zarqa Ma'in. The predominant rock constituent is sandstone. But due to the presence of shale and clays, the aquifer becomes extremely complex with many differences in permeability in the lateral and vertical directions. The impermeable zones are of relatively limited lateral extent and individual aquifers within the system are to some extent interconnected.

In Zarqa Ma'in area the lower Zarqa shale and clays form a local aquiclude confining the underlying saturated Cambrian sandstone. This in turn forms a local artesian aquifer in the Cambrian in which the geothermal water is believed to occur.

The Zarqa shale and clays is absent in most parts of the study area, therefore, the whole sequence can be treated as one hydraulic connected aquifer. The average permeability of the whole aquifer is 4.48 E -5 m/s (Salameh & Udluft, 1985).

The lower aquifer sandstones are exposed in the low rainfall areas along the Dead Sea coast. So, direct recharge to the aquifer within the study area is limited to these outcrops and can be neglected. The main recharge source to the lower aquifer is the downward leakage from the upper aquifer system in the eastern parts of Jordan. The major outflow from the aquifer is the thermal springs in Zara and Zarqa Ma'in areas. The total annual discharge as base flow from the aquifer in Wadi Zarqa Ma'in is about 20 MCM/y and about 3 MCM/y as flood flow (Abu Ajameih, 1980). The aquifer also discharges about 5 MCM/y at the lower reaches of Wadi Heidan. All the discharged water used to flow directly into the Dead Sea. Recently, a new project is being implemented to treat about 15 MCM/y from the thermal water to be used for domestic uses.

The groundwater flows in the lower aquifer from the east towards the Dead Sea in the west. Not much data on the potentiometric level in the aquifer is available. Therefore, a potentiometric surface is drawn as straight line from Zarqa Ma'in thermal springs elevation to the water level of Qastel deep well No-3 to the artesian level of Azraq deep well, further east (Figure-3.11).

3.3.2 Aquitards

The formations: Na'ur, Fuheis, Hummar and Shueib (A_{1-6}) are forming the main aquitard, which separates the two main aquifer systems in the study area. It consists of about 400 m of marl, marly limestone intercalated occasionally with limestone bands.

It crops out in the western areas, therefore it becomes locally saturated due to the presence of fractured and jointed limestone bands within the marly sequence of this aquitard, but of course permeability is low. It supports some small springs which seep along the steep slopes, such as, Al Zarqa spring in the upper part of Wadi Zarqa Ma'in.

4. GEOTHERMAL ANOMALY OF THE STUDY AREA

4.1 General description and occurrences

The study area contains two geothermal manifestations; the Zara-Zarqa Ma'in thermal springs systems and the thermal wells at the areas of Madaba and Jiza region.

The Zara hot springs, at the Dead Sea Shore, together with Zarqa Ma'in hot springs, about 4km to the NE, form the main geothermal manifestation in Jordan.

More than 1000m of sedimentary rocks are exposed in Zara-Zarqa Ma'in area ranging in age from Middle Cambrian to Recent. Cenozoic vesicular olivine basalts and significant quantities of travertine deposits are found in the area (Hakki and Teimeh, 1981). The topography of the area drops from about 800m asl down to 400m bsl within a distance of less than 7km. The area is very rugged with steep slopes and without any remarkable soil cover. The wadis are V-shaped with an average slope of 15%.

In Zara-Zarqa Ma'in area there are more than 100 thermal springs issuing from the Kurnub sandstone aquifer (Lower Cretaceous) with temperatures of up to 63°C. These springs have been of great importance since ancient times due to their therapeutic properties.

About 60 thermal springs used to issue along the northern side of the, east-west trending, Wadi Zarqa Ma'in Fault Zone at altitudes between 80 to 120m asl. All springs issue from the Kurnub Sandstone Formation as typical fault contact springs. No thermal springs were found at the southern side of the wadi where the down faulted Na'ur Limestone Formation is standing against the Kurnub Sandstone Formation at the northern side. Al Shallal (Waterfall), Al Magharah and Al Amir are the major springs in terms of their temperatures and flows. The mean flow rate of Zarqa Ma'in thermal springs is 1887 m^{3}/hr (Abu Ajameih, 1980) discharging westwards into the Dead Sea. The area attracts many tourists, especially after establishing the modern spa in the location. Photos-4.1 and 4.2 show the modern spa and the waterfall in Zarqa Ma'in area.

In Zara area, more than 40 thermal springs used to discharge along the eastern slopes of the Dead Sea with 20% slope. It is of 3-4km in north south extension and 1.5 km in east west direction. Zara springs discharge from the Kurnub Sandstone Formation as normal springs. Photo-4.3 shows one of the thermal springs in Zara area (Zara-1). The thermal spring, Zara-22 (photo-4.4), has the highest temperature (57°C) and the highest flow rate (252 m^{3}/hr). The average flow rate of the major 18 springs is 832 m^{3}/hr (Abu Ajameih, 1980).

Photo-4.1: The modern spa in Zarqa Ma'in area.

Photo-4.2: The waterfall in Zarqa Ma'in area

Photo-4.3: Thermal Spring (Zara-1) in Zara area

Photo-4.4: Thermal spring (Zara-22) in Zara area

These springs together with the remaining 27 thermal springs in the area discharge into Dead Sea through several small streams. Part of the thermal water is used in bathing before it discharges into the Dead Sea. Recently, about 15 MCM/y from the thermal springs water were planed to be desalinated and used for domestic purposes.

The second geothermal manifestation is found in the thermal wells in the eastern part of the study area, where, many wells have been drilled by the private sector for agricultural purposes. The wells were drilled to the upper aquifer (B_2/A_7) ranging in depth from 250 to 350m. Most of these wells are discharging thermal water ranging in temperature from 30 to 46°C. The water of these wells is used in irrigation after it cooled in pools with out making any use of its energy. The thermal wells are generally located within the eastern extension of Zarqa Ma'in Fault and the other several faults in the area, mainly Daba'a and Wadi Al Hammam faults (Figure 4.1).

The water temperature distribution at wellheads shows that the thermal wells are subdivided into two heat anomalies (Figure 4.2). The first anomaly located around well-5 (Abu Shweimeh) east of Madaba (Photo-4.5) at the intersection of Jiza fault with covered unknown NW-SE trending fault. The latter was detected by radon measurements carried out around well-5 by NRA (Jaser et al. 2002) in the course of the geothermal project. The measurements were carried out using the Track-Etch method (CR39 films for 3 days duration) in 101 wells drilled for 2m in depth and 1000*500m spacing (Figure-4.3). The figure shows that well-5 is located at the intersection of Jiza fault with NW-SE trend of high radon values i.e. two faults. Therefore, the intersection of the two faults is forming the up flow path for the thermal water from the lower to the upper aquifer causing this anomaly around the well.

The second anomaly is located at the eastern-southern part of the study area, where Daba'a and Wadi Al Hammam faults are located (wells 2,3,4,10,11,16,29 and 31).

58
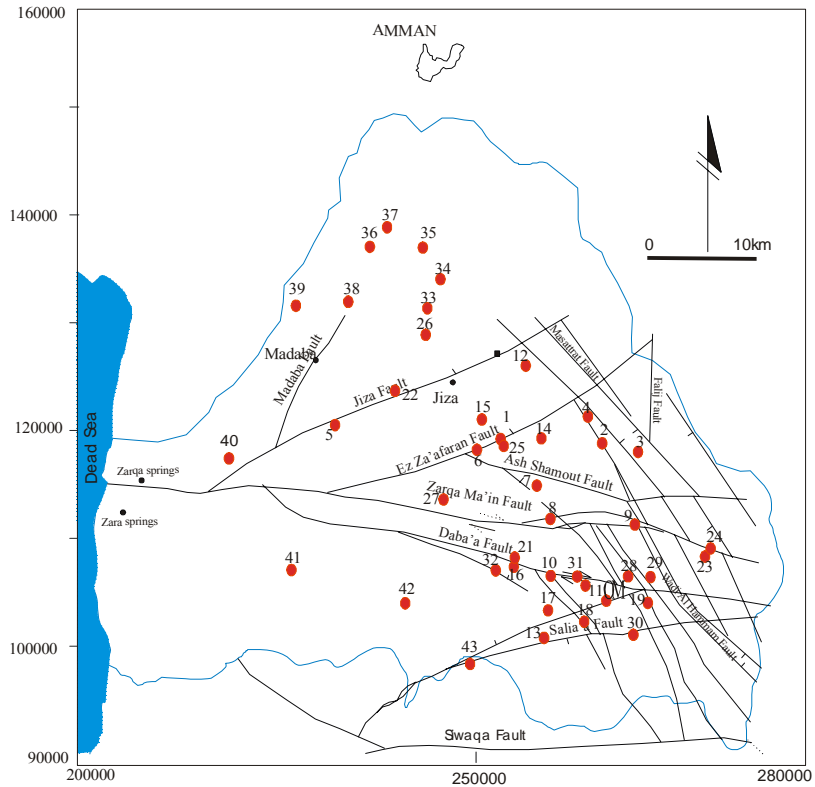
Figure-4.1: Location of the sampled water wells along the main faults
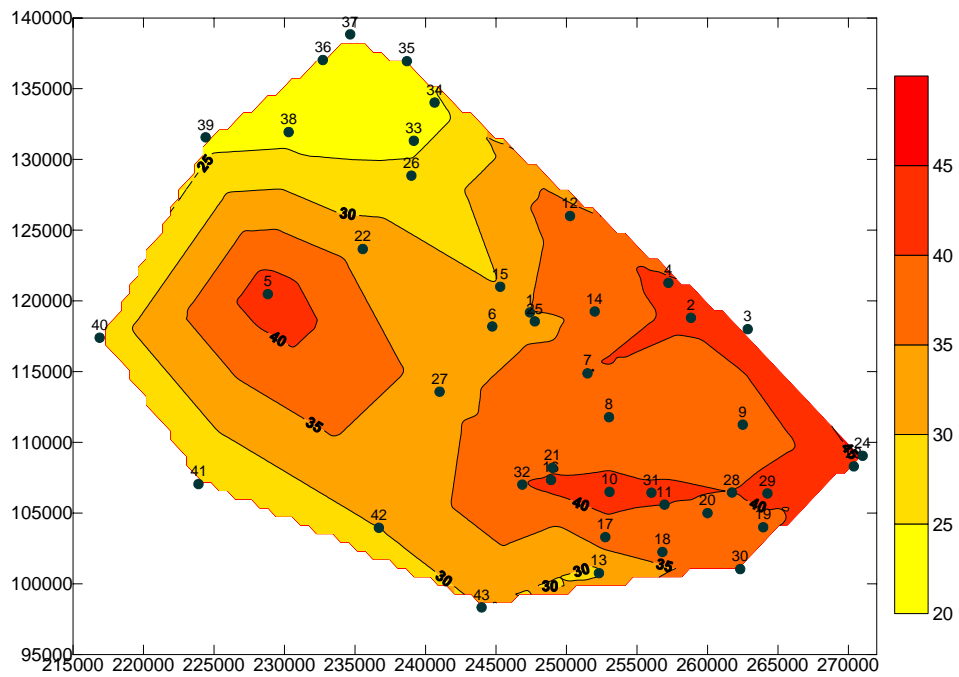
Figure-4.2: Isothermal contour map in the upper aquifer

Photo- 4.5: Abu Shweimeh thermal well, Madaba.
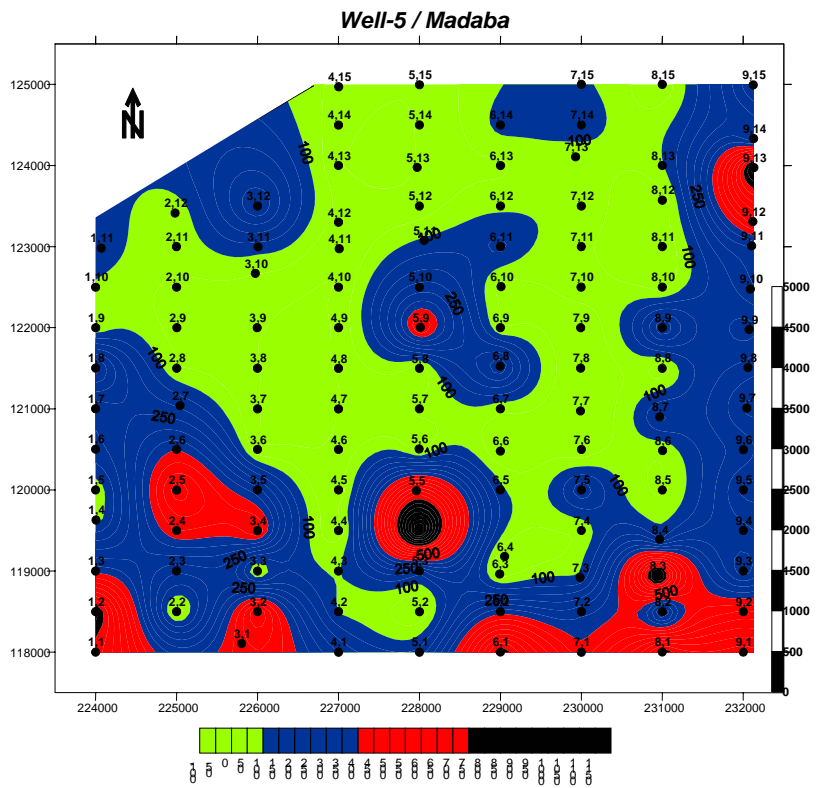
Figure-4.3: Radon concentration map (Track-Etch Method)

4.2 Previous work on geothermal anomaly

Many investigations of the geothermal energy potential in Jordan have taken place over the last four decades. Most of these studies were done for, or directed by the NRA. Thermal waters of Zara-Zarqa Ma'in have been subjected to many studies regarding their chemistry, heat source, therapeutic properties and their potential as source of energy. On the contrary, only limited work has been done on the thermal wells in the eastern part of the study area, these studies are reviewed below:

The first study was undertaken by Sir M. Mac Donald and partners in 1965, and comprised chemical analyses of samples from Zarqa Ma'in.

Bender (1968b) described the major and minor spring areas and provided chemical analyses of the Zarqa Ma'in thermal springs.

McNitt (1976) reviewed the existing chemical data for the Zarqa Ma'in system and recommended a resistivity survey and drilling to investigate the area.

On the basis of temperature and fluid chemistry, Marinelli (1977) concluded that the east escarpment of the Dead Sea Rift and particularly the Zarqa Ma'in and Zara areas possessed the most favorable geothermal potential in Jordan and recommended a program for further investigations.

Truesdell (1979) gave a comprehensive evaluation of the geothermal potential based on geochemical evidence. He concluded that, the Zarqa Ma'in and Zara springs, are fed by waters circulating deep within the Paleozoic Sandstone aquifers and receiving heat from a normal geothermal gradient. He suggested that these waters exist at a maximum temperature of $110^{o}C$ at depth and are cooled during their ascent by mixing.

Abu Ajameih (1980) reported on a major exploration exercise using a variety of exploratory techniques carried out by the NRA in the Zara-Zarqa Ma'in thermal area in 1977-78. The main conclusion of the report was that an important geothermal reservoir is indicated in the area of the springs most probably heated by Hammamat Umm Hasan basalt plug. The moderate radioactivity of the waters was also noticed.

Mabey (1980) studied previous data for the Zarqa Ma'in-Zara area and proposed a program of investigation beginning with interpretation of magnetic data, then developing a geological model and undertaking gravity and geochemical survey. Followed by micro-earthquake, thermal gradient, resistivity surveys and finally deep drilling.

Hakki and Teimeh (1981) carried out a detailed geological study of the Zarqa Ma'in-Zara area. Their work related the hottest springs to the highest intensity of shearing in the area.

Di Paola (1981) concluded that the existing geochemical and isotopic results for the Zarqa Ma'in area indicated that the thermality of the springs is most probably due to the uprising of deeply circulating waters under a normal geothermal gradient.

McEwen and Holcombe (1982) applied terrain correction to the resistivity data reported by Abu Ajameih (1980). The corrected data suggested that four areas of low resistivity existing in the Zarqa Ma'in-Zara area, but that none had the lateral extent normally characteristic of high temperature geothermal reservoir.

Salameh and Khdeir (1983) reported on the thermal water system in Jordan and the reservoir temperatures, which were determined by geothermometers to be around 85°C.

Salameh and Rimawi (1984) studied the isotope content and the hydrochemistry of the thermal springs along the eastern side of the Dead Sea Rift, including those of Zara and Zarqa Ma'in.

Flanigan and El Kaysi (1984) reported on preliminary audio-magneto telluric studies in the Zarqa Ma'in–Zara area. They found that the rocks in the area ranged from moderately conductive to very conductive. The most conductive materials exist at 100-200m depth. The authors related this zone to alteration of sedimentary rocks associated with the movement of thermal waters.

Khoury and others (1984) studied the hydrochemistry, geochemistry and isotopic composition of the Travertine in Zarqa Ma'in area.

Salameh (1986) studied the reason of the elevated temperatures in the lower aquifer system in Jordan. He concluded that it is due to heat stowing horizon within the overlying sedimentary sequence.

Salameh and Udluft (1985) studied the Zara-Zarqa Ma'in thermal springs and presented a flow model showing the hydrodynamic pattern of the central part of Jordan, where the groundwater flow in the upper aquifer towards the east while it flows towards the west in the lower aquifer system.

In 1985, based on the results of the thermal gradient logs, Kappel Mayer proposed a 1000m well in Zarqa Ma'in area to investigate geothermal conditions below the Kurnub sandstone.

In late 1985, the NRA drilled well number GTZ-4A. The well was drilled to 407m and a bottom hole temperature of $46^{o}C$ was recorded indicating a temperature gradient of $52.8^{o}C$/km.

Galanis and others (1986) concluded that the heat flow in Zarqa Ma'in–Zara area is high (up to 472 mw/m^2) and that the area of highest heat flow is associated with the Zarqa Ma'in fault zone rather than the local basaltic eruptions.

In 1986, a French company (Enersystem) concluded that medium enthalpy (140-160°C) geothermal energy could be utilized in Jordan and proposed a pre-feasibility study, followed by the drilling of two deep slim boreholes to 1500–2000m.

Jeries (1986) in MSc thesis study the types of groundwater in Jiza region and concluded that there are three groundwater types according to Rimawi (1985) groundwater classification in Central Jordan.

Duffield and others (1987) studies the age, chemical composition and geothermal significance of Cenozoic basalt near the Jordan Rift Valley. The study showed that the lavas are too old and of too small volume to represent the surface expression of an active reservoir of magma within the crust.

Between 1987-1988, Strojexport Company drilled two deep wells at Zarqa Ma'in-Zara area. Well GTZ-2D was drilled to a depth of 1314m (Trimaj, 1987). A bottom hole temperature of 68.5°C was determined with temperature gradients of 55°C/km to around 300m, falling to around 10-15°C/km between 400m and the bottom of the well. GTZ-3D well, was drilled to a depth of 1100m; the maximum measured temperature in the well was 55.4°C at the depth interval from 242.5 to 318.5m, which lies in the Triassic sandstone of the Zarqa Group.

Myslil (1988) re-evaluated the heat flow data presented by Galanis, 1986 and included recent data and presented temperature gradient maps and identified two favorable zones for future exploration. The most favorable area was the eastern escarpment of the Dead Sea Rift, north of El-Lisan where gradients of 50°C/km could be expected. The second area was the region near the border with Syria and Iraq where temperature gradients of the order of 40°C/km were identified.

Faraj (1988) from NRA jointly with Petro-Canada carried out a study on the variation of the geothermal gradient across Jordan. The results have been incorporated into a map, which is broadly similar to that of Myslil, although lower gradients are indicated for the area east of the Dead Sea.

Rimawi and Salameh (1988) studied the hydrochemical and the groundwater system of Zara-Zarqa Ma'in thermal field. They related the high salinity of Zarqa Ma'in thermal water to a possible mixing with the Dead Sea water.

Between the year 1989 and 1991, Allen, Evans and Darling from the British Geological Survey (BGS) visited Jordan as part of the technical cooperation between BGS and NRA. They review the available data, reports and the availability of the instrumentations within NRA regarding geothermal exploration. Three reports were produced on geothermal resources evaluation in Jordan and a geothermal exploration program was recommended.

Sawarieh (1990) based on hydrogeological and hydrochemical data from the thermal wells near Queen Alia Airport, concluded that there is a water mixing between the thermal water of the lower deep sandstone aquifer and the fresh cold water of the upper limestone aquifer (B2/A7).

Dermage and Tournage (1990) reported on the potential and uses of the geothermal resources in Jordan.

Salameh and others (1991) carried out a medical treatment experiment on the curative ability of the thermal water in Jordan. The results of the experiment show the ability of the thermal water in treating several diseases.

Sawarieh and Massarweh (1996) studied the thermal springs in Zara and Zarqa Ma'in area. The conclusion of the study is that the heat source in Zara-Zarqa Ma'in area seams to be due to deep circulation of water in more or less normal geothermal gradient.

Saudi (1999) used the data of Sawarieh (1990) and concluded that the maximum reservoir temperature predicted by calculation of various geothermometers exceeds $100^{o}C$.

In the years 2001-2002, the NRA conducted a study on the thermal wells in Jiza region. In the course of this project, geological, hydrogeological, hydrochemical and geophysical investigation were made. The main outcome of this work is that the thermal water in the area is as a result of mixing between different types of water and the maximum reservoir temperature is more than $80^{o}C$ (Jaser et al. 2002).

4.3 Heat Source

Four possible heat sources were considered for Zara-Zarqa Ma'in thermal field, these are:

1- The presence of the Late Cenozoic basaltic lavas in the area led earlier investigators (Bender, 1974 and Abu Ajameih, 1980) to conclude that the thermal water is heated by a crustal magma body or solidified hot pluton, that represents the intrusive roots of the lavas. The radiometric-age determinations show that the lavas (Hammamat Umm Hasan plug) are too old (1.8 ±.1 million year) and of too small volume, less than 1km^3. Also, the chemistry of the thermal water suggest that it is probably equilibrated with crustal rocks of about 110°C (Truesdell and others, 1983). Therefore, a magmatic heat source for this thermal water seems unlikely.

2- Friction associated with lateral movement along faults of the Dead Sea Rift. Hakki and Teimeh (1981) related the hottest springs to the highest intensity of shearing in the area. Galanis and others (1986) concluded that the heat flow in Zarqa Ma'in-Zara area is high (up to 472 mW/m^2) and that the area of highest heat flow is associated with the Zarqa Ma'in Fault Zone rather than the local basaltic eruptions.

3- Salameh (1985) suggested a heat stowing horizon consisting partly of dry sandstone overlain by marls with heat conductivities of only about half that of wet sandstone results in temperature gradient of about twice the gradient of the whole sequence, maintaining herewith a constant heat flow.

4- An alternative hypothesis that the waters are heated during deep circulation through crust with more or less normal geothermal gradient appears more likely. The isotopic and chemical properties of the water indicates an origin in the Paleozoic (Disi) sandstones, which extend to depths of 2500-3500m below the level of the Jordanian plateau (Bender, 1974). The geothermal gradient in these sandstones is normal, thus circulation to 2.5-3 km could produce the estimated temperature of about 100°C. By this model, deep circulation in nearly flat lying Paleozoic sandstones is directed upwards along the deep faults to feed the hot springs and wells. This suggest that a widespread resource of moderate temperature thermal water exists in the Paleozoic sandstones of Jordan.

Zara-Zarqa Ma'in thermal field is controlled by tectonic, so the feeding system follows the vertical faults, which acts as conduits for the rapid ascent of hot waters from deep confined aquifers. This up flow can feed laterally some permeable layers where aquifers can be developed on more or less large characteristic temperature curve with rapid increase of temperature followed by an inversion of the gradient. It is well represented on the temperature profile of GTZ-3 well (1100m) in Zara area, where the out flow seems to be localized at the depth interval from 242.5 to 318.5m, which lies in the Triassic sandstone of the Zarqa Group. The temperature decrease from $55.4^{o}C$ in the out flow zone to $51^{o}C$ at the down hole. Therefore, the only way to find hotter water is to intercept the vertical feeding system.

Truesdell and others (1983) concluded that the Zarqa Ma'in and Zara springs, are fed by deep circulating water. The maximum temperature of this water at depth is about $110^{o}C$ cooling down during ascendance and by mixing with shallower cold water before it discharges as thermal springs.

This interpretation for the heat source is similar to that reported by Mazor and others (1980) for many thermal springs elsewhere in the western side of the Dead Sea Rift and appears to reflect a regional similar geothermal regime along this major structural zone.

The study area is dissected by numerous faults of different trends. Renewed acting of the NW–SE compressional forces during the Late Cretaceous to Tertiary and Quaternary times lead to the reactivation of the old faults and weakness zones. These forces are also responsible for creating new faults, fractures and discontinuities. This suggested that there is a hydraulic connection between the two-aquifer systems within the study area. This allows the thermal water from the lower aquifer to flow up via faults (conduits) to the upper aquifer raising the water temperature in vicinity of these faults. Despite the head differences between the two aquifers, the faulting system may introduced a reverse head around the faults. Also, the water is driven toward the upper aquifer by a gradient caused by the lower density of the water in the hotter parts of the system. Therefore, the next chapter of this study will concentrate on the hydrochemistry of the thermal wells and their relation with the thermal water of the lower aquifer to find out the heat source by examining the mixing process between the two aquifers.

5. HYDROCHEMISTRY

5.1 Hydrochemical Data

A total of 49 chemical analysis were used in this study (Table-5.1). The samples 1-32 were taken from the thermal wells during the course of the NRA geothermal project (2001-2002) in Jiza region. The chemical analysis from Zara springs (Z-8 and Z-22) and Zarqa Ma'in springs (ZM-21 and ZM-53) were taken from a previous study carried out by Sawarieh and Massarweh (1996). Table-5.1, also shows the chemical analysis of 13 samples taken in the course of this study (Dec. 2002); 11 samples (33 to 43) from the upper aquifer mainly from the recharge area, south of Amman and 2 samples (Zm-8 and Z-25) from the Zara and Zarqa Ma'in thermal springs. The samples from Zara and Zarqa Ma'in springs represent the water of the lower aquifer system since there are no wells taping the lower aquifer in the area of Jiza region, except Qastel deep well-3.

All samples were analyzed in the Water Authority Labs, Amman for the major cations and anions as well as the trace elements (Na, K, Mg, Ca, Cl, HCO_3, SO_4, SiO_2, F, Br, NO_3, B, Li). Among these samples, 37 samples were analyzed for stable isotopes (^2H,^{18}O) and some for radioactive isotope (^3H ,^{14}C and ^{13}C) in the same labs. The basic field measurements (T°C, pH ,TDS and EC) were also carried out and are shown in table-5.2.

5.2 Groundwater Characteristics

The chemical analysis and the field measurements of groundwater samples from the upper aquifer (Tables 5.1 and 5.2) show that the water is of HCO_3 type with pH between 6.5 and 7.5. The electric conductivity ranges from 500 to 2580μs, increasing from the recharge areas in the north-west towards the south-eastern parts of the study area (Figure- 5.1).

The chloride content ranges from 59 to 433 ppm and the sodium content from 26 to 245 ppm. Both, Cl and Na contents increase from the recharge areas towards the southern eastern corner of the study area where wells 8,9,10,16,21 and 31 are located. Figures-5.2 shows the Cl concentration contour map. The location of high Cl and Na concentrations along Daba'a and Wadi Al Hammam faults suggests that these faults are the main up flow zones of thermal water from the chloride water in the lower aquifer to the bicarbonate water in the upper aquifer.

68

TABLE-5.1: Chemical analysis results in mg/l.

No.	Na	K	Mg	Ca	Cl	HCO3	SO$_4$	NO$_3$	SiO$_2$	Li	F	Br	B
1	36.6	2	34.8	94.2	59.2	397.7	51.8	4.49	13.8	0.01	0.46	0.05	0.11
2	72.9	3.1	54.6	110	158.1	418.5	100.8	0.4	17.6	0.01	1.1	0.71	0.17
3	112.2	4.7	49.6	105.6	178.7	337.9	177.1	0.5	21.8	0.02	1.34	0.84	0.34
4	83	3.1	51.3	123.2	204.9	385.5	103.2	0.4	16.7	0.01	1	0.96	0.21
5	64.1	15.2	52.9	76.6	164.1	269.6	119	0.5	19.4	0.03	1.7	0.88	0.23
6	42.6	2	30.3	100	70.6	365	50.1	3.3	9.7	0.01	0.61	0.05	0.24
7	121	7.1	66	159	208	445	289	0.3	11.1	0.02	1.62	0.85	0.53
8	213.1	10.6	99.8	211.2	402.4	464.8	450.7	0.4	19.9	0.03	1.03	1.71	0.93
9	245	8.2	133	223	424	432	570	1	11.2	0.03	1.29	0.05	0.9
10	238.7	8.2	79.8	176.6	375.9	396.5	431	0.53	20	0.04	1.4	1.6	0.93
11	102.6	7.8	54.6	219.8	344.4	419.7	419	0.32	16.6	0.03	1.24	1.28	0.53
12	71.3	2.7	40.7	124	120	469	84.5	3	14	0.01	1.26	0.69	0.1
13	86.7	3.1	58.4	133	151	506	121	0.2	15.1	0.01	1.48	0.77	0.04
14	79.4	5.1	56.1	140	124	479	190	0.6	11	0.02	1.49	0.58	0.27
15	37.5	2	30.8	79.4	59.2	312	55.7	4.9	9.5	0.01	0.5	0.44	0.12
16	198	7	69.9	145	433	307	225	0.8	12.3	0.03	1.48	0.05	1.53
17	174	7	79.4	187	263	476	433	0.8	11.2	0.03	1.16	0.05	0.97
18	174	5.9	65.3	171	254	420	386	0.6	10.6	0.03	1.21	0.05	0.88
19	134	5.1	49.9	140	172	431	246	0.3	13	0.02	1.15	0.94	0.2
20	170	5.5	78.1	204	267	488	422	0.5	13.9	0.02	1.01	2.74	0.36
21	174.8	6.6	60.1	137.5	372	305	197.8	0.6	12.1	0.03	1.41	0.05	1.49
22	80.7	5.5	35.3	113	205.5	327	91.7	5.55	13	0.01	0.79	1.27	0.02
23	153.2	7.4	62.4	157.7	225.1	419.7	311.5	0.5	20.2	0.02	1.54	0.74	0.5
24	154.1	8.2	57.8	140.9	226.1	406.3	262.6	0.5	20.5	0.02	1.43	0.77	0.44
25	45.8	2.94	32	85	75.4	427	50	X	20.6	0.03	1.36	1.05	X
26	41.2	5.1	25.2	70.7	65	452	50.9	13.7	11.6	0.01	0.8	0.31	X
27	54	2.8	26	100	77.7	451	43	X	9.67	X	0.91	0.94	X
28	189.5	7	66.2	182.4	249.6	458.7	411.4	0.1	17	0.02	0.99	0.81	X
29	186.8	8.6	70.3	173.5	258.8	445.3	385	0.1	14.2	0.02	1.23	0.99	X
30	124.7	4.3	42.4	110.2	174	292.8	240	0.1	17.4	0.01	1.12	0.53	X
31	206.5	7.8	69.3	182.4	337.8	400.8	387.4	0.1	17.7	0.02	1.07	1.43	X
32	160.5	7.8	60.3	145.1	329.8	372.1	186.2	0.4	16	0.02	1.28	1.51	X
33	43.9	2.7	23.5	71.9	70.3	260	34.6	20.6	X	0.01	X	X	X
34	43.9	2.74	23.5	71.94	70.3	260.5	34.56	54.5	X	0.01	X	X	X
35	44.6	6.26	25.3	73.2	65	284	26.4	37.1	X	0.01	X	X	X
36	26.4	3.1	21.	77.4	40.5	300.1	14.4	32.7	X	0.01	X	X	X
37	39.6	5.87	22.1	99.80	70.29	320.3	17.76	58.7	X	0.01	X	X	X
38	37.5	2.35	17.3	66.3	45.1	237.9	34.56	20.5	X	0.01	X	X	X
39	30.6	2.74	22	58.52	46.50	218.4	30.72	29.5	X	0.01	X	X	X
40	45.1	2.74	30	59.92	73.13	248.9	35.52	28.3	X	0.01	X	X	X
41	96.6	4.69	51.3	116.4	145.5	413	145	15.1	X	0.01	X	X	X
42	147.7	6.65	79.5	152.5	274.8	489.2	228.5	2.65	X	0.01	X	X	X
43	146.7	4.69	66.5	143.9	251	527	152.64	2.71	X	0.01	X	X	X
44/Zm8	382.3	46.5	27.4	132.3	666.7	261.8	173.76	4.43	X	0.18	X	X	X
45/Z25	208	27	24	88.8	374.2	186	118.56	0.18	X	0.11	X	X	X
Z-8	275	38	21	137	515	232	150	X	24	X	0.39	4.68	X
Z-22	195	30	18	115	408	180	118	X	29.5	X	0.37	4	X
ZM21	500	49	34	157	799	288	196	X	20	X	0.25	7.7	X
ZM53	410	63	35	170	740	299	254	X	25	X	0.52	6.7	X

TABLE- 5.2: The basic field measurements

Sample	Well owner name	T (°C)	Ph	T.D.S (ppm)	EC (μS/cm)	Eh
1	Faleh Al Fayez	35	7	427	875	
2	B.Mothafer	41	6.8	796	1624	
3	Attalah Zaben	43	6.8	876	1787	
4	Al Sayegh Hani	41	7	659	1332	
5	Abu Shweimeh	43	7.4	556	1129	47
6	Kina Company	32	7	548	1118	
7	Abu Shahmeh-1	40	6.7	850	1706	
8	Abu Shahmeh-2	35	6.8	1291	2540	
9	F. Akef	36	6.8	1313	2580	-140
10	M. Adhoub	42	6.9	1141	2280	-57
11	G. Abu Jaber	40	6.7	1374	2804	
12	Masharbash	38	6.9	603	1220	
13	Dr. Jaber	29	6.8	677	1367	
14	Kadrawi	38	6.7	648	1310	
15	HakimAl Fayez	30	7	429	875	
16	Amouri	41	7	1058	2100	
17	Dr. Huneiti	38	6.8	1387	2830	
18	A. Abu Shihab	39	6.9	1337	2728	
19	Dr. T. Ghnaim	38	6.8	815	1635	
20	S. R. Zaben	37	6.7	1085	2150	
21	A. Madhoor	39	7	981	1956	
22	M. Al Fayez	33	7	628	1272	
23	M. Abdullah	45	6.7	936	1870	
24	M. Abo Jaber	46	6.8	907	1813	
25	M. Al Fayez	33	6.9	449	850	
26	HmaidiAlFayez	26	7.6	378	785	
27	M. Al Sattel	33	7	657	1326	
28	Abu Haidh	40	6.8	1038	2006	
29	Awamleh	42	6.8	1022	2030	
30	Anwar Khamis	39	6.9	703	1417	
31	Salim Raheeleh	41	6.5	1124	2230	
32	Emarati	40	6.8	903	1797	-193
33	Qastel-15	25	7	513	802	
34	A. Abu Jnaib	25	7.3	686	1072	
35	Harran Bakhit	26	7	518	810	
36	H. Salfiti	22	7.37	448	700	
37	Bsharat	22	7.28	594	928	97
38	M. Nablsi	25	7.4	433	677	
39	H. Saba'awi	23	7.1	407	636	
40	ZarqaMainCold	27	7	513	802	
41	Waleh well-14	25	6.8	941	1470	
42	Qatari	30	6.85	744	2030	31
43	Agil Hgaish	30	7	928	1970	
44	Zarqa spring -8	63	6	1950	3050	-118
45	Zara spring -25	53	6.2	1210	1890	
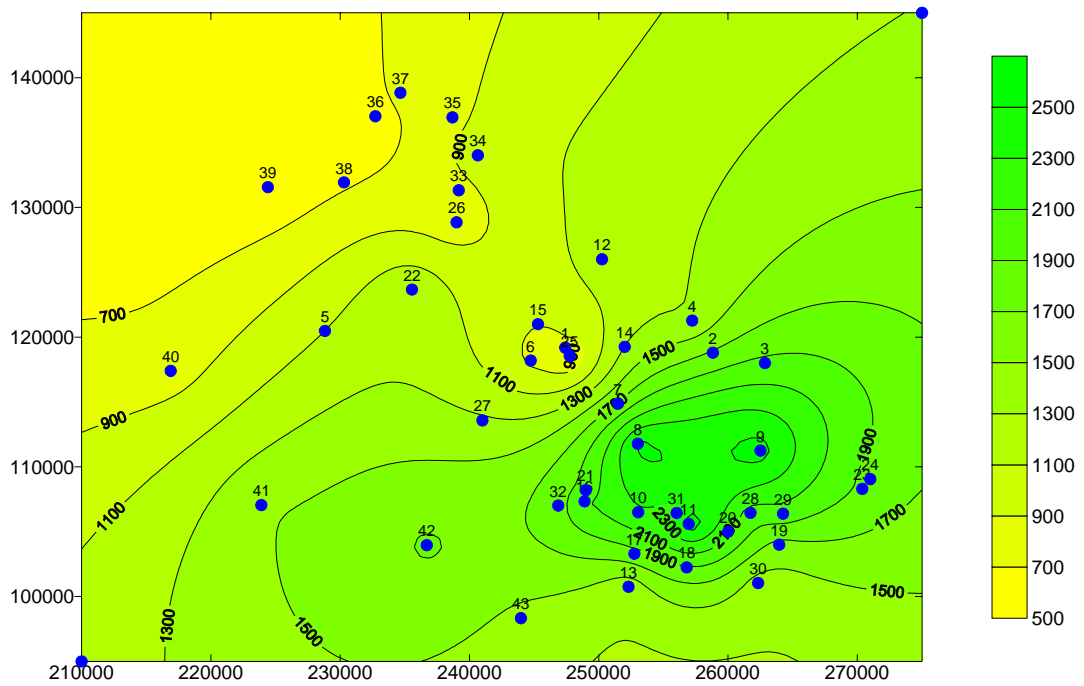
Figure-5.1 : The Isosalinity contour map (μs/cm)
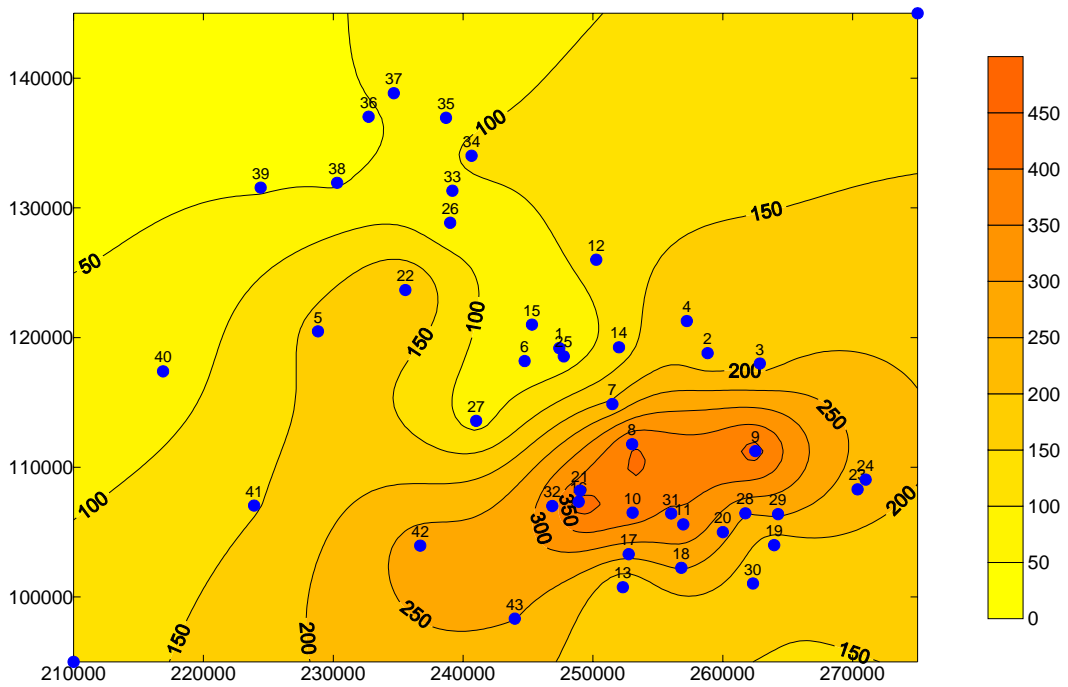
Figure-5. 2: Chloride concentration contour map (mg/l)

71

It can be seen from figure-5.3 that the So_4 concentration increases towards the south east area where the high concentrations of Cl and Na are occurred.
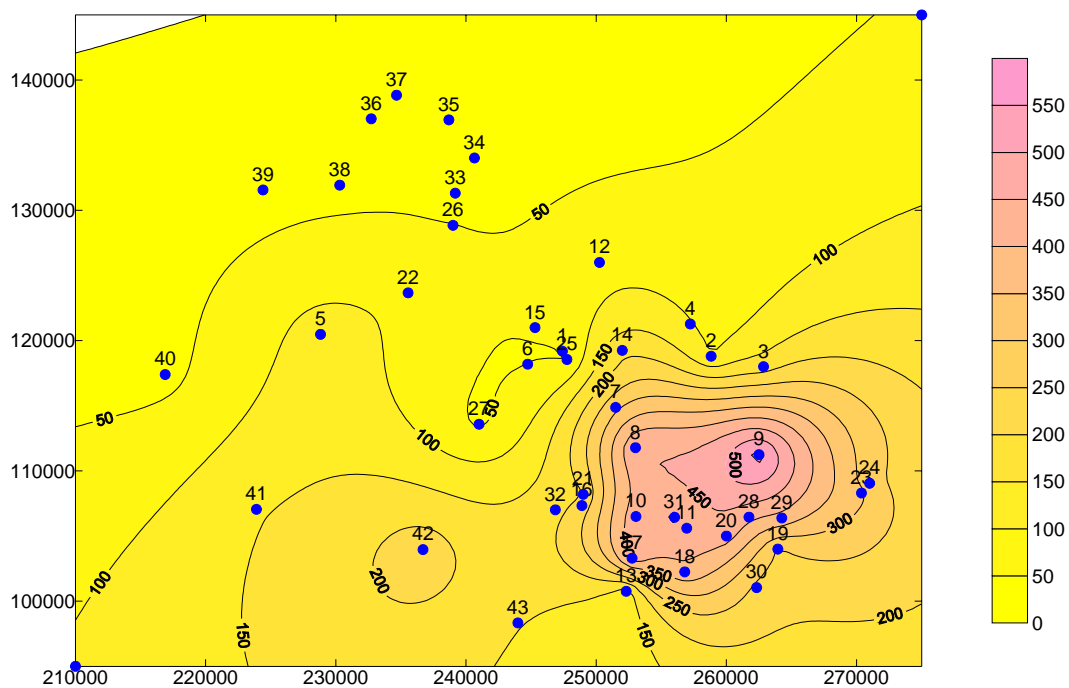
Figure-5.3: Sulfate concentration contour map (mg/l)

5.3 Classification of groundwater

The chemical analysis were plotted on different classification diagrams:

5.3.1 Cl-SO$_4$–HCO$_3$ graph

All chemical analyses were plotted in Cl- SO$_4$ – HCO$_3$ graph (Giggenbach, 1991) to show the thermal water classification (Figure-5.4). This graph helps to discern immature unstable waters and may give an initial indication of mixing relationships or geographic grouping and trends. It can be seen from the figure that all samples from Zara-Zarqa Ma'in thermal springs, lower aquifer (Zm8, Zm21, Zm53, Z8 , Z22, and Z25) are located in the chloride water type area. Whereas, the samples (33 to 39) from the cold water wells in the recharge area are located in the high bicarbonate part. Most of the samples from the thermal wells fall in the bicarbonate area, and are therefore classified as bicarbonate water. Only two samples (16, 21) can be classified as chloride groundwater type. Another two samples (9, 10) are located in the sulfate water type. The position of some samples namely 8, 11, 31, and 32 show a shift towards the sulfate and chloride areas, but still within the bicarbonate water range.

The figure shows a clear mixing trend (triangles) between the bicarbonate cold water of the upper aquifer (circles) with the chloride thermal water of the lower aquifer (stars). Also it shows a shift towards the sulfate water. The SO$_4$ increase could be as a result of reducing or dissolution conditions or may be both. The Eh values (positive and negative) show that both conditions reducing and oxidizing are present. Under reducing condition when the reducing hot mineralized water of the lower aquifer mixes with the oxidized cold water of the upper aquifer, the sulphides reduce and release sulphates. Also, sulphates are produced from the dissolution of gypsum, which occurs in several horizons in the aquifer matrix.
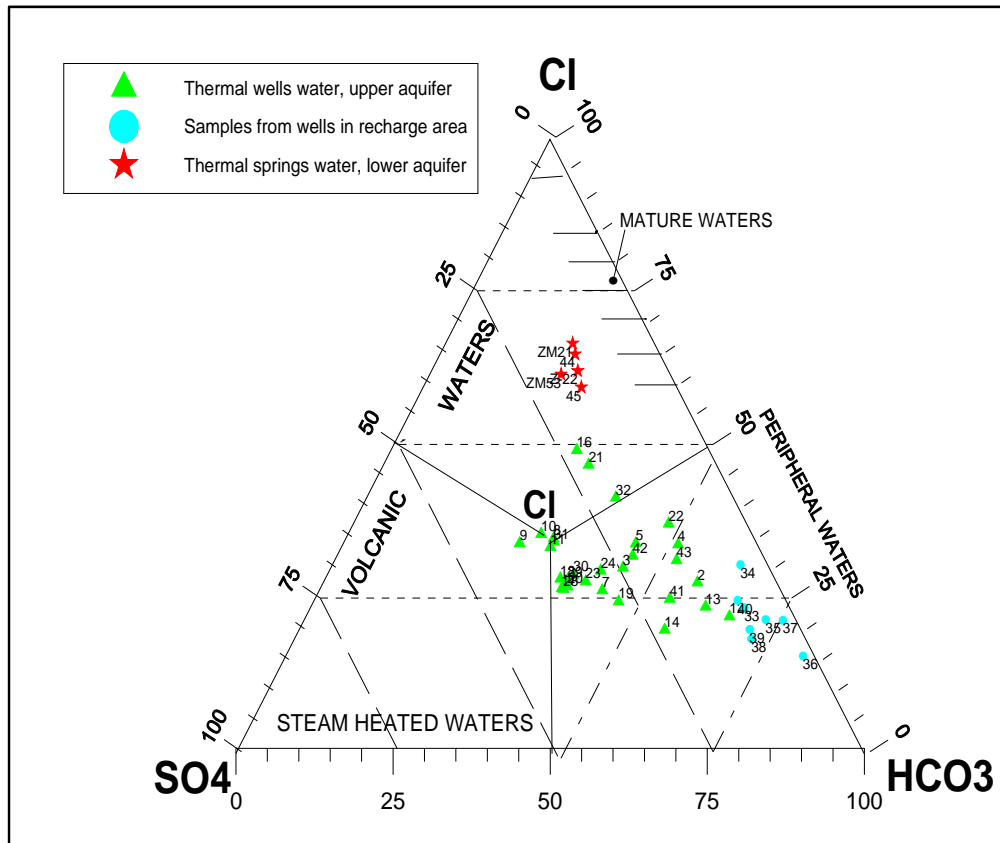
Figure-5.4: Giggenbach (1991) diagram for samples from the thermal and cold wells, upper aquifer and Zara-Zarqa Ma'in thermal springs, lower aquifer.

5.3.2 Schoeller graph

Schoeller diagram is used to classify the type of water. It may be also used to show the changes over time of the different water types. In this diagram the log concentrations of fluid constituents from a number of analyses are connected with a line. Because logarithmic values are used, a wide range of concentrations can be shown. The effect of mixing with dilute water, as well as gain or loss of steam, is to move the connecting line vertically without changing its shape (Truesdell, 1991). Different water types will be displayed by crossing lines.

Figure-5.5 is a Schoeller diagram shows that the cold water wells, recharge area, is of bicarbonate type (blue circles) and the thermal springs water of the lower aquifer is of chloride water type (red stars). Thermal wells samples (green triangles) show a degree of mixing between these two types.
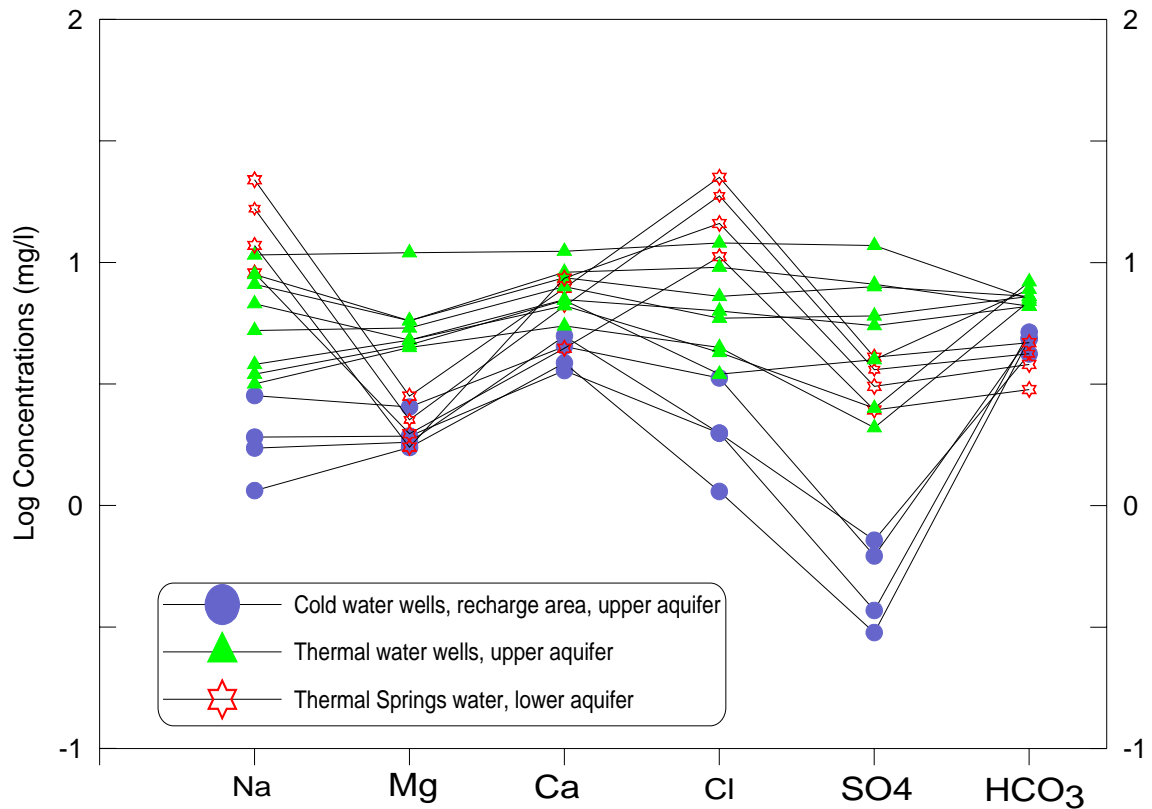
Figure-5.5: Schoeller diagram for samples from thermal and cold wells, upper aquifer.

5.3.3 Durov Diagram

This diagram is composed of two triangles and one square. The square is subdivided into 9 zones according to Lloyd and Heathcoat (1985) classification of the diagram. Each zone indicates a different water type and conditions. For example, zone one indicates recharge water in limestone, sandstone and other aquifers, Zone 5 indicates that there is no dominate anion or cation.

Eleven samples from cold wells in the recharge area to thermal wells in the southern eastern area along the flow line were plotted on Durov diagram (Figure-5.6). The figure shows that sample 36 fall in the recharge water zone while samples 8, 9, 12 , 14, 24, 28, and 31 fall in the mixing zone which coincide with their location sample36 from well in the recharge area and the samples 8, 9, 12 , 14, 24, 28, and 31 from wells in the up-flowing zone.
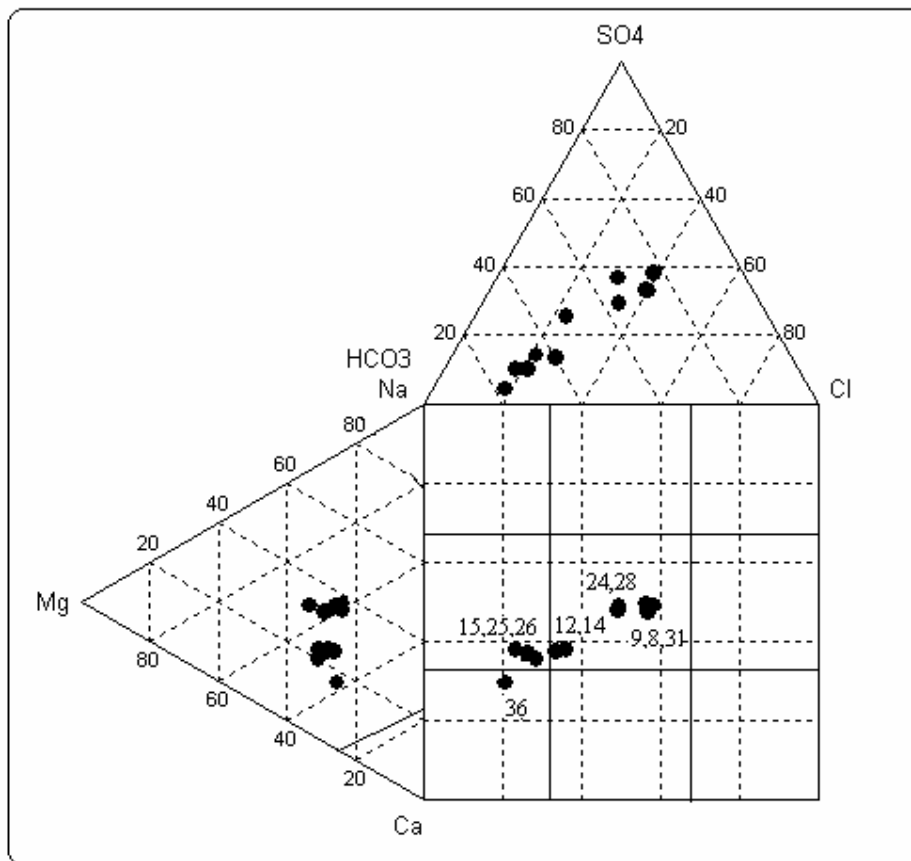
Figure-5.6: Durov diagram for selected samples from cold and thermal wells.

5.3.4 Na-K-Mg diagram

The Na-K-Mg diagram of Giggenbach (1988) is used to evaluate the equilibrium conditions between the thermal water and the reservoir rocks (Figure-5.7). This diagram has the ability to picture the position of a large number of samples, allowing the delineation of mixing trends and grouping. The figure shows that all samples fall in the area of immature water, very close to the Mg corner indicating that the water is in partial equilibrium with reservoir rock, either as a result of mixing or water-rock reaction during up-flow.
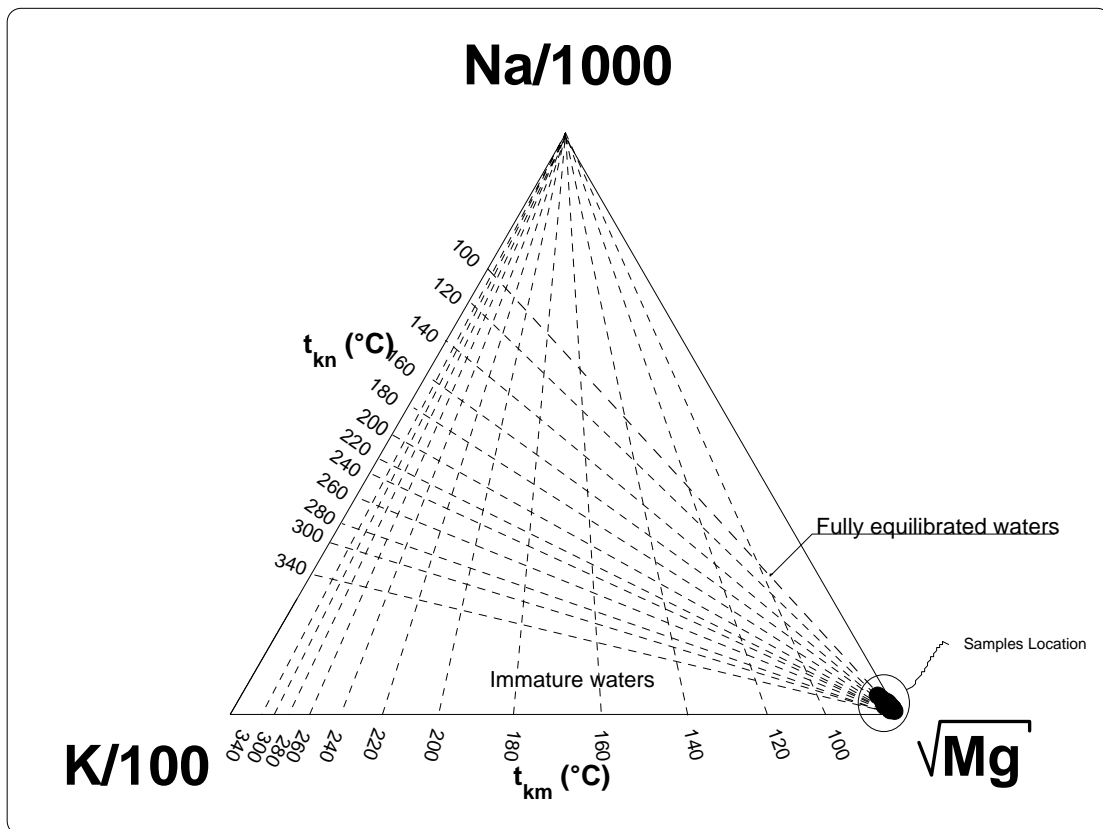
Figure-5.7: Giggenbach, 1988 diagram for samples from the thermal and cold wells and springs, upper and lower aquifers.

5.4 Geothermometers

The use of chemical geothermometers is one of the important methods applied in geothermal resources investigations. It is useful to predict the subsurface temperature and to determine the main up-flow zones in a geothermal system. Cooling of the water may occur by conduction, boiling and or mixing with cold water. Comparison of different geothermometers may be helpful to interpret those processes. The temperatures in geothermal reservoirs are generally not homogeneous, but variable, both horizontally and vertically, so geothermometry is useful for revealing the temperature of the aquifer feeding the wells. Temperatures encountered in a deep well may be higher than those indicated by chemical geothermometry, particularly if the waters investigated are fed by shallow aquifers (Arnorsson, 1991).

Silica and cations are the main chemical geothermometers used in geothermal investigations.

5.4.1 Silica geothermometers.

The solubilities of the most common silica minerals have been determined experimentally as functions of temperature at the vapor pressure of the solution. Pressure and added salts have little effect on the solubilities of quartz and amorphous silica below 300°C. These experimental information allow the dissolved silica concentration in a hydrothermal solution to be used as a chemical geothermometer after making an assumption about the particular silica mineral that is controlling the dissolved silica. Below 340°C, the solubility of all silica minerals decreases sharply as temperature decreases. Therefore, silica may precipitate from solution as a result of conductive or adiabatic cooling before reaching the surface, resulting low estimated reservoir temperatures. The basic reaction for the solution of silica minerals to give dissolved silica is:

$$SiO_2 \text{ (s)} + 2H_2O = H_4SiO_4 \text{ (aq)}$$
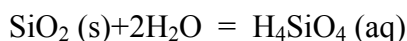
   Mineral------------silica acid

The silica temperature is based on the equilibrium between quartz or chalcedony and the unionized silica in a thermal water.

Silica enters the thermal water from dissolution of several different mineralogic species, mainly: quartz, feldspars, clays and various forms of amorphous silica. Taking into

78

account that the study area is underlain by a thick sequence of mainly marine carbonate rocks which are underlain by another thick sequence of clastic sediments of various origins, it is unlikely that the silica in the water originated from dissolution of feldspars. The silica content of the studied thermal water is much larger than that could be contributed by clays. Amorphous silica is abundant in some parts of the carbonate sequence as nodules, lenses and fully developed layers.   The approximate solubility of amorphous silica below 200°C can be calculated by Fournier and Truesdell (1974) equation:

T °C = (731 / (4.52-log (SiO$_2$))) - 273.15

Using this equation shows that the process of dissolution of amorphous silica up to a concentration slightly above 100ppm/l is entirely independent of temperature. And the studied thermal water shows clear relationship between silica concentration in the range of 10-30 ppm/l, and temperature between 30 to 60°C. Therefore, it seems that the silica in the thermal water is originated from dissolution of quartz, which is abundant in the thick sandstone units.

Both quartz and chalcedony geothermometers were used to estimate the reservoir temperatures. Three equations applicable in the temperature range 20-250°C were used to predict the reservoir temperature in the study area:

1- Quartz - no steam loss equation by Fournier (1977):

T °C = (1309 / (5.19 - log (SiO$_2$))) - 273.15

2- Chalcedony - no steam loss by Foumier (1977):

T °C = (1032 / (4.69-log (SiO$_2$))) - 273.15

3- Chalcedony - no steam loss by Arnorsson et al. 1983:

T °C = (1112 / (4.91-log (SiO$_2$))) -273.15

Because there is no known fumarolic activity in the study area which would indicate the possibility of steam release directly from the thermal system in the subsurface, other equations can be neglected.

The calculation results (Table-5.3) show that the chalcedony equations (2 and 3) does not apply to the samples, they give very low temperatures even lower than the orifice temperatures. While the quartz equation (1) gives more reliable results, but still it gives lower estimation of the reservoir temperature, which may be due to silica precipitation from the solution as a result of conductive or adiabatic cooling during upflow before reaching the surface.

TABLE 5.3: Silica geothermometers results (^{o}C)

Sample Number	Quartz (Fournier, 1977)	Chalcedony (Fournier,1977)	Chalcedony (Arnorsson et al, 1983)
1	50.05	17.54	21.80
2	58.71	26.46	30.30
3	66.71	34.77	38.20
4	56.80	24.49	28.43
5	62.30	30.18	33.85
7	42.68	10.00	14.58
8	63.25	31.17	34.79
9	42.97	10.31	14.87
10	63.44	31.37	34.97
11	56.58	24.27	28.21
12	50.55	18.06	22.29
13	53.20	20.78	24.89
14	42.38	9.70	14.29
15	37.61	4.85	9.64
16	46.11	13.51	17.94
17	42.97	10.31	14.87
18	41.16	8.46	13.10
19	47.99	15.44	19.79
20	50.30	17.80	22.05
21	45.56	12.94	17.40
22	47.99	15.44	19.79
23	63.82	31.76	35.34
24	64.37	32.33	35.89
25	64.56	32.53	36.07
26	44.14	11.50	16.02
28	57.44	25.15	29.06
29	51.04	18.56	22.77
30	58.29	26.03	29.89
31	58.91	26.67	30.51
32	55.26	22.90	26.91
44/Zm8	75.11	43.55	46.52
45/Z25	78.01	46.59	49.39
Z-8	70.44	38.65	41.88
Z-22	78.71	47.33	50.09
ZM53	72.04	40.33	43.47

5.4.2 Cation Geothermometers

Cation geothermometers are widely used to estimate reservoir temperatures of waters collected from hot springs and wells. There are many different cation geothermometers and it is rare when they give about the same result, especially when applied to hot spring waters. Under the best of conditions, cation geothermometers have an uncertainty of at least $\pm 5\text{-}10^{\circ}C$, and commonly much greater than $20^{\circ}C$. Despite that they can be useful for estimating approximate temperatures in geothermal systems and for investigating effects of partial water-rock re-equilibration during up flow. Cation geothermometers are likely to be more reliable for highly saline waters and least reliable for dilute water when applied to hot spring waters.

Cation geothermometry is based on ion exchange reactions that have temperature-dependent equilibrium constant. For example, the exchange of Na^+ and K^+ between coexisting alkali feldspars:

$K^+ + NaAlSi_3O_8 = KAlSi_3O_8 + Na^+$

(albite) ------------ (orthoclase)
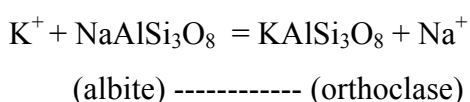
And the equilibrium constant, K^+, for this reaction is:

$K_{eq} = [KAlSiO_3O_8][Na^+] / [NaAlSi_3O_8][K^+]$

If the activities of the solid reactants are assumed to be in unity and the activity of the dissolved species is about equal to their molal concentrations, the equation will be simplified to:

$$K_{eq} = [Na^+]/[K^+]$$

5.4.2.1 Na-K Geothermometer

The Na-K geothermometer is believed to take longer to reach equilibrium at a given temperature than other commonly used geothermometers. Therefore, it is used to estimate the possible highest temperatures in deeper parts of a system where the water resides for relatively long periods of time. It is based on ion exchange reactions whose equilibrium constants are temperature dependent partitioning of Na and K between hydrothermal altered aluminum silicates and solutions.

The following equations, based on empirical correlation, are used to estimate the reservoir temperature, the concentrations of Na^+ and K^+ are in ppm:

1- Na/K temperature by Arnorsson et al. (1983), 25 – 250 °C :

T °C = (933 / (0.993 + log (Na/K))) - 273.15

2- Na/K temperature by Giggenbach (1988):

T°C = (1390 / (1.75 +log (Na/K)))- 273.15

5.4.2.2 K-Mg geothermometer

The K-Mg geothermometer is based on the equilibrium between water and the mineral assemblage K-feldspar, K-mica and chloride (Giggenbach, 1988). It is found that it responds fast to the changes in the physical environment and, thus, usually gives a relatively low temperatures in mixed and cooled waters as compared to other geothermometers. The equation of Giggenbach (1988) is used to estimate the reservoir temperature, concentrations are in ppm:

T °C = (4410 / (14.0 - log (K/√Mg))) - 273.15

Table-5.4 shows the results of the cation geothermometers. It can be seen from the table that the Na/K geothermometers give high estimation for the reservoir temperature. The K/Mg geothermometers gives low estimation for samples from thermal wells but it is more reliable in estimation the reservoir temperature for samples from Zara-Zarqa Ma'in thermal springs.

TABLE- 5.4: Cation geothermometers results (^{o}C)

Sample Number	Na/K (Arnorsson, 1983)	Na/K (Giggenbach,1988)	K/Mg (Giggenbach,1988)
1	140.51	188.27	22.04
2	121.46	172.17	25.74
3	120.37	171.24	34.14
4	112.27	164.27	26.29
5	303.48	312.11	56.95
7	146.26	193.05	39.24
8	133.16	182.10	43.01
9	104.83	157.81	35.32
10	106.58	159.33	40.19
11	168.60	211.33	42.91
12	113.23	165.10	25.90
13	109.28	161.68	25.15
14	153.80	199.28	34.51
15	138.59	186.66	23.09
16	108.51	161.01	38.42
17	117.48	168.76	37.20
18	105.70	158.57	35.82
19	113.58	165.40	35.61
20	102.59	155.85	32.85
21	113.03	164.92	38.74
22	158.89	203.45	40.35
23	130.92	180.21	40.58
24	138.41	186.51	43.34
25	153.75	199.23	29.56
26	217.82	249.93	42.16
28	111.51	163.61	38.94
29	127.30	177.14	42.35
30	106.83	159.55	33.94
31	113.05	164.95	40.58
32	131.38	180.60	41.94
44/Zm8	215.86	248.44	91.23
45/Z25	223.21	254.02	79.16
Z-8	230.48	259.51	89.44
Z-22	243.49	269.20	85.36
ZM53	243.33	269.09	96.03

5.4.3 Enthalpy–Silica Mixing Model

The disagreement between all geothermometers estimations suggest that the water is a mixture of hot thermal water and cold water of shallower depth. Therefore, to take account of the effect of mixing of different waters, the Enthalpy-silica diagrams (Truesdell and Fournier, 1977) can be used for better temperature estimations.

Under some conditions; no steam loss, no conductive cooling after mixing and the quartz is controlling the silica solubility in the high temperature water, the concentration of a mixed water and a silica-enthalpy diagram can be used to determine the temperature of the hot water component. In this diagram, a straight line drawn from a point representing the non-thermal component (cold wells) of a mixed water through the mixed water (thermal wells and springs) to the intersection with the quartz solubility curve gives the initial silica concentration and enthalpy of the hot-water component.

Figure-5.8 (A, B) , shows the silica concentrations in thermal water from Zara-Zarqa Ma'in thermal springs, lower aquifer (A) and in thermal wells water, upper aquifer (B). It can be seen from figure (A) that the maximum reservoir temperature in Zara-Zarqa Ma'in is about $105^{\circ}C$ and it is quite close to the estimated temperature ($111^{\circ}C$) concluded by Truesdell (1978) for the same springs field. Figure (B) shows that the reservoir temperature for the thermal wells ranges from 65 to $105^{\circ}C$ depending on the mixing ratio from the lower aquifer.
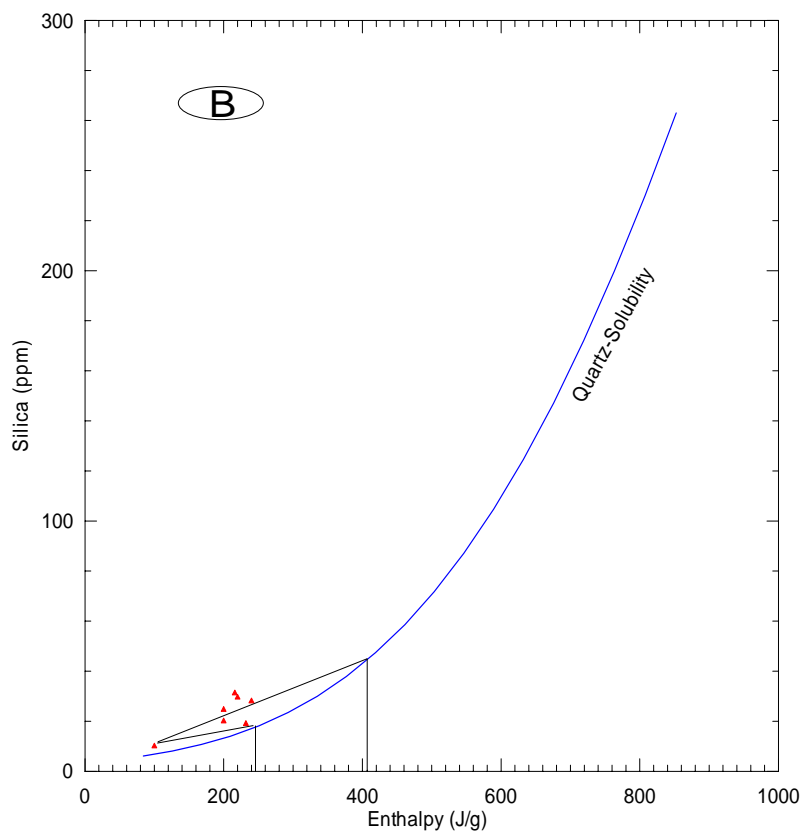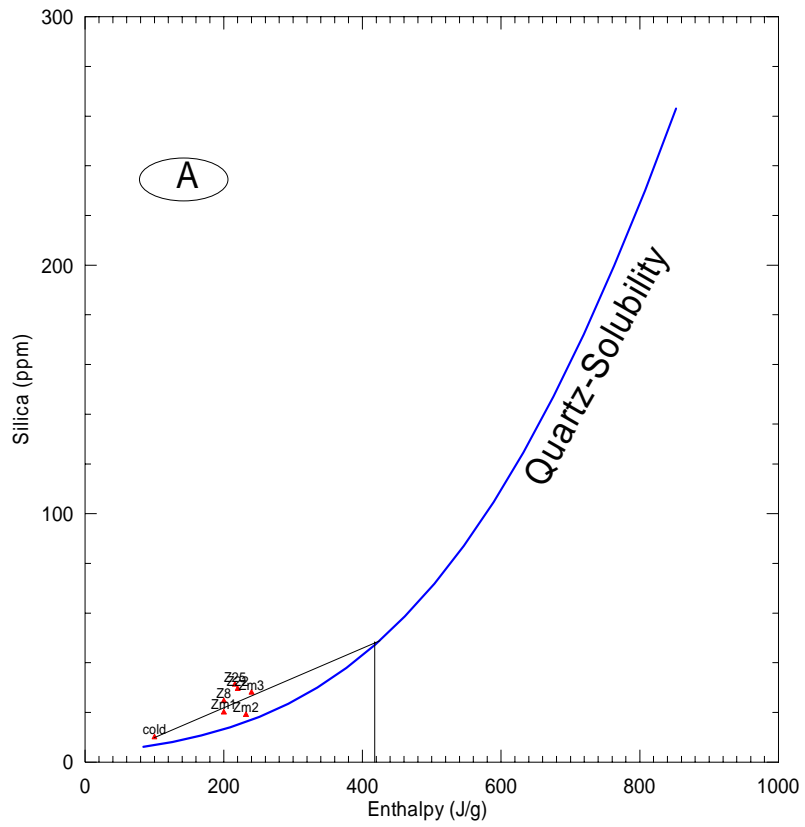
Figure-5.8: Silica-Enthalpy graphs for thermal water from the study area

5.5 Isotope analysis and thermal water origin

The stable isotope analysis of the samples (33 to39) from cold water wells in the recharge area, the samples (1 to 26) from the thermal water wells in the upper aquifer and the samples from the Zara–Zarqa Ma'in thermal springs, lower aquifer are shown in table-5.5. The table also shows the stable isotope content in two rainfall stations (Waleh and Rabba).

Isotopic data can well differentiate between the three possible types of thermal waters i.e. of magmatic, oceanic and meteoric origin. The $\delta^{18}O$ (V-SMOW) of all samples from the study area ranges from –6.71 to –3.88 ‰ with an average of -5.59‰ and –4.43 ‰ for the upper and the lower aquifers, respectively. The δ^2H of the upper aquifer ranges from –34.9 ‰ to –22.9 ‰ with an average of 29.18‰, while it ranges in the lower aquifer from -32‰ to –37.8 ‰ with an average of –34.9 ‰. These isotope values, do not show the presence of any significant amount of magmatic water which, generally, shows $\delta^{18}O$: +6 to +9 ‰ and δ^2H: -40 to –80‰ (Pearson et al. 1980). The possibility of oceanic origin of these waters is ruled out because the $\delta^{18}O$ and δ^2H of the oceanic water is about zero. Therefore, the origin of these waters is obviously meteoric.

A cross plot of $\delta^{18}O$ vs. δ^2H is shown in figure5.9 together with Global Meteoric Water Line (GMWL: $\delta^2H = 8^{18}O + 10$ %) after Craig (1961) and the Mediterranean Meteoric Water Line (MMWL: $\delta^2H = 8* {}^{18}O + 22$ %) after Dansgard (1971). All samples from cold and thermal wells from the upper aquifer are located between the MMWL and the GMWL on a line that originates from the MMWL indicating that the water origin is from the Mediterranean water type. The slope of this line is less than 8 indicating that the water has been either subject to evaporation or mixing with water of different origin. Water samples from the Zara-Zarqa Ma'in thermal springs (lower aquifer) fall below the GMWL with an oxygen shift. The oxygen shift takes place when oxygen isotopes are exchanged between hot rock and the circulation water at enhanced temperature. Generally, low temperature, high water–rock ratio and low interaction time result in a low oxygen isotope shift. If the $\delta^{18}O$ shift is neglected and the location of the lower aquifer samples (red stars) brought back to their origin, then the location of the thermal wells water samples (green triangles) of the upper aquifer become between the cold water (blue circles) of the upper aquifer and

the thermal water of the lower aquifer suggesting a mixing between the water of the two aquifers.

In a geothermal system, ^{34}S of sulphates with a magmatic origin ranges between 0‰ and +2‰ CDT (Canyon Diablo Troilite) and sulphates resulting from the dissolution of evaporates can have ^{34}S from +10 to +35‰ whereas in modern oceanic sulphates its value is about +20‰ (Krouse, 1980). Five samples (4,7,8,9,24) were analyzed for ^{34}S in PINSTECH labs, Pakistan in the year 2001. Their ^{34}S contents (Table-5.5) are in the range of +6.56 to +10.81‰, showing that the sulphates are neither of magmatic nor of modern oceanic origin. Samples 7, 8 and 24 indicate that the sulphates is a result of dissolution process of the evaporates mainly gypsum. While, samples 4 and 9 show lower values indicating that the major contribution of sulphates is derived from reduced sulphur compounds such as sulphide minerals and/or organic sulphides (Pearson et al. 1980). Also the reducing condition is confirmed by the linear relationship between the isotope content and the Eh values, more depleted water more negative Eh values.

The ^{34}S and Eh content of the samples indicates that sulphate in the thermal water results from both processes; dissolution and reduction.

TABLE-5.5: Isotope analysis of thermal wells, cold wells and springs from both aquifers as will as rain water samples :

Sample No.	$\partial\ ^{18}O$ ± 0.15	∂^2H ± 1.0	D ex	Tritium ±1	$\partial\ ^{13}C$ ± 0.15	^{14}C (PMC)	∂S^{34} (CDT)
1	-5.56	-26.3	18.1	<1	-12.62		
2	-6.6	-32.1	20.7	X			
3	-6.07	-31.4	17.2	X			
4	-6.4	-32	19.2	X			6.76
5	-5.61	-27.4	17.4	<1	-4.86	0.79	
6	-5.06	-25.3	15.1	X			
7	-5.67	-29.7	15.7	X			9.04
8	-6.33	-32.8	17.9	X			10.81
9	-6.44	-34.3	17.2	X			6.56
11	-6.6	-32.7	20.1	X			
12	-6.05	-32.1	16.3	X			
13	-6.03	-31	17.3	X			
14	-5.37	-27.8	15.2	X			
15	-5.07	-24.8	15.7	X			
16	-6.24	-32.1	17.8	X			
17	-6.44	-33.4	18.2	<1	-15.57	1.75	
18	-6.59	-33.5	19.2	X			
19	-6.71	-34.6	19	X			
20	-6.68	-34.2	18.8	X			
21	X	X	X	<1	-11.36	1.24± 0.6	
22	-5	-26.3	13.7	X			
24	-6.41	-34.9	16.4	<0.9	-14.8	0.6± 0.53	9.89
25	-5.35	-26.5	16.3	<0.7	-13.525	4.83± 0.54	
26	-5.3	-26.2	16.2	X			
33	-4.85	-24.1	14.7	1.5			
34	-5.12	-25.6	15.4	1.9			
35	-5.28	-25.7	16.5	1.7			
36	-5.51	-25.2	18.9	3.7			
37	-5.31	-26.7	15.8	5.3			
38	-4.95	-22.9	16.7	1.8			
39	-5.24	-23.9	18	2.7			
40	-5.19	-22.9	18.6	2.5			
41	-5.16	-25.9	15.4	1.5			
42	-5.99	-31.4	16.5	1.1			
43	-6.21	-32.7	17	<1			
44/Zm8	-3.88	-32	-0.96	2.7			
45/Z25	-4.99	-37.8	2.12	<1			
Rain Airport	-6.1	-24.5					
Rain Rabba	-5.6	-21.5					
Rain Waleh	-5.4	-22.4					
Kurnub Sst.	-6.6	-45.2					
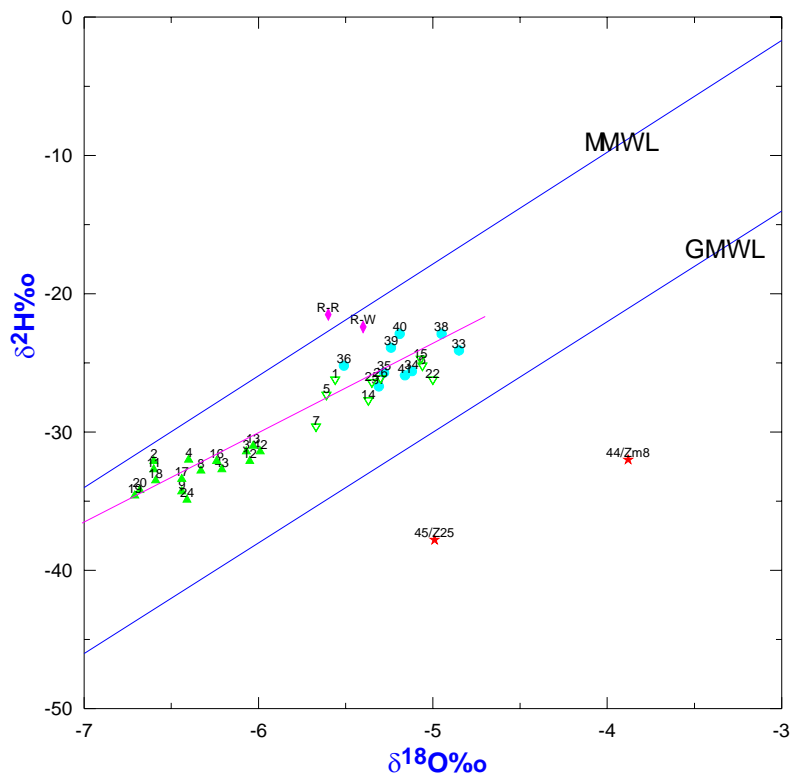
Figure-5.9: Stable isotopes content of rain water (violet rhombs), thermal wells (green triangles), cold water wells in recharge areas (blue circles) and the thermal springs water of Zara and Zarqa Ma'in (red stars).

5.6 Age of the thermal water

The radioactive ^{14}C as a dating method can date carbon-containing material from the last 50,000 to 60,000 years. Generally, carbon in groundwater can be derived from several different sources such as atmospheric CO_2 , soil CO_2 of organic origin, CO_2 leached from rocks and from magmatic sources in volcanic areas. Age based on the ^{14}C method shows the time since groundwater became isolated from the atmosphere and the soil zone.

The age of the thermal water in five samples 5,17,21,24 and 25 (Table-5.4) ranges from 20,000 and 37,000 years. The age increases along the groundwater flow path from northwest towards the southeast. This is in agreement with the other models which suggests that the mixing of the thermal water is taking place in the south-eastern parts of the study area where more older water is flowing up along the faults and mixing with the upper aquifer water.

5.7 Mixing Assessment

Thermal water resulting from mixing between geothermal water and cold groundwater or surface water may possess chemical characteristics, which serve to distinguish it from unmixed geothermal water. This is because the chemistry of the geothermal water is characterized by equilibrium conditions between solutes and alteration minerals, while the composition of the cold water appears mainly to be determined by the kinetics of leaching process. The final chemical composition of the mixed water is governed by the residence time in the bedrock after mixing, temperature and salinity of the mixed water. The main chemical properties of the mixed thermal waters which serve to distinguish them from equilibrated geothermal waters, include: relatively high concentration of silica in relation to discharge temperatures, low pH relative to the water salinity and high total carbonate (Arnorsson, 1985).

Chemical and isotope composition of the thermal water from the thermal wells in the study area strongly suggest mixing due to the following reasons:

1- The location of high Cl concentrations along Daba'a and Wadi Al Hammam faults suggests that these faults are the main up flow zones of thermal water from the lower to the upper aquifer (Figure-5.2).

2- On the Cl- SO_4- HCO_3 diagram (Figure-5.4), most of the thermal water samples (triangles) show a mixing trend between the thermal water samples (red stars) of the lower aquifer and the upper aquifer water samples from the cold water wells (blue circles) in the recharge area.

3- On Schoeller graph (Figure-5. 5) the thermal wells samples fall between the recharge wells samples and the thermal springs samples.

4- On Durov diagram (Figure-5.6) thermal wells samples fall in the mixing zone (Zone 5).

5- The positive relationships between Cl and B, Br, SiO_2, SO_4, Li, Mg, Ca, K and Na is an indication for mixing (figure-5.10) between the two aquifers.

In addition the following observations may also support the mixing process:

On the Na- K- Mg diagram all thermal water samples fall in the partial equilibrated mixed water area (Figure-5.7). The disagreement among all the geothermometers used in estimating the reservoir temperature may results from mixing between water of the two aquifers without water-rock re-equilibration after mixing.

On the graph of $\delta^{18}O$ vs δ^2H (Figure-5.9) the thermal water samples of the upper aquifer fall on a line with a slope of less than 8 indicating that the thermal water is either subject to evaporation or that mixing of water of different genesis is taking place. The evaporation process is ruled out by the negative relationship between ^{18}O and Cl , and the absence of the negative relation between ^{18}O and temperature (Figure-5.11), which indicates mixing process.

The positive relations of temperature versus Cl and temperature versus F indicate mixing between the two aquifers in the study area (Figure-5.12).
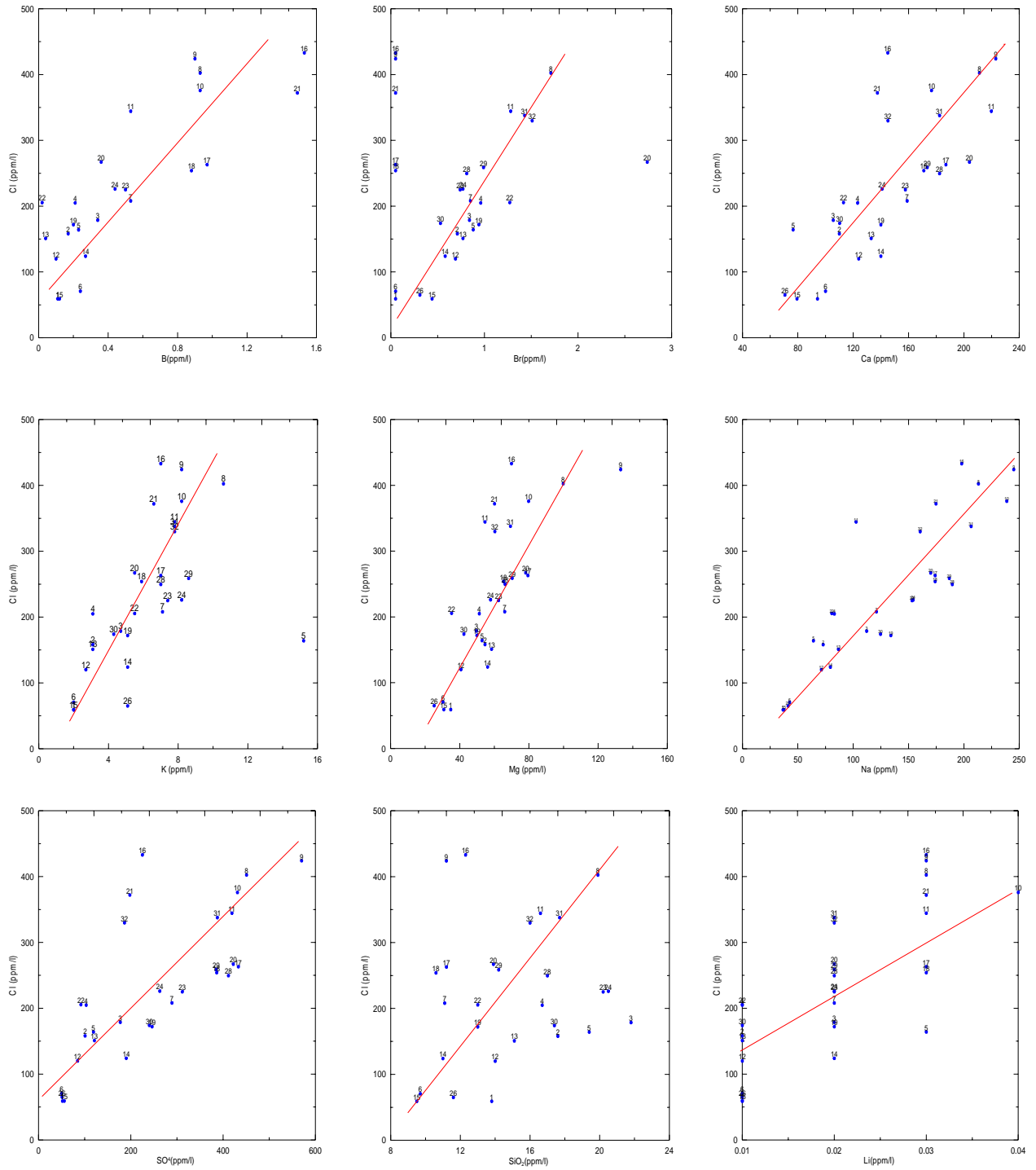
Figure-5.10: Relationships between Cl and Na, Br, Li, SiO$_2$, SO$_4$, Mg, Ca, K and B
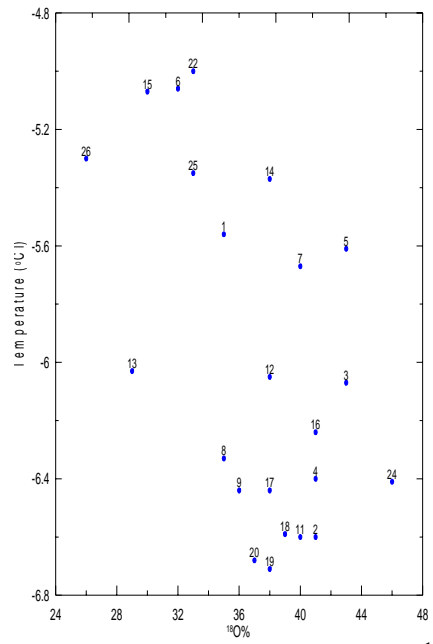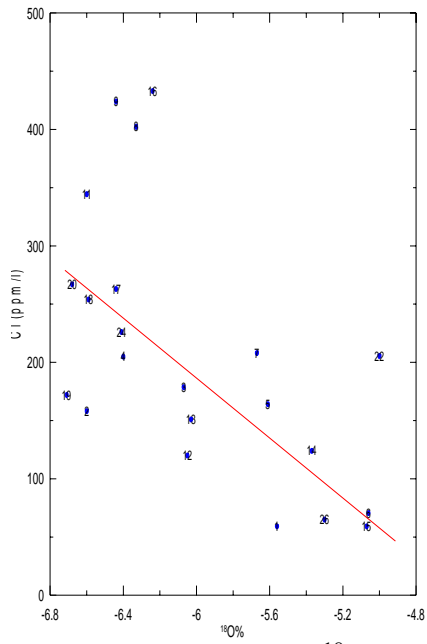
Figure-5.11: Cl versus ^{18}O negative relation and the non-negative relation of ^{18}O versus temperature
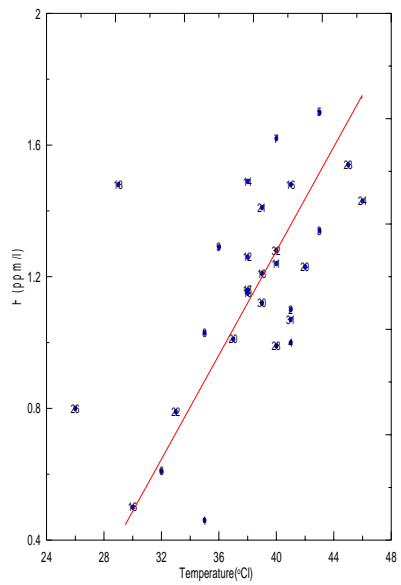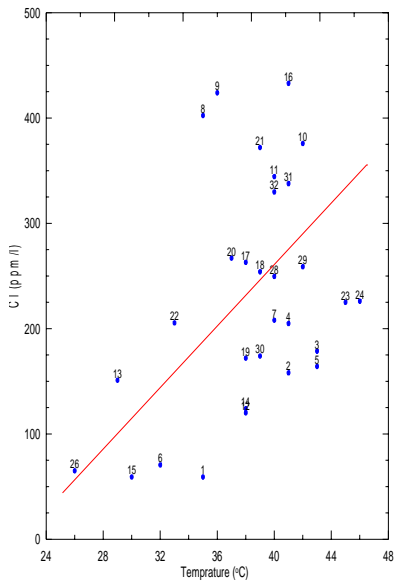
Figure-5.12: Temperature versus Cl and F relationship

6. MODELING

6.1 General background on modeling

Analytical and numerical methods were used to obtain solutions to a mathematical model of groundwater flow or solute transport.

The flow of groundwater in an aquifer is described by two basic equations; these are Darcy's Law and the continuity equation. The storage parameters of an aquifer material and the permeability are used in these equations to describe groundwater flow. The boundary conditions must be described and for transient solution it is necessary to specify the starting conditions. The solution to the equations is normally required in the form of the head in the aquifer at specific place and time.

Generally, a number of assumptions has to be made about the aquifer in order to analytically solve the equations. The most common assumptions are those regarding the uniformity of the aquifer properties and the aquifer geometry. The boundary conditions also have to be set in a simple way, i.e. the aquifer is assumed to be of infinite extent or bounded by no flow boundaries. Therefore, with analytical solutions the complexity of aquifer geometry, boundary conditions and aquifer properties can't be properly represented. When these parameters are important in the problem under consideration, then the numerical solutions to the equations probably give the correct solution.

Numerical solutions are based on the discretisation of space and time into 'blocks', where the various parameters do not vary within each block. Two main methods are commonly used to discretise the spatial dimensions of the aquifer. These are the finite-difference and the finite-element, which are the most commonly used in groundwater modeling. The problem to be solved and the desire of the user determine which method should be used.

The finite difference was initially applied to the flow of fluids in petroleum reservoirs. Then, it was applied to the groundwater flow and solute transport in the mid-1960's (Ashcroft et al. 1962; Remson et al. 1965 and others). The method is easier to understand,

a specific program and in general fewer input data are needed to create a finite difference grid. The method works best for rectangular or prismatic aquifer uniform composition and the accuracy of solutions to solute transport problems is lower than that of the finite element method.

The finite element method was first used to solve groundwater flow and solute transport problems in the early 1970's (Zienkiewicz et al. 1966; Price et al. 1968; Zienkiewicz, 1971 and others). With finite element, irregular shaped boundary, an-isotropic and heterogeneous aquifers properties can be easily incorporated to the numerical model. Also, it is easier to adjust the size of individual elements as well as the location of boundaries, making it easier to test the effect of nodal spacing on the solution. Finite elements are better in handling internal boundaries and can simulate point sources and sinks, seepage faces and moving water tables (Istok, 1989).

On regional scales (10's–1000's of kilometers), numerical models are used to help in aquifer resources management. Generally they are 2D models with a fairly course grid spacing. Regional models usually overcome the problem of defining realistic boundaries by extending to the geographical extremities of the aquifer. The required input data of the aquifer properties are average values over large areas. Usually, the model is calibrated by comparing it's output with water level maps and, where appropriate, with river flow hydrographs.

To investigate the aquifer behavior in the vicinity of pumping wells, radial flow models are usually used (Near well simulations). Where it is assumed that the regional behavior of the groundwater has little effect compared to the effect of the pumping in the vicinity of the well (Anderson and Woessner, 1992).

Numerical models are often used for predicting the effect of future changes on the aquifer system. This may be for management purposes or for water resources protection. Resources management models are generally regional, transient models. It is essential to consider the effects of uncertainty when predictions are made on the basis of the model output. Therefore, it is useful to perform a series of model runs using a variety of possible values for the most influential parameters (Monte Carlo Simulation).

Also, numerical models can be used in contaminant transport problems; this can be carried out in two ways. The first is to use the model to determine the value of dispersion coefficients for an aquifer where data of pollutant concentrations are known. The second is to predict the possible pathways for pollutants should spill or leak occurs. The contaminant transport models are used to delineate the protection zones .

Setting up and running a model requires a large amount of data. Depending on the model, the input data include; the boundary conditions, recharge rates, hydraulic conductivity, storage coefficient, effective porosity, specific yield, transport parameters (dispersion coefficients, adsorption isotherms and decay coefficient) and river/aquifer interactions where rivers form the main natural out flow of the aquifer (Anderson and Woessner,1992).

Object-oriented (OO) software concepts become more and more important in order to meet scientific computing challenges, such as the treatment of coupled non-linear multi-field problems with extremely high resolutions. The implementation of numerical methods involving geometrical description of geo-systems with the application of numerical meshes is of vital importance for investigation and modeling of complex coupled natural or man-induced processes. Innovative application of CAD-Systems in combination with computer aided modeling of such systems provides a user-friendly powerful tool for the often-complex geometrical descriptions necessary for comprehensive modeling of the dominant processes (Kolditz et al. 2003).

In the course of this study the GeoSys/RockFlow scientific modeling software (Kolditz et al. 2003) is used in two applications: firstly to model (2D) the water flow and heat transport across one of the major faults (Kolditz et al. 2004). Secondly to develop a 3D numerical groundwater flow and heat transport model, based on GIS Project, for the whole investigated area. This is the first application of using the GeoSys/RockFlow Software to model the groundwater flow and heat transport based on GIS Project (Sawarieh et al. 2004). Where the hydrogeological conceptual model of the study area is converted to shape files (GIS Project) using the ArcGIS software. All required data for modeling, such as aquifer geometry, boundary conditions, material properties, well positions and pumping rates etc. are kept in the GIS Project. These data are directly imported to GeoSys for modeling purposes.

6.2 GeoSys concept

The GeoSys software concept consists of three components (Libs), which are connected via a graphical user interface (GUI), (Kolditz et al. 2003). These components are described below:

1- GeoLib:

The GeoLib contains basic geometric objects such as points, lines, polylines, surfaces, and volumes, which form domains. All these geometric entities are implemented as C++ classes: CGEO Point, CGEO Polyline, CGEO Surface, CGEO Volume, CGEO Domain. Examples of these objects can alternatively be stored in vectors and lists for convenience and specific purposes.

2- MshLib:

The MshLib contains the basic topological objects such as finite elements (triangles, tetrahedral, hexahedral etc.), which form the basis for mesh generation.
For the meshing of complex geo-systems such as fractured and karstified aquifers very flexible mesh generators are necessary. Currently, the following build-in mesh generators can be used: PrisGen, TetMesh as well as open and commercial systems such as Gmsh and gOcad.

3- FEMLib:

This concept contains numerical methods for solving partial differential equations (PDEs) for example, the finite element method. It has been applied for a large variety of situations in geo-system modeling such as geo-technical, geothermal, geochemical and geo-hydrological problems. In this study, the concept is focused on the groundwater and geothermal modeling.

6.3 GeoSys theoretical background

6.3.1 Multi-field problems

In multi-field problems, several types of processes might be involved such as flow (hydraulic), heat (thermal) and component transport (componential) as well as deformation (mechanic). These processes are described by different types of partial differential equations (PDEs); parabolic, mixed parabolic-hyperbolic, and Elliptic. The PDEs are derived from the basic conservation principles of mass and energy together with the corresponding material laws. Associated with each PDE are the corresponding initial and boundary conditions, as well as the appropriate numerical and solution techniques (Kolditz et al. 2003).

The general form of the microscopic differential balance equation of an extensive thermodynamic property (e.g. mass, linear momentum, energy) is given by

$$\partial e/\partial t + \nabla . (ev^E) = \rho f^E \quad \ldots\ldots\ldots\ldots\ldots\ldots\ldots\ldots\ldots\ldots\ldots\ldots\ldots\ldots\ldots(1)$$

Where: e is the density of an extensive thermodynamic quantity E, t is time, v^E is particle velocity of E properties, ρf^E is a source term of E.

Equation (1) is a classical balance law of continuum mechanics expressing the conservation principle of any thermodynamic property.

Considering a continuum consisting of a number of particles: a representative velocity of the continuum must replace the particle velocity, which will be a certain average velocity of a cloud of particles (e.g. mass or volume-weighted velocities). So, the total flux of an extensive quantity E may be sub-divided into two parts: an advective flux ($\nabla.(ev^c)$) corresponding to an average velocity, and a diffusive flux ($\nabla.J$) relative to this average velocity. Then the balance law takes the general form:

$$\partial e/\partial t + \nabla . (ev^c) + \nabla . J = \rho f^E \quad \ldots\ldots\ldots\ldots\ldots\ldots\ldots\ldots\ldots\ldots\ldots(2)$$

This universal description of any physical process in terms of a general balance equation is the basis for the process-orientation of multi-field problems.

6.3.2 Density-dependent flows in confined/unconfined aquifers

A summary of the governing equations of variable-density groundwater flow and solute transport based on the general balance equation (2) is presented (Kolditz et al. 2003). Employing the equations of state for the bulk fluid density and porosity, the mass balance equation of the fluid phase can be written as:

$$\rho S_0{}^P (\partial p/\partial t) + \nabla. (\rho n v) = \rho Q_\rho - \rho n \beta_\omega (\partial \omega/\partial t) \dots\dots\dots\dots\dots\dots\dots\dots\dots(3)$$

Where: ρ is water density, $S_0{}^P$ is storage coefficient, p is water pressure, t is time, n is porosity, v is pore water velocity, Q_ρ is source term, β_ω is an expansion coefficient and ω is salt mass fraction.

The momentum balance equation for variable-density fluid flow in a porous medium leads to the generalized form of Darcy's law:

$$q = n v = -(k/\mu) . (\nabla P - \rho g)$$
$$\dots\dots\dots\dots\dots\dots\dots\dots\dots\dots\dots\dots\dots\dots\dots\dots\dots\dots(4)$$

Where: k is permeability tensor, μ is water viscosity, g is gravity vector, p is water pressure, ρ is water density and n is porosity .

If density and porosity variations are neglected for the balance equation of the solute mass conservation, salt mass conservation can be written in a simplified form:

$$n(\partial C/\partial t) + n v . \nabla C - \nabla. (n D . \nabla C) + C Q_\rho = Q_C \dots\dots\dots\dots\dots\dots\dots\dots.(5)$$

Where: n is porosity, v is fluid velocity, t is time, C is salt concentration, Q_ρ is source term, Q_C is salt mass and D is a diffusion-dispersion coefficient.

For the case of heat transport, the governing equation can be obtained based on the heat balance equation for the porous medium consisting of two phases, i.e. the solid and the liquid phase. The following thermal energy equation for the temperature T is obtained:

$$((1 - n) c^s \rho^s + n c^l \rho^l) (\partial T/\partial t) + (c^l \rho^l n v \nabla T) - ((1-n) \lambda^s + n \lambda^l) \nabla^2 T = Q_T \dots\dots(6)$$

Where: n is porosity, t is time, ρ is fluid density, c is thermal capacity, λ is thermal conductivity, v is fluid velocity and Q_T is the heat source term. The superscripts l and s refer to the liquid and the solid phase respectively.

6.4 Model setup

6.4.1 Model domain information

The study area is located in the central part of Jordan, east of the Dead Sea and covers the northern third of the Wadi Mujib groundwater catchment and Wadi Zarqa Ma'in sub-catchment with total area of about 2300 km^2 (Figure-1.2).

The area consists of two major aquifer systems: the upper and the lower. The upper aquifer (B_2/A_7) is mainly recharged along the northern and northwestern parts of the study area where it crops out and receive the highest rainfall averages, 250–400 mm/y (cf. chapter 3). Another recharge enters the area in the southeastern part of the study area and flows into the area from the southern part of Wadi Mujib catchment. In Wadi Waleh sub-catchment the long term (1975-2003) infiltration average amounts to 21.5 MCM/y as 6% of the average total rainfall (357MCM/y) for the same period (Rimawi, 2004). The direct and indirect recharge to Wadi Zarqa Ma'in sub-catchment is amount to 6 MCM/Y (Abu Ajameih, 1980). The groundwater within this aquifer flows mainly from north (recharge area) to south then to the west and from south to north then join the other flow to the west. Part of the water flows further to the east towards the Azraq groundwater catchment (Figure-3.12). The main natural outlets from the aquifer are the Heidan springs and the Zarqa Ma'in spring with an average annual discharge of about 15.09 MCM/y and 0.7 MCM/y respectively (WAJ open files).

The lower aquifer consists mainly of sandstone of Lower Cretaceous and older ages. The major contribution to the aquifer recharge comes from the upper aquifer by water infiltration, mainly in the eastern parts of Jordan. The infiltrated water receives heat under a normal to slightly elevated geothermal gradient and flows to the west towards the Dead Sea, where it enters the Dead Sea as subsurface flow or discharges to the ground surface as thermal springs, as in Zara and Zarqa Ma'in springs. The average discharge of the Zara-Zarqa Ma'in thermal springs amount to 20 MCM/y (Salameh and Udluft, 1985). The lower aquifer discharge about 5 MCM/y along the lower part of Wadi Heidan, increasing the total discharge in the wadi to about 23 MCM/y at the confluence with Wadi Mujib.

In the last three decades about 300 wells were drilled to the upper aquifer in the study area. The private sector drilled most of these wells for agricultural purposes and the rest by the government for drinking purposes. Wells drilled mainly east and south east of Jiza town discharge thermal water ranging in temperatures from 30 to 46°C. The average annual discharge of all wells is about 35.6MCM/y.

The dense faults net affecting the area, strongly suggested that the two-aquifer systems, upper and lower are hydraulically connected, especially in the eastern parts of the study area. This allows the thermal water in the lower aquifer to flow up via faults (conduits) to the upper aquifer. The isotope content indicates that the thermal water in both aquifers is of meteoric origin. The chemical analysis and the isotope content of the thermal water of the upper aquifer show that it is a result of mixing process between waters from upper and lower aquifers (cf. chapter 5).

6.4.2 GIS project

The first step in setting up the model is creating the GIS Project, where geological data of the study area such as the geological formations, faults, wadis and the hydrogeological data like aquifers, aquitards, wells, water table, top and base of aquifers and boundary conditions were converted to shape files (layers) using the ArcGIS software (digitizing feature) and kept in this project. These layers are described below:

6.4.2.1 Hydrological units

The sedimentary sequence, which covers the study area, is grouped into four divisions. These are from bottom to top: the lower aquifer (the Kurnub sandstone formation and the sandstone of older ages), the aquitard (A1-6 marl and marly limestones formations), the upper aquifer (B2/A7 limestone formations) and the confining beds (B3 and B4 chalk and marly limestone formations). Figure-6.1 shows the simplified surface distribution of these units.
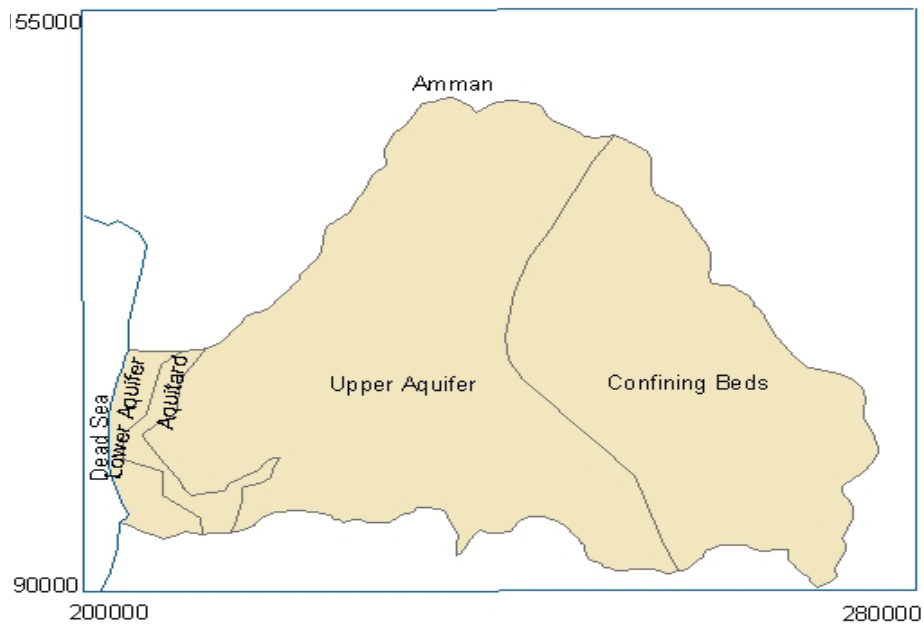
Figure-6.1: Surface distribution layer of the hydrological units in the study area

6.4.2.2 Wadis and springs

The study area is drained westwards to the Dead Sea by two major wadis: Wadi Zarqa Ma'in and Wadi Waleh/Heidan and their numerous tributaries such as Wadi Ez Za'afaran and Wadi Es Sufuq. The tributaries are dry except for a short period after rainfall. Perennial base flow is seen only on the lowest reaches down stream of Wadi Waleh/Heidan, between the elevations 450 and 250m where the major springs group (Heidan springs) is located at an elevation of 350m and on the lowest reaches of Wadi Zarqa Ma'in from a short distance east of the Zarqa Ma'in thermal springs at elevation of about 200m (Al Zarqa spring). Figure-6.2 shows the model domain including the layers of the major wadis and springs discharging from the upper aquifer.

6.4.2.3 Faults
The study area is highly affected by faults especially in the eastern part. Figure- 6.3 shows the major faults layer in the model domain (Zarqa Ma'in, Jiza, Ez Za'afaran, Masattarat, Daba'a, Falij and Wadi Al Hammam). Daba'a, Masattarat and Wadi Al Hammam faults have tensional forces (Diabat and Masri, 2002), which allow them to act as conduits for the thermal water of the lower aquifer to flow up and mix with the upper aquifer water, raising the temperature of the water in the vicinity of these faults.

102

Figure-6.2: Major wadis and springs layers in the model domain
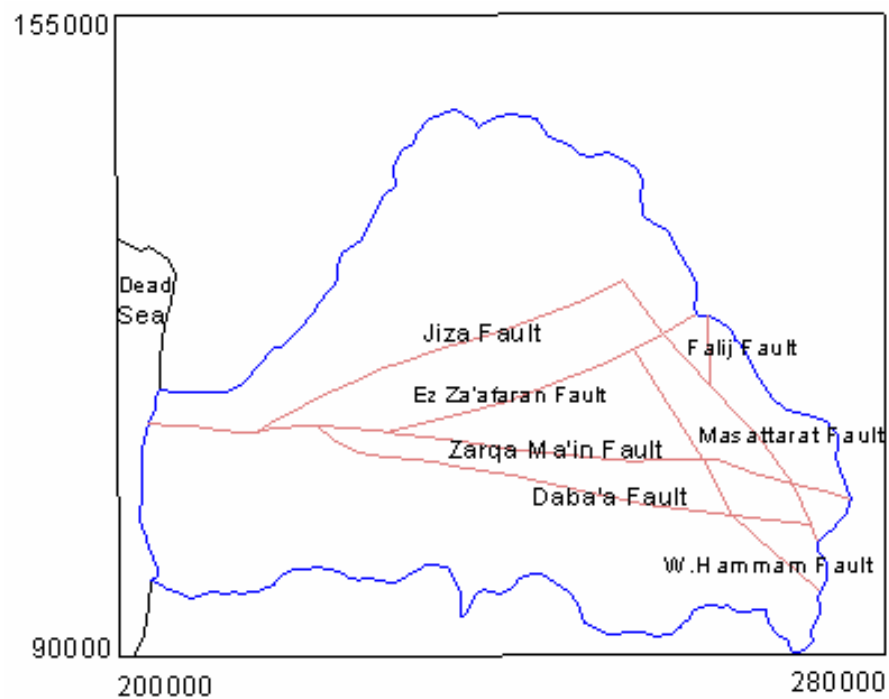
Figure- 6.3: Major faults layer in the model domain

6.4.2.4 Wells location

During the last three decades more than 300 wells were drilled in the study area.   The majority of these wells are private wells, which have been drilled for agricultural purposes. The Government drilled several well fields (Qastal, Waleh, Heidan,…etc.) for drinking purposes, mainly pumped to the Capital City.   The location of 298 wells, that have pumping records for the five years period (1999-2003) is shown in figure-6.4.   The five years (1999-2003) average pumping rate for these wells amounts to 35.6 MCM/y.
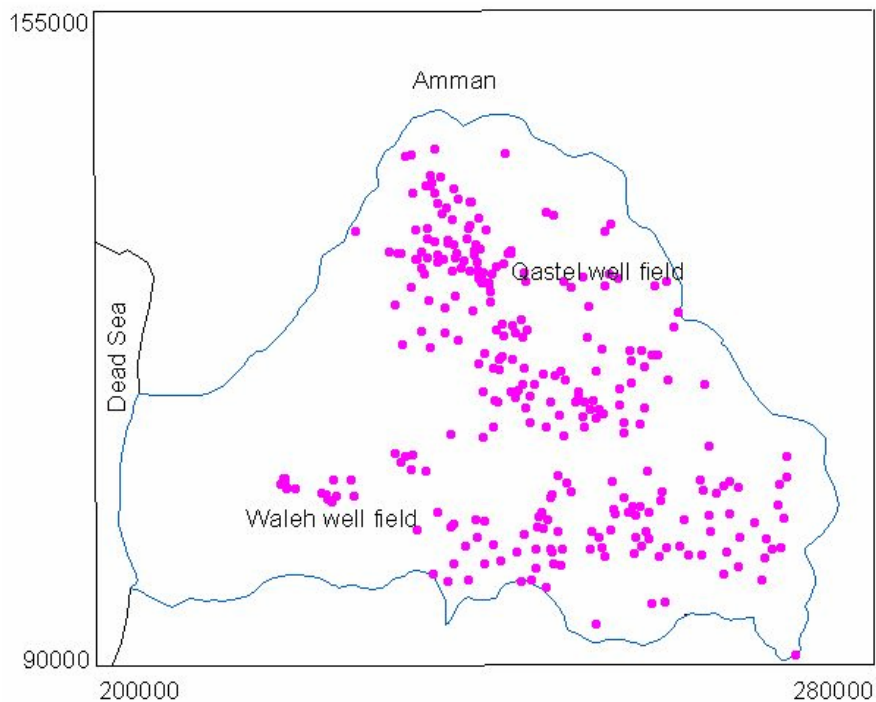
Figure-6.4: Wells location layer in the model domain

6.4.2.5 Water level contour map

The water level measurements in 1985 are used to represent the steady state conditions in the aquifer i.e. before the heavy pumping from the aquifer was started.   Therefore, the available water level measurements are used in constructing a water level contour map for the upper aquifer system (Figure-6.5).
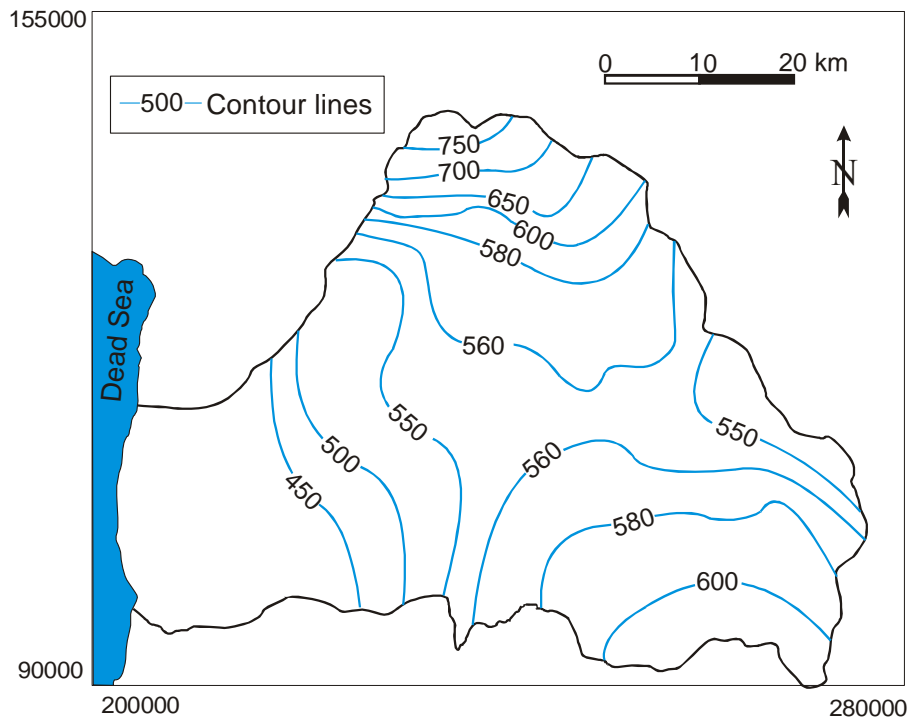
Figure-6.5: Water level contour map layer for the upper aquifer before development (steady state)

6.4.2.6 The study area domain

The whole study domain is subdivided into 29 areas (surfaces) by adding the major faults and wadis to the hydrological units. 22 surfaces representing the upper aquifer system (0-21), 3 surfaces formed the aquitard and 4 representing the lower aquifer system (Figure-6.6). The hydraulic conductivity values computed from all wells located in each surface is averaged and given as a hydraulic conductivity value for that surface.
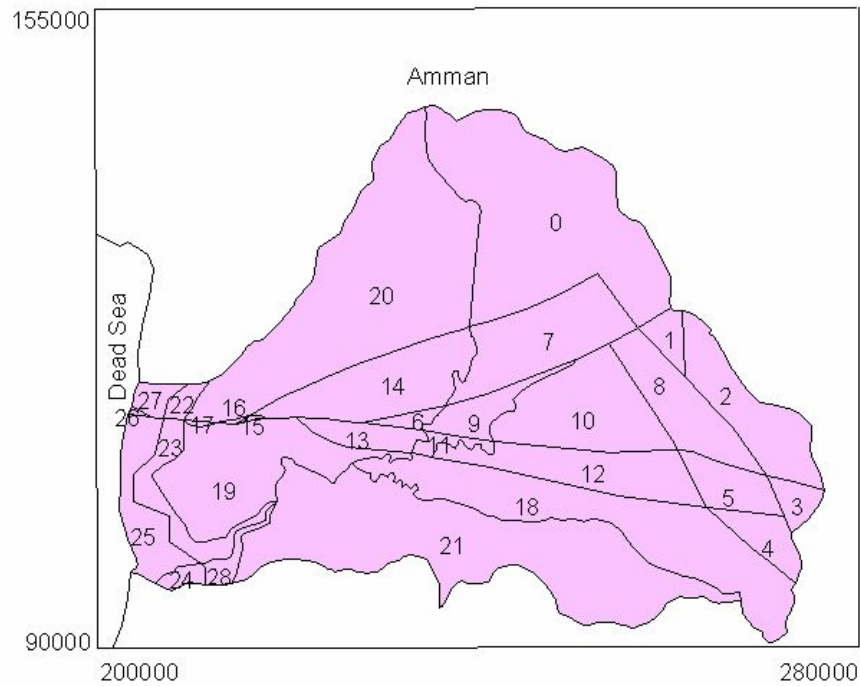
Figure 6.6: The study area modelling domain (surfaces)

6.4.2.7 Boundary conditions

Recharge boundary is set at the northern and western highlands, where the major recharging points are located. A no-flow boundary is set along the western border except for the main discharging outlets (Heidan springs and Al Zarqa spring) in the lower reaches of the wadi. An out-flow boundary is set along the eastern boundary, where the water is leaving the system to the Azraq groundwater basin in the east. The southern border is divided into two parts: recharge boundary in the southern eastern corner and no-flow boundary in the western part (Figure-6.7).

106
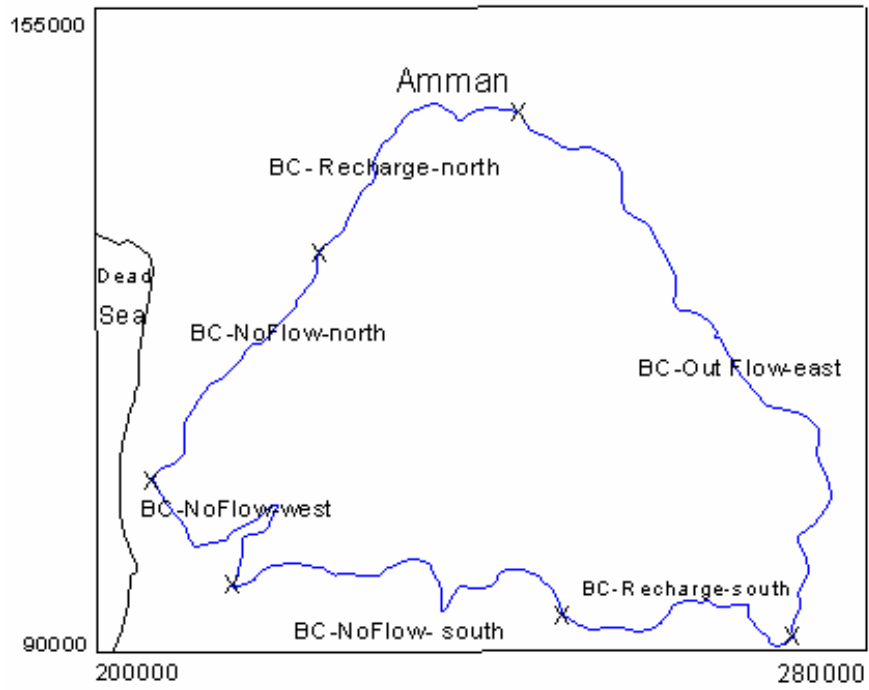
Figure-6.7: Boundary condition layer of the upper aquifer system

Boundary conditions for the lower aquifer are set as no-flow boundary condition at the northern and southern borders, recharge-flow boundary at the eastern border and out-flow boundary at the western border (Figure-6.8).
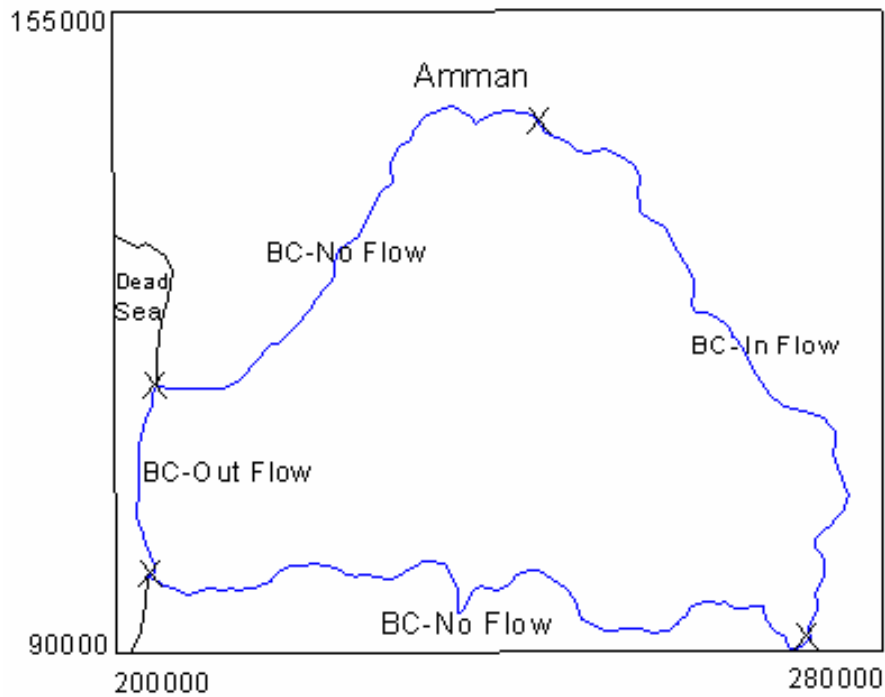
Figure-6.8: Boundary condition layer of the lower aquifer system

107

6.4.3 GeoSys project

The second step is the GeoSys Project (GSProject) creation, as follows:

 New project file is created in GeoSys and saved. All the data reference for the model such as geometry data (GSProject.gli), meshing data (GSProject.rfi), processing data (GSProject.rfo), are stored in this project file (Jordan Project File) to keep the connection between the project and its data components.

6.4.3.1 Geometry data

In this step, shape files in GIS Project are imported into GeoSys/RockFlow and converted into their own geometric data structure (GeoLib) as basic geometric data for the modeling area. The geometry file (GSProject.gli) is the input data format for GeoLib. It is composed of points, polylines, surfaces, volumes and domains. Point is the basic element of all other geometry type, which is used to define 1D geometry elements like: source terms (springs and wells), boundary condition. Figure-6.9 shows the points display after removing the double points.
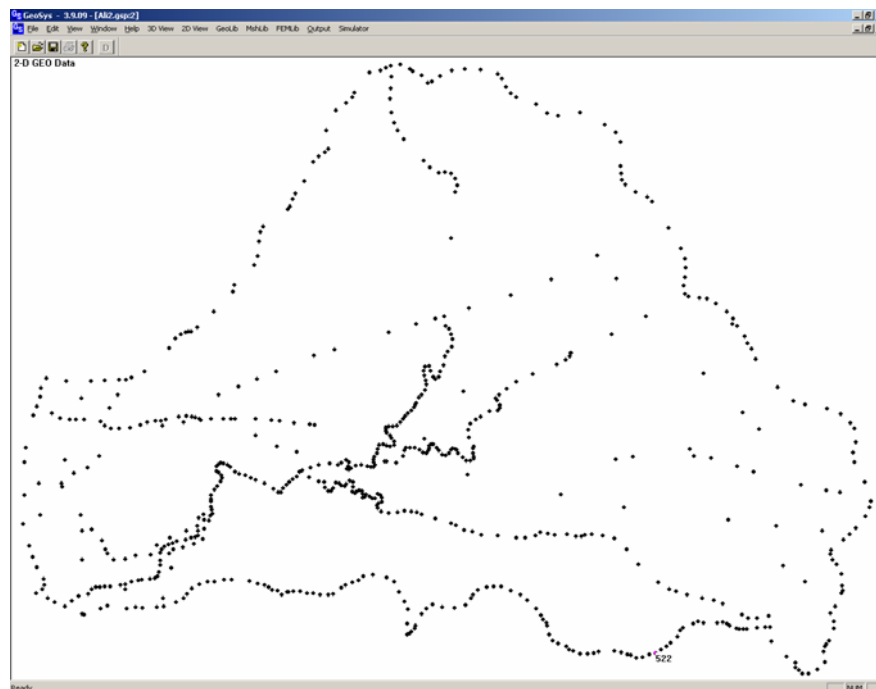
Figure-6.9: The point's display in GEO View

Polyline consists of points and it is used to define 2D geometric elements as; boundary of study domain, boundary to assign boundary condition and line structures (faults). The surface is composed of one closed polyline and used as 2D boundary domain. The volume is composed of surfaces and it is the component of the domain.

The whole study area (domain) is subdivided into 29 parts, which means surfaces in GeoSys Project. One surface could be created from one closed polyline (polygon) or from several polylines, which form a closed area. In this study, each surface is created from one closed polyline, i.e. the last point of the polyline is connected to the first one. Figure-6.10 shows the created surfaces with different colors and their names on the center of each one.
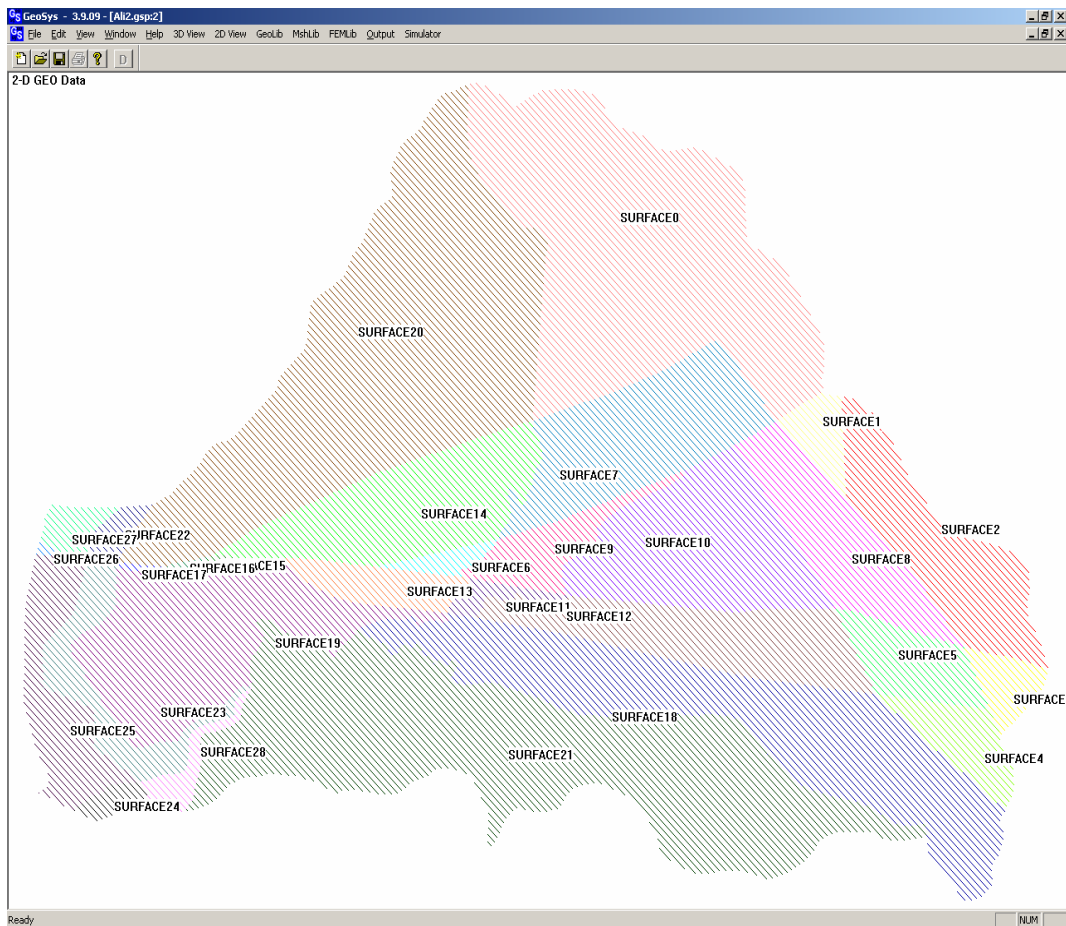
Figure- 6.10: Surfaces display with their names

After having the surfaces ready, the meshing generation is the following step by using an external program (GMSH), which creates triangulations for all 2D surfaces. The results are stored in RFI file, which consists of geometric information of nodes and elements of the triangulations. The existing triangulation is needed to create the TINs (triangulated irregular networks) for the discrete geometric description of surfaces and then for volumes as well.

Each TIN file has the same base name of the corresponding surface (surface_name.tin). The conceptual model of the study domain consists of three layers: the upper aquifer, the lower aquifer and the aquitard in between. So three copies of the surfaces are needed to create 3D layer model based on the TINs for the original 2D model. Figure-6.11 shows the volume objects of the 3D geometric model
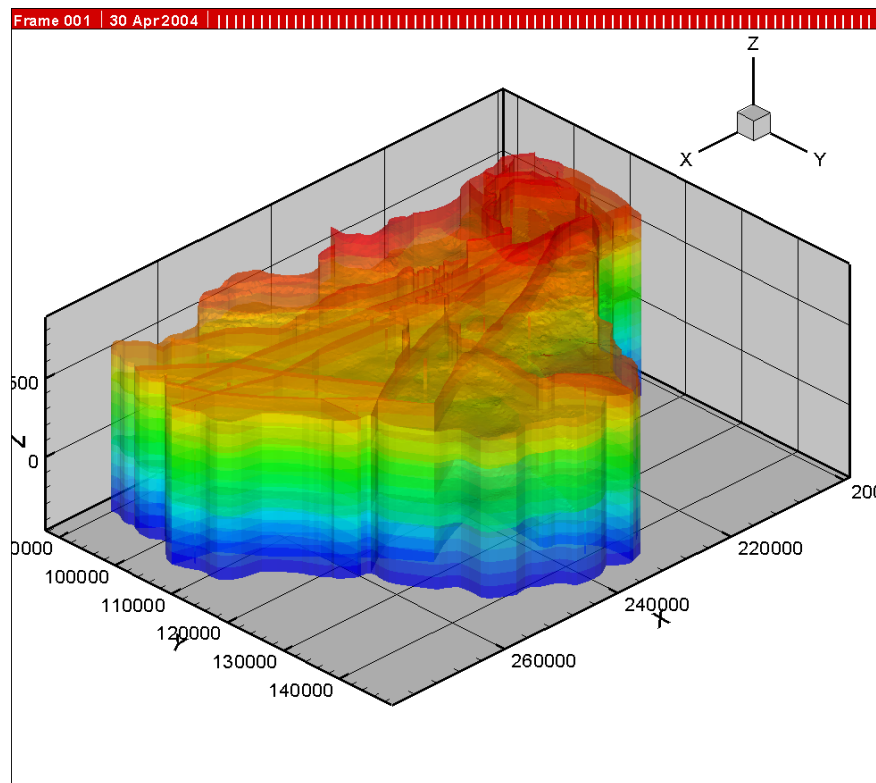
Figure-6.11: The volume objects of the 3D geometric model

110

6.4.3.2 Meshing data

The general steps for the hybrid meshing procedure in this application are:

1- Create a triangulation based on surfaces for the 2D surface model. The surfaces must be topologically consistent.

2- Create the line elements for the 1D Wadis model based on the triangulation.

3- Create the prismatic elements for the 3D subsurface model by extending the triangles to the vertical direction.

4- Create the quadrilateral elements for the 2D fracture/faults model.

All the above created elements are added to the existing (.rfi) file with triangulations. Figure-6.12 shows the 2D finite element mesh.
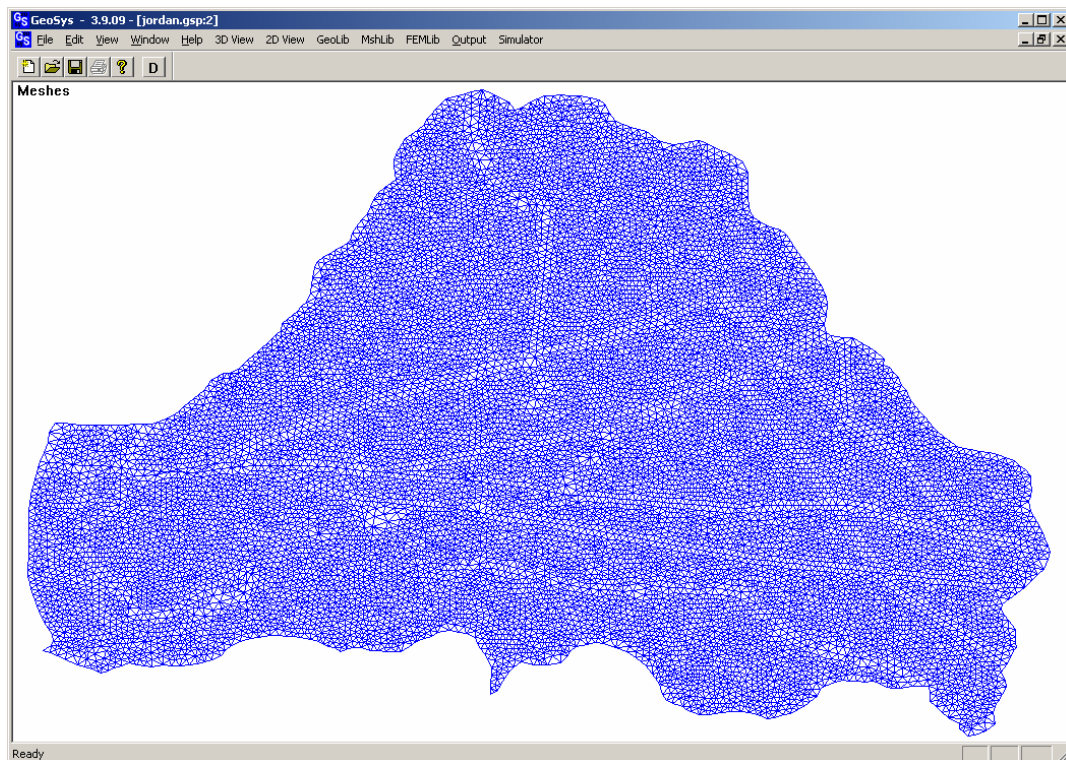
Figure-12: The 2D finite element mesh

Surface mapping is the process of making the mesh conforms to stratigraphic irregularities, i.e. thickness and orientation of the mesh slices can be deformed. The types of mapping data, which can be used, are grid files created by either Surfer or Arc View and saved as asc files. Four grid files have been created for the upper aquifer (B2/A7) and the lower aquifer (Ks). These files are: top_b2a7.asc, base_b2a7.asc, top_ks.asc and base_ks.asc. The files: base_b2a7.asc and top_ks.asc represent the top and the base of the aquitard in-between.

Figure-6.13 shows the mapped (inside the hybrid) finite element mesh including; line, triangle, quadrilateral and prismatic elements to represent the wadis, surfaces, faults as well as aquifers and aquitards.
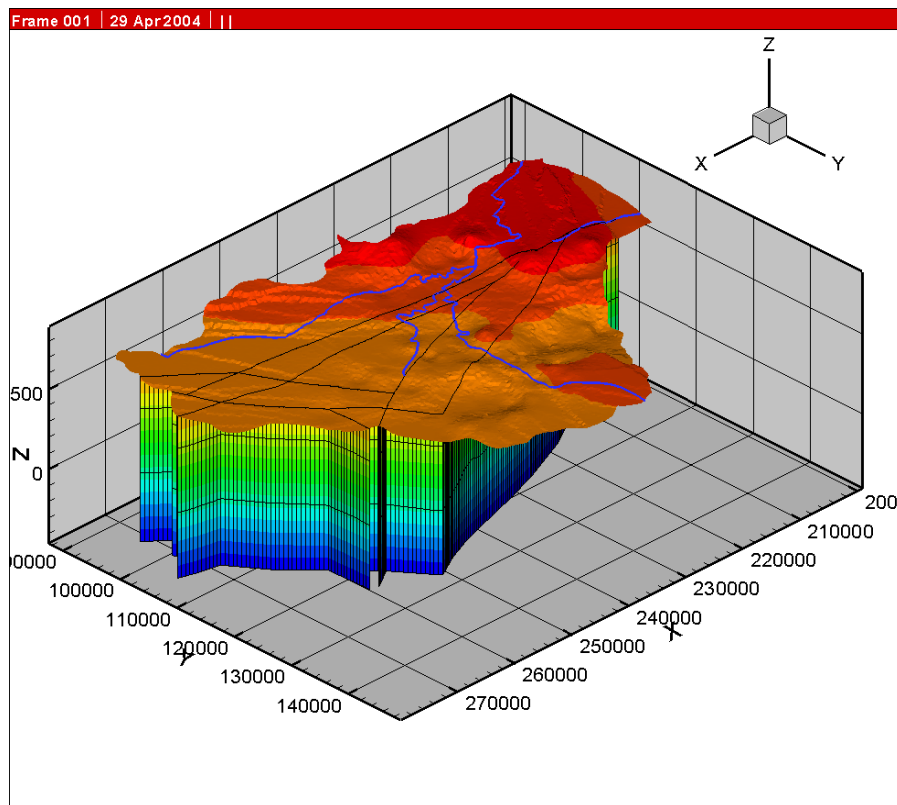
Figure-6.13: Inside the hybrid finite element mesh

6.4.3.3 processing data

112

After having finished all geometric and meshing operations, it comes to specify data for the processes to be simulated.

- Boundary conditions and source terms:

The hydraulic system is controlled by recharge and discharge conditions to or from the model area as well as by discharges from several springs. The heat flow from the base ($100mW/m^2$) is represented by source terms distributed at the bottom surface.

Points, polylines and surfaces (from GIS Project) are used to set the boundary conditions and to specify source terms. Three boundary condition types are set to the upper aquifer and three for the lower aquifer as well by importing their shape files as polylines. The boundary conditions at surfaces were assigned identical to that for polylines and shown in figure- 6.14.

The water table measurements of the year 1985 (Figure-6.5) are used as steady state condition; so, heads at the study domain boundary are used as initial boundary condition, fixed heads to simulate the hydraulic conductivity within the study area. Points are used to specify the springs as source terms.
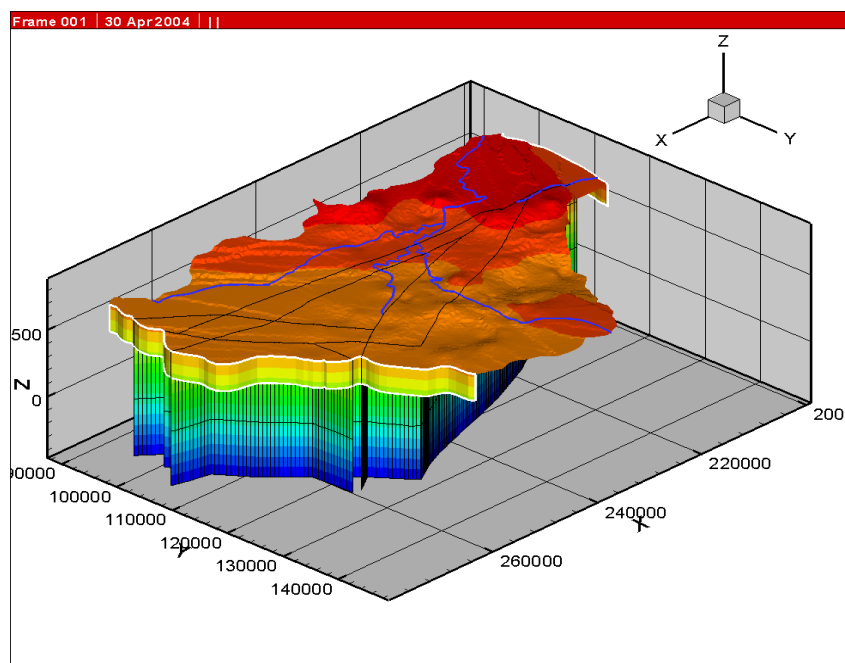
Figure-6.14: The boundary conditions at surfaces along eastern and western borders.

- Material properties

Material properties have to be specified for fluids, solids and the porous medium itself. They are element data, i.e. connected with the finite elements by a material group number. For convenience the material data have been prepared in Excel tables, which can be easily imported.

Figure-6.15 shows the geometrical distribution of material groups in the aquifer layers based on the hydrogeological data. In the 3D model all material groups are linked to volume objects. In a finite element model all elements belonging to a specific geometric object inherit data from the material group connected to this volume.
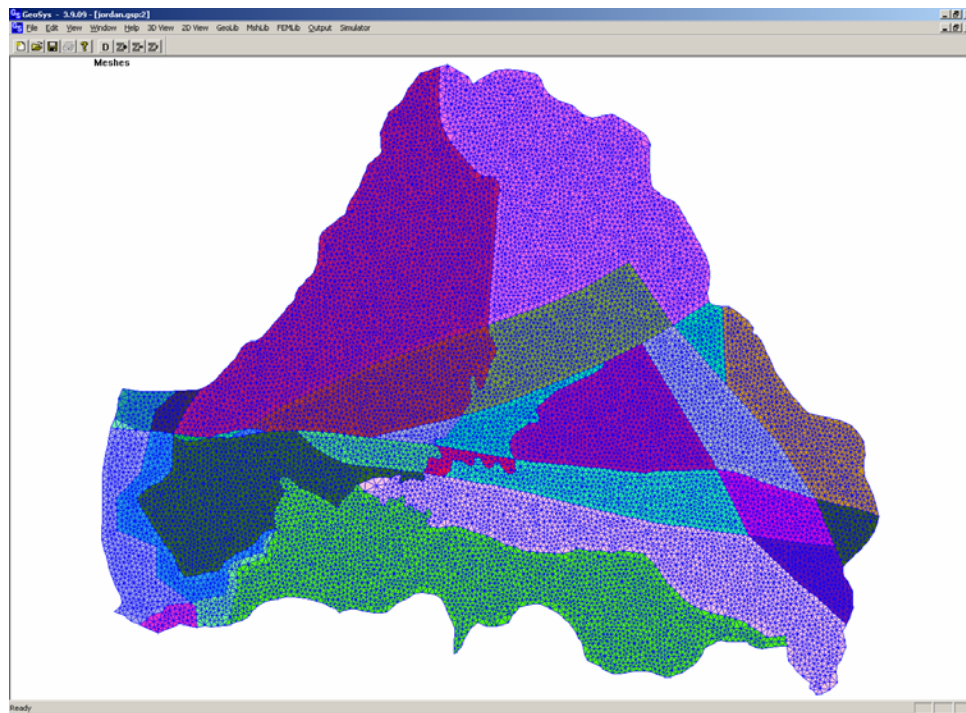
Figure-6.15: The geometrical distribution of the material properties

6.5 Simulation Results

6.5.1 Groundwater Flow modeling

1- Steady state

The hydraulic system in the area is controlled by recharge and discharge conditions to or from the model area as well as by discharges from Heidan springs. Figure 6.16 shows the simulation results of heads in the steady state. It can be seen from the figure that high heads are found in the recharge areas in the north and in the southeast. It also shows the effect of the Heidan spring on the groundwater flow. The simulated heads are quite similar to the water heads measured in 1985 (Figure-6.5).
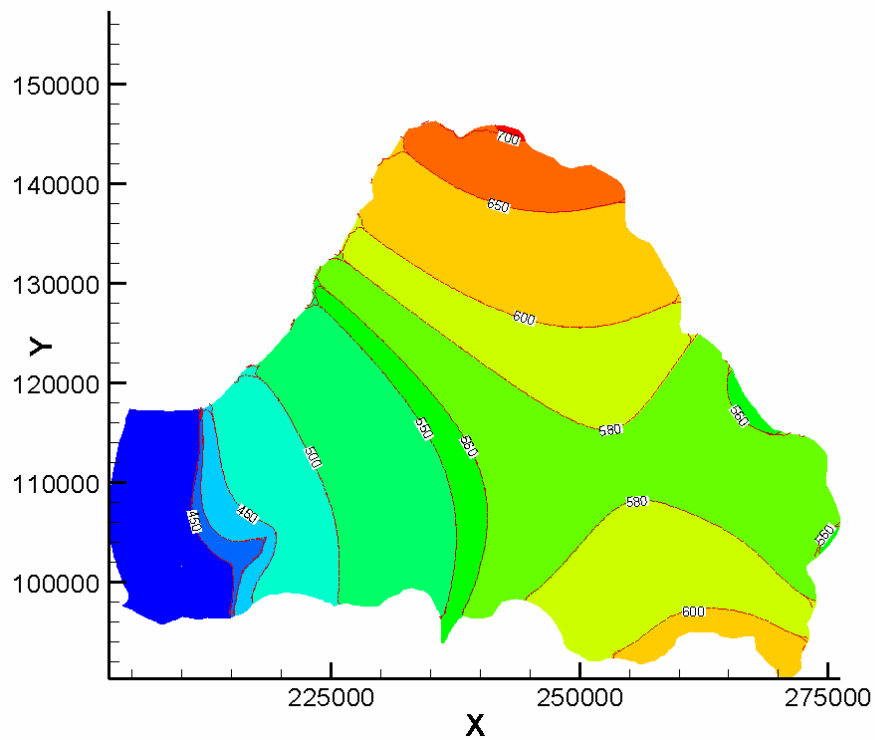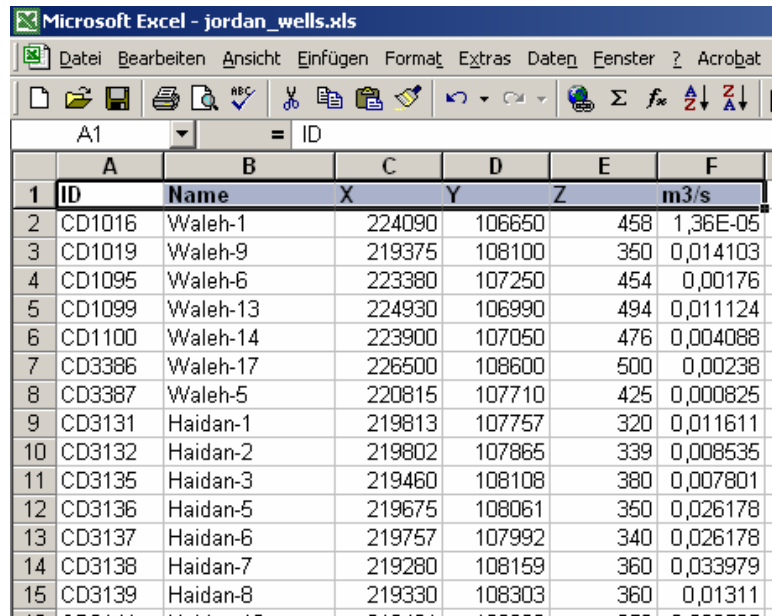
6.16:   Figure-
Heads distribution in the steady state

2- Transient state

In the transient state, well data have to be involved in the hydro-system model. Information from about 300 wells was available in an Excel data base (Figure-6.17). These data, i.e. well positions (Figure-6.18) and pumping rates, are directly imported by the software. Figure-6.19 shows the resulting hydraulic head distribution.

Figure-6.17: Excel data base for the wells

Figure-6.18: well locations in the model domain

116

Figure-6.19: Hydraulic head in the model domain including well pumping data
(Transient state)

Both simulation results, for the steady and transient states, gave reasonable results despite that this is the first implementation of the software in modeling the groundwater flow based on GIS data.   The model was not calibrated for the transient state simulation, therefore, the simulation results form a solid base for further work to develop a 3D calibrated flow model for the area using the present GIS Project.

6.5.2 Heat transport modelling

Two applications were carried out to model heat transport in the investigated area:

In the first application we used a vertical cross section, 12km long, crossing Daba'a fault. Aquifer layers are represented by 2D rectangular elements while the fault zone is represented by 1D line elements and given high permeability. The heat transport (T process) has to be modeled and coupled to the water flow process. The temperature distribution in the aquifer influences some material parameters, like fluid density and fluid viscosity. Warm water has lower density and thus rises in comparison to colder water.

The up-coning effect of warm water at the fault can be clearly seen by the higher temperatures along the vertical fracture (Figure-6.20). Vertical heat transport in the model area without fractures is much less pronounced, which shows the relative importance of heat transport by water movement compared to heat conduction in the aquifer material and stagnant water.
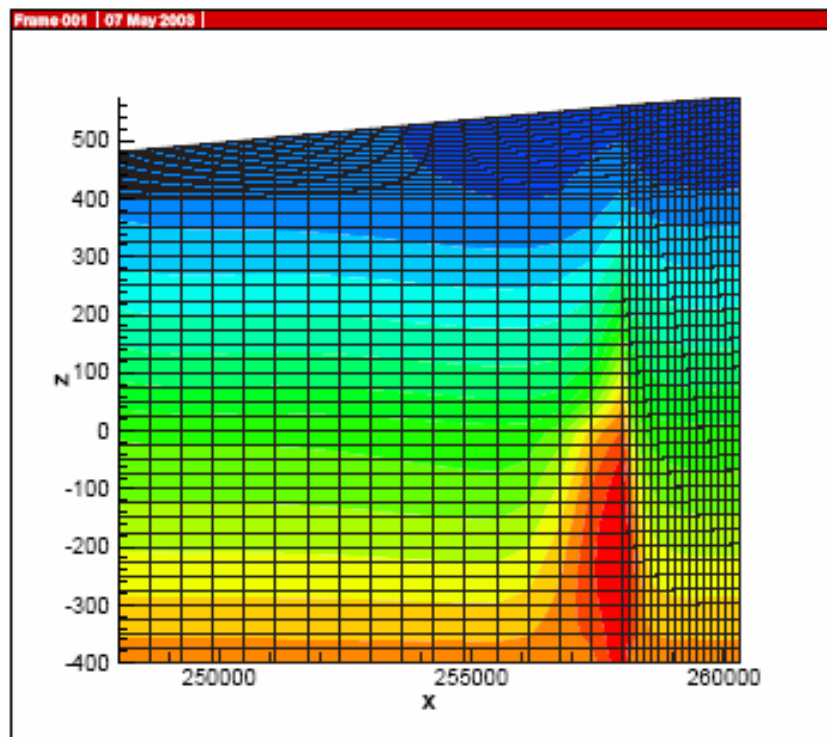
Figure-6.20: Vertical temperature distribution in the aquifer

In the second application, based on the 3D model of the groundwater flow regime in the model domain, a fully 3D heat transport model is set up to investigate the long-term

thermal regime in this region. The heat flow from the base, assumed to be 100mW/m^2, is represented by source terms distributed at the bottom surface.

The thermal basic processes are illustrated in figure-6.21. The figure shows a permanent heat flow from the base to the system. In the eastern area, groundwater is entering the lower aquifer causing increase in temperature and in the northern area, groundwater is entering the upper aquifer. The latter has to cool the whole groundwater system; otherwise the temperature will increase permanently.

Groundwater entering the system

Heat flux from the base
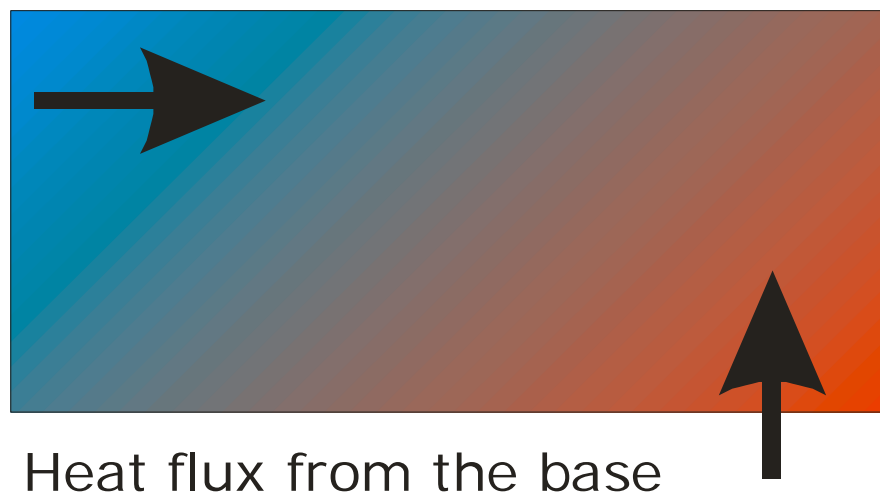
Figure-6.21: Thermal basic process in the area.

Figure-6.22 shows a first long-term simulation (30000 years) of the thermal system based on the hydraulic model presented before. It shows that there is a clear temperature increase along the faults, but it also shows a permanent increase of temperatures in the whole system. In other words, the groundwater entering the system is not equilibrating the base heat flux. This indicates to possible defects in the current model due to the underestimation of recharge groundwater to the domain or the base heat flux is overestimated. This means that by involving thermal data in the simulation, the hydraulic model might be improved.
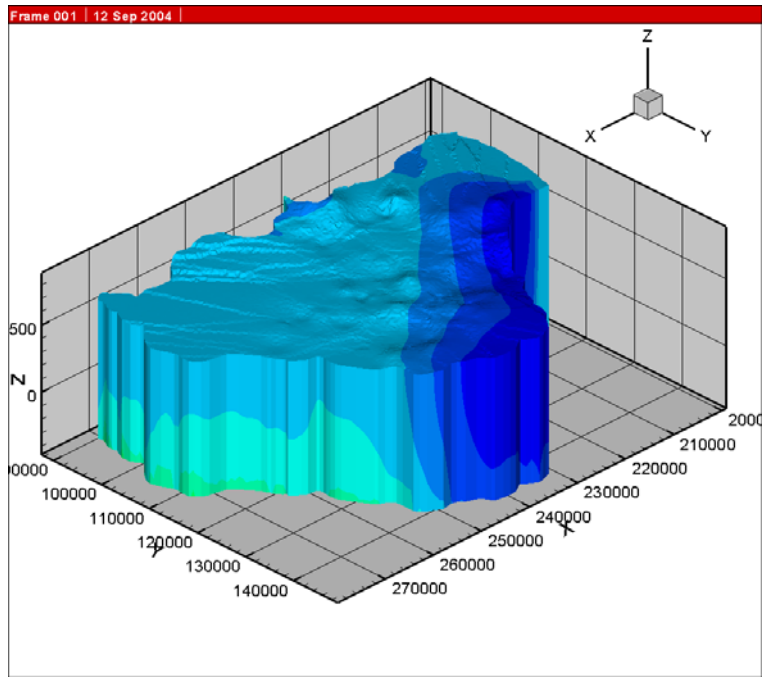
Figure-6.22: Simulated temperature distribution in the model area

7. SUMMARY AND DISCUSSIONS

Jordan is located in the northern western part of the Arabian Peninsula. The main structural element governing the morphology, hydrology and hydrogeology of Jordan is the Dead Sea Rift fault zone. It forms an active part of the African-Syrian Rift, which extends about 6000km, from east Africa through the Red Sea, Wadi Araba, Dead Sea, Jordan Valley to south Turkey. Long time before the formation of the Dead Sea Rift, the northward movement of the African plate including the Arabian plate caused the formation of the Syrian Arc Fold Belt, which was formed in two stages: the first in the Turonian-Maastrichtian and the second in the Oligocene (Burdon,1959; Bandel and Mikbel, 1985; Abed, 1989). After that, in the Miocene the Arabian plate separated from the African plate and continued its movement to the north causing the creation of the Transverse Fault System in the Miocene-Pliocene. This system accompanied by a group of tensional faults trending NW-SE and dextral shears trending E-W and compressional structures trending NE-SW.

The Dead Sea Rift was created. It trends nearly N-S and extends southwards beyond the Gulf of Aqaba into the Red Sea and northwards through Lebanon into Turkey with total length of 1100km. It consists of two faults: The southern fault, called Risha or Wadi Araba Fault and the northern fault, known as Jordan Valley Fault. Wadi Araba Fault starts from Gulf of Aqaba to Risha area in the middle of Wadi Araba to Dead Sea basin along the eastern shore and ends at its northern eastern corner. The Jordan Valley Fault starts at the southern western part of the Dead Sea and continues to the north along the western shore of the Dead Sea to the east of the Tiberias lake.

The left-lateral strike slip displacement along this transform boundary comprehends in Jordan about 107km (Quennell, 1956). According to results from Midyan peninsula (Bayer et al. 1988; Purser and Hoetzl, 1988) the movement started in the Mid-Miocene time, between 12-15 million years, and continued more or less continuosly the last 12 million years with a movement of about 9mm/year.

As a result of the major structures (Syrian Arc, Transverse Fault System and Dead Sea Rift) and the continuous northward movement of the Arabian plate faults of different trends and ages have developed (Figure-2.1). The different trends are due to different stress fields resulting from the different tectonic movements in different ages. These faults are mainly of two major trends (N-S, E-W) and (NW-SE, NE-SW). The crossing of the two fault systems acted locally as conduits for the Neogene-Pleistocene basaltic intrusions and flows. Several of the E-W faults are traceable for tens of kilometers from the Rift inside the country.

Sedimentary rocks cover almost the whole area of Jordan with a thickness of more than 5000m in Azraq Basin. The Precambrian basement rocks are only exposed in the south-west of the country and deepen northward and northeastward.

The sedimentation began in Late Pre-Cambrian with the deposition of the Saramuj Conglomerates. During the Cambro-Ordovician, the Disi sandstones were deposited through out Jordan and northwest Saudi Arabia. Then Khryim silty sandstone series were deposited in east Jordan during the major marine transgression, which occurred from Lower to Middle Ordovician up to lower Devonian. In north Jordan, alteration of transgressions and regressions during Triassic and Jurassic resulted in the deposition of Zarqa complex. From Cretaceous to Eocene the whole country was covered by an extensive marine transgression and caused the deposition of the Kurnub, Ajlun and Belqa groups. In the Upper Eocene, the sea regressed and a period of erosion began which lasted to the present day. This period has been characterized by volcanic activity resulting in the extensive basalt flows mainly in northeast Jordan and extended to Syria, and by localized lacustrine and fluviatile deposits in the Azraq and Jafer basins as well as the Rift Valley.

Jordan has an area of about 90,000km^2 and its relief is extremely of diverse nature: the western part consists of the world deepest rift (410m bsl). Eastwards, the highlands range in elevation from about 1000m in the north to around 1200m in the south. East of the highlands comes the plateau with desert basins (500m asl).

This sharp variation in topography within a small country leads to great differences in its climate. Therefore, the highlands have a semi-arid Mediterranean climate, characterized

by cold, wet winter and moderate, dry summer. The plateau (desert) has arid Mediterranean climate, with dry cold winter and hot summer. But the climate in the Jordan Valley and the Dead Sea can be classified as arid climate with hot summer and warm winter.

The study area is located in central part of Jordan and consists of two catchments: Wadi Waleh sub-catchment (2030 km^2) and Zara-Zarqa Ma'in thermal springs area (272 km^2). It extends from Zara hot springs at the eastern shore of the Dead Sea in the west through Zarqa Ma'in thermal springs to Jiza region in the east.

A sequence of more than 1000m thick of sedimentary rocks is well exposed in the study area, it ranges in age from Cambrian to recent. This sequence consists of the Paleozoic Ram Sandstone Group, the Permo-Triassic Zarqa Sandstone Group, the Lower Cretaceous Kurnub Sandstone Group and the Upper Cretaceous Ajlun and Belqa Limestone Groups. The area is dissected by numerous faults with several trends, which probably originated during the Paleozoic or earlier times. Renewed activation due to the separation of the Arabian plate and its northward movement occurred during the Late Cretaceous to Tertiary and Quaternary times leading to new movements along the old faults and weakness zones. These forces are also responsible for creating new faults, fractures and discontinuities, which are important for the hydrogeological situation.

The investigated area characterized by semi-arid to arid. An essential feature of this climate is receiving rainfall during the cool winter season (October-April) and having very marked drought summer. Most of the study area receives less than 200 mm/y as long-term average rainfall. The average all over Wadi Waleh sub-catchment is about 189 mm/y (Khdeir, 1997), and for Wadi Zarqa Ma'in sub-catchment it is about 200mm/y.

The area drains westwards to the Dead Sea via the two major wadis and their numerous tributaries. The tributaries are dry except for a short period after rainfall. Perennial base flow is seen only on the lowest sections down stream of Wadi Waleh/Heidan and on the lowest parts of Wadi Zarqa Ma'in from a short distance east of the Zarqa Ma'in thermal springs.

Hydrogeologically, the study area belongs to the hydraulic pattern model of the central part of Jordan, described by Salameh and Udluft (1985). According to the model, Central Jordan consists of two major aquifer complexes. The upper aquifer complex, consists of limestone, chert, and marly limestone of the Upper Cretaceous age. This main aquifer complex is known as B_2/A_7 aquifer and is considered as a major source for fresh water for domestic uses in Jordan. The lower aquifer complex, consists mainly of sandstone of Lower Cretaceous and older ages. The two aquifer systems are separated by more or less an impermeable sequence forming an aquitard. This aquitard is known as A_{1-6} and consists of about 400m of marl and marly limestone of the Upper Cretaceous.

The hydraulic system of the study area (Figure-3.11) shows that most of the recharge enters the upper aquifer in the structurally high outcrop area in the western highlands, where the rainfall is relatively high, and where the aquifer is cropping out at the west flank of the mountains blocks of Amman, Madaba and Ma'in. And most of the groundwater in this aquifer flows to the west. The main outflows from the aquifer are flowing springs. The major group of springs with annual average flow discharge of 15 MCM/y is located in Wadi Waleh/Heidan, where ground elevation is about 350m asl.

The upper aquifer has a hydraulic conductivity values (Appendix-2) ranging from 1 E -3 m/s to 1 E -7m/s with an average of 2.7 E –5. The wide range in the hydraulic conductivity values is related to karst features, including enlarged joints, sinkholes, caves and solution breccias that developed in and around the fault zones. The transmissivities values differ widely from one well to another and this is due to the wide range in permeability rather than the variation of the saturated thickness. Transmissivity varies from very low values, as low as 2 m^2/d to very high values, of 51000 m^2/d. But, the majority of the values are less than 120 m^2/d.

The lower aquifer sandstones are exposed in the low rainfall areas along the Dead Sea coast. So, direct recharge to the aquifer within the study area is limited to these outcrops and can be neglected. The main recharge source to the lower aquifer is the downward

leakage from the upper aquifer system in the eastern parts of Jordan. The major outflow from the aquifer is the thermal springs in Zara and Zarqa Ma'in areas. The total annual

discharge as base flow from the aquifer in Wadi Zarqa Ma'in is about 20 MCM/y and about 3 MCM/y as flood flow (Abu Ajameih, 1980). The aquifer also discharges about 5 MCM/y at the lower reaches of Wadi Heidan. All the discharged water used to flow directly into the Dead Sea. The groundwater flows in the aquifer from east towards the Dead Sea in the west. Recently, a new project is being implemented to treat about 15 MCM/y from the thermal water to be used for domestic uses. The average permeability of the whole lower aquifer is 4.48 E -5 m/s (Salameh and Udluft, 1985).

The study area contains two geothermal manifestations: the Zara-Zarqa Ma'in thermal springs systems and the thermal wells at the areas east of Madaba and Jiza region. The Zara hot springs, at the Dead Sea shore, together with Zarqa Ma'in hot springs, form the main geothermal manifestation in Jordan. Thermal springs in both areas, Zara and Zarqa Ma'in, issue their water from the Lower Cretaceous and older sandstone with temperatures ranging from 30 to 63°C. The thermal waters of Zara-Zarqa Ma'in have been subjected to many studies regarding their chemistry, heat source, therapeutic properties and their potential as source of energy. They are fed by water circulating deep within the Paleozoic sandstones and receiving heat from a normal to slightly elevated geothermal gradient. The maximum temperature of the water at depth is up to 110°C, cooling down during ascendance and by mixing with shallower cold water before discharge as thermal springs.

Beside these natural thermal water outflows along the Jordan Rift System there is a second geothermal manifestation, the thermal wells field of the Madaba-Jiza region, eastern part of the study area, where many wells discharge thermal water (30 to 46°C) from the Upper Cretaceous limestone. These wells are generally located within the eastern extension of Zarqa Ma'in Fault and the other faults in the area (Figure-4.1). The water temperature distribution at wellheads shows that this region has two heat anomalies (Figure-4.2). The first anomaly is located around well number-5 (Abu Shweimeh) east of Madaba at the intersection of Jiza fault with covered unknown NW-SE trending fault (cf. chapter 4). The

second anomaly is located at the southern eastern part of the study area, along Daba'a and Wadi Al Hammam faults.

The dense faults net of the different trends, strongly suggested that the two-aquifer systems are hydraulically connected, especially in the eastern parts of the study area. This allows the thermal water from the lower aquifer to flow up via faults (conduits) into the upper aquifer raising the groundwater temperature in the vicinity of these faults. Despite the head differences between the two aquifers, the faulting system may introduced a reverse head around the faults. Also, the water is driven toward the upper aquifer by a gradient caused by the lower density of the water in the hotter parts of the system.

A bout 50 chemical analyses were used to classify the water types in the upper and lower aquifers in the study area. Of these samples, 24 samples were also analyzed for stable isotopes. All samples were analyzed in the Water Authority Labs, Amman. The chemical and isotopic analyses were interpreted using several chemical graphs.

On Cl-SO_4–HCO_3 graph of Giggenbach (1991) all samples from Zara-Zarqa Ma'in thermal springs are located in the chloride water type area (Figure5.4). Whereas, most of the samples of the thermal wells fall in the high bicarbonate part, so they classified as HCO_3 water type. The figure suggests that there is a mixing between the water of the two aquifers.

The SO_4 increase could be as a result of reducing or dissolution conditions or may be both. The Eh values (positive and negative) show that both conditions reducing and oxidizing are present. Under reducing conditions when the reducing hot mineralised water of the lower aquifer mixes with the oxidized cold water of the upper aquifer, sulphides reduce and release sulphates. Sulphates are also produced from the dissolution of gypsum, which occurs in several horizons in the aquifer matrix.

On Schoeller diagram (Figure-5.5), thermal well samples fall between the thermal springs samples and samples from wells in the recharge area suggesting mixing between the two aquifers.

The Durov diagram (Figure-5.6) shows that sample 36 falls in the recharge water zone while samples 8, 9, 12 , 14, 24, 28, and 31 fall in the mixing zone, which coincide with their location in the field; sample36 from a well in the recharge area and the samples 8, 9, 12 , 14, 24, 28, and 31 from wells in the up-flowing (mixing) zone.

The Na-K-Mg diagram of Giggenbach (1988) shows that all samples fall in the area of immature water, very close to the Mg-corner indicating that the water is in partial equilibrium with reservoir rock, either as a result of mixing or water-rock reaction during up flow.

The chemical geothermometers (silica and cations) are used to predict the subsurface temperature and to determine the main up-flow zones in a geothermal system. Both quartz and chalcedony geothermometers were used to estimate the reservoir temperatures. Three equations applicable in the temperature range 20-250°C were used to predict the reservoir temperature in the study area. The calculation results (Table-5.3) show that the chalcedony equations does not apply to the samples, they give very low temperatures even lower than the orifice temperatures. While the quartz equation gives more reliable results, but still it gives lower estimation of the reservoir temperature, which may be due to silica precipitation from the solution as a result of conductive or adiabatic cooling during up flow before reaching the surface.

Cation geothermometers are widely used to estimate reservoir temperatures of waters collected from hot springs and wells. There are many different cation geothermometers and it is rare when they give about the same result, especially when applied to hot spring waters. Two cation geothermometers (Na-K and K-Mg) are used to predict the reservoir temperature. The calculation results (Table-5.4) show that the Na/K geothermometers give high estimation for the reservoir temperature. The K/Mg geothermometers gives low estimation for samples from thermal wells but it is more reliable in estimation the reservoir temperature for samples from Zara-Zarqa Ma'in thermal springs.

The disagreement between all geothermometers estimations suggest that the water is a mixture of hot thermal water and cold water of shallower depth. Therefore, to take account of the effect of mixing of different waters, the Enthalpy-silica diagrams (Truesdell and Fournier, 1977) can be used for better temperature estimations.

The enthalpy-silica diagram (Figure-5.8a,b), shows that the maximum reservoir temperature in Zara-Zarqa Ma'in is about 105°C and it is quite close to the estimated temperature (111°C) concluded by Truesdell (1979) for the same springs field. It also shows that the reservoir temperature for the thermal wells ranges from 65 to 105°C depending on the mixing ratio from the lower aquifer.

Isotopic data can well differentiate between the three possible origin types of thermal waters i.e. magmatic, oceanic and meteoric origin. The $\delta^{18}O$ content of all samples from the study area ranges from -6.71 to- 3.88 ‰ and the δ^2H content ranges from -37.8 to -22.9 ‰. These isotope values, do not show the presence of any significant amount of magmatic water which, generally, has $\delta^{18}O$: +6 to +9 ‰ and δ^2H: -40 to -80‰ (Pearson et al. 1980). The possibility of oceanic origin of these waters is ruled out because the $\delta^{18}O$ and δ^2H content of the oceanic water is about zero. Therefore, the origin of these waters is obviously meteoric water.

The stable isotopes content of all samples were plotted on $^1\delta^8O$ against δ^2H graph (Figure-5.9). The figure shows that all samples from cold and thermal wells from the upper aquifer are located between the MMWL and the GMWL on a line that originates from the MMWL indicating that the water is of Mediterranean water type. The slope of this line is less than 8 indicating that the water has been either subject to evaporation or that mixing of water of different genesis has taken place.

Water samples from the lower aquifer fall below the GMWL with low oxygen shift for the thermal water samples from Zara-Zarqa Ma'in springs. The oxygen shift takes place when oxygen isotopes are exchanged between hot rock and the circulation water. It depends on the interaction temperature, water rock ratio, interaction time and permeability of the rock. Generally, low temperature, high water-rock ratio and low interaction time result in a low oxygen isotope shift. If the $\delta^{18}O$ shift is neglected and the location of the lower aquifer samples brought back to their origin, then the location of the thermal wells water samples of the upper aquifer become between the cold water of the upper aquifer, rain water and the thermal water of the lower aquifer suggesting a mixing between the water of the two aquifers.

The above mentioned chemical and isotope composition of the thermal water of the thermal wells strongly suggest mixing between bicarbonate water of the upper aquifer in the recharge areas and the Na-Cl thermal water of the lower aquifer.

In the course of this study, the GeoSys/RockFlow scientific modeling software (Kolditz et al. 2003) is used in two applications: firstly to model in 2D groundwater flow and heat transport a cross Daba'a fault, secondly to develop a 3D numerical groundwater flow and heat transport model based on GIS Project for the whole investigated area.

In the first application, a vertical cross section of about 12km long, crossing Daba'a fault is used, where the aquifer layers are represented by 2D rectangular elements while the fault zone is represented by 1D line elements and given high permeability (Kolditz et al. 2004). The heat transport (T-process) has to be modeled and coupled to the water flow process (H-process). The temperature distribution in the aquifer influences some material parameters, like fluid density and fluid viscosity. Warm water has lower density and thus rises in comparison to colder water.

The up-coning effect of warm water at the fault can be clearly seen by the higher temperatures along the vertical fracture (Figure-6.20). Vertical heat transport in the model area without fractures is much less pronounced, which shows the relative importance of heat transport by water movement compared to heat conduction in the aquifer material and stagnant water.

The second application represents the first implementation of GeoSys/RockFlow Software in modeling groundwater flow and heat transport based on GIS Project (Sawarieh et al, 2004). The first step in setting up the model is creating the GIS Project, where geological data of the study area such as the geological formations, faults, wadis and the hydrogeological data like aquifers, aquitards, wells, water table, top and base of aquifers and boundary conditions were converted to shape files (layers) using the ArcGIS software (digitizing feature) and kept in this project. The whole study domain was subdivided into 29 areas (surfaces) by adding the major faults and wadis to the hydrological units. The second step is the creation of the GeoSys Project, where all the data reference for the

model such as geometry data, meshing data and processing data are stored in this project file to keep the connection between the project and its data components. The shape files in GIS Project are imported into GeoSys/RockFlow and converted into their own geometric data structure as basic geometric data for the modeling area.

The results confirm that the hydraulic system is controlled by recharge and discharge conditions to or from the model area as well as by discharges from Heidan springs. The simulation results of the hydraulic head in the steady state are shown in figure 6.16. The figure shows that high heads are found in the recharge area in the north and in the southeast. It also shows the effect of the Heidan springs on the groundwater flow. The simulated heads are quite similar to the water heads measured in 1985 (Figure-6.5).

In the transient state, well data (locations and pumping rates) are included in the hydro-system model. Figure-6.19 shows the resulting hydraulic head distribution after involving pumping from about 300 wells scattered in the model domain.

Both simulation results, for the steady and transient states, gave reasonable results despite that this is the first implementation of the software in modeling the groundwater flow based on GIS data. The model was not calibrated for the transient state, therefore, the flow simulation results form a solid base for further work to develop a 3D calibrated flow model for the area using the GIS Project of this study.

In the second application , based on the 3D model of the flow regime in the model domain, a fully 3D heat transport model was set up to investigate the long-term thermal regime in this region. The thermal basic processes are illustrated in figure-6.21. The figure shows a permanent heat flow from the base to the system. In the eastern area, groundwater is entering the lower aquifer causing increase in temperature and in the northern area, groundwater is entering the upper aquifer. The latter has to cool the whole groundwater system; otherwise the temperature will increase permanently.

Afirst long-term simulation (30000 years) of the thermal system based on the hydraulic model presented before was carried out. It shows that there is a clear temperature increase along the faults, but it also shows a permanent increase of temperatures in the whole system. In other words, the groundwater entering the system is not equilibrating the base heat flux. This indicates two possible defects in the current model due to the underestimation of recharge groundwater to the domain or the base heat flux is overestimated. This means that by involving thermal data in the simulation, the hydraulic model might be improved.

8-CONCLUSIONS AND RECOMMENDATIONS

8.1 Conclusions

The hydrogeological conceptual model of the study area shows that most of the recharge enters the upper aquifer in the mountains blocks of Amman, Madaba and Ma'in. The lower aquifer sandstones are exposed in the low rainfall areas along the Dead Sea Shore. So, direct recharge to the aquifer is limited and can be neglected. It can be concluded from the hydraulic system of the investigated area that it belongs only to the western part of the hydraulic system of Central Jordan and the groundwater flows in both aquifers towards the Dead Sea in the west.

The dense faults net affecting the area, strongly suggested that the two-aquifer systems are hydraulically connected. Especially in the eastern parts of the study area, where the NW-SE trend faults such as Daba'a, Wadi El Hammam and Masattarat faults demonstrates an extensional regime. This may allows the thermal water from the lower aquifer to flow up via faults (conduits) into the upper aquifer, raising the groundwater temperature in the vicinity of these faults.

The heat source of the thermal water in the lower aquifer is a result of the deep circulation of water within the Paleozoic sandstones receiving heat from a normal to slightly elevated geothermal gradient. Cation (Na-K and K/Mg) and silica (quartz and chalcedony) geothermometers were used to estimate the reservoir temperatures. The results show disagreement between all geothermometers estimations. Therefore, the Enthalpy-silica diagram is used for better temperature estimations. The diagram shows that the maximum reservoir temperature in Zara-Zarqa Ma'in is about 105°C. It also shows that the reservoir temperature for the thermal wells ranges from 65 to 105°C depending on the mixing ratio from the lower aquifer.

The chemical and isotope analysis confirm that the water of thermal wells is a mixture of two components: bicarbonate water of the upper aquifer and chloride water of the lower aquifer and there is no third component from the east as mentioned before in literature. The location of high Cl concentrations and higher water temperatures along Daba'a and Wad El Hammam faults suggests that these faults are the main up flow zones of the thermal water.

131

GeoSys/RockFlow scientific modeling software is used in two applications: A vertical cross section, crossing Daba'a fault, is used in the first application to model (2D) the water flow and heat transport. The simulation results show the clear up-coning effect of warm water at the fault i.e. higher temperatures along the vertical fracture. And the vertical heat transport in the model area without fractures is much less pronounced, which shows the relative importance of heat transport by water movement compared to heat conduction in the aquifer material and stagnant water.

The second application represents the first attempt to use the Software to model (3D) the groundwater flow and heat transport based on GIS Project. In the steady state, the simulation results of water flow are quite similar to the water heads measured in 1985. In the transient state, well data (locations and pumping rates) are included in the hydro-system model and the flow simulation gave good results. The flow model was not calibrated, therefore, the simulation results form a solid base for further improvement of the model using the GIS Project of this study.

Based on the flow 3D model, a fully 3D heat transport model was set up to investigate the long-term (30000 years) thermal regime in this region. The simulation shows that there is a clear temperature increase along the faults, but it also shows a permanent increase of temperatures in the whole system. In other words, the groundwater entering the system is not equilibrating the base heat flux. This indicates a possible defect in the current model most likely due to the overestimation of the base heat flux. This means that by involving thermal data in the simulation, the hydraulic model might be improved.

The hydrological, chemical and simulation results indicate that the heat is transported to the thermal wells by water up-flow movement via faults forming the heat source for these thermal wells. Thus, to find higher temperatures the thermal water should be intercepted in the faults (conduits) before it reaches the upper aquifer.

8.2 Recommendations

As a result of this study the following investigations are highly recommended to be carried out in the area:

1- Further chemical and isotopic specialized research such as; noble gases measurements in Zara-Zarqa Ma'in thermal field and additional isotopic analysis.

2- The water flow simulation needs to be improved on the bases of the simulation results of this study.

3- One or two deep wells, about 1200m in depth, are needed to be drilled to investigate the lower aquifer system in the areas where the hottest wells are located.

4- In Jiza region, the temperature drop sharply in winter (some times below zero) affecting the agricultural activities. The heat of the water in the area should be used by introducing the protected agricultural and fish farming activities in this region.

9. REFERENCES

1- Abed, A. M. (1989): On the genesis of the phosphate-chert association in the Amman Formation in Tel es Sur area, Ruseifa, Jordan. Science Geologie Bullittin, Strasburg 42 , 141-153.

2- Abed, A. M. (1982): Geology of Jordan. Al- Nahda El-Islamih Library. Amman, Jordan. 232pp (in Arabic).

3- Abed, A. M. (2000): Geology, Environment and Water of Jordan. Jordanian Geological Association Publications Amman, Jordan. 570 pp (in Arabic).

4- Abu Ajameih, M. (1980): The geothermal resources of Zarqa Ma'in and Zara. Report of phase-1. Of the geothermal energy project in Jordan, Natural Resources Authority, Amman. 82 pp.

5- Al Hunjul, N. (1995): The geology of Madaba area. Map sheet No. 3153II. Bulletin No. 31, NRA, Amman, Jordan.

6- Al Hunjul, N. (1991c): Eth-Thamad oil shale deposit: Geological setting and evaluation. In: Rimawi et al., (eds): Geology of minerals and industrial rocks and environmental geology-Proceedings of the fourth Jordanian geological conference, Special publication, No. 4, Amman.

7- Allen, D. (1988): Preliminary Evaluation of the Geothermal potential of Jordan Recommendations for future studies. BGS. Keyworh, UK. 34pp.

8- Anderson, M. P. and Woessner, W. W. (1992). Applied Groundwater Modeling. Academic Press, San Diego.

9- Andrews, I. J. (1992): Cretaceous and Paleocene Lithostratigraphy in the subsurface of Jordan. Subsurface Geology Bulletin No. 5. NRA, Amman, Jordan.

10- Arabtech-Jardaneh, (1996): Study and evaluation of surface and underground water in Zara and Ma'in areas. Contract no. 140/93. Feasibility study report submitted to Jordan Valley Authority, Amman, Jordan.

11- Arad, A. and Bein, A. (1986): Saline versus fresh water contribution to the thermal water of the Northern Jordan Rift Valley, Israel. Journal of hydrology, 83:49-66.

12- Arnorsson, S., Gunnlaugsson, E., and Svavarsson, H. (1983): The chemistry of geothermal waters in Iceland III. Chemical geothermometry in geothermal investigations. Geochim. Cosmochim. Acta, 47, 567-577.

13- Arnorsson, S. (1985): The use of mixing models and chemical geothermometers for estimating underground temperatures in geothermal systems.- Journal of Volcanology and Geothermal Research, 23, 3-4: 299-235.

14- Arnorsson, S. (1991): Geochemistry and geothermal resources in Iceland, In: D'Amore,F. (coordinator), Applications of geochemistry in geothermal reservoir development. UNITAR'UNDP publication, Rome, 145-196.

15- Ashcroft, G., Marsh, D. D., Evans, D. D. and Boersma L. (1962): Numerical method for solving the diffusion equation: 1. horizontal flow in semi-finite media soil. Science Society of America Proceedings, Vol.9, No.2, pp.97-156.

16- Bandel, K. and Khoury, H. (1981): Lithostratigraphy of the Triassic in Jordan. Facies4, 1-26, Erlangen.

17- Bandel, K. and Mikbel, Sh. (1985): Origin and deposition of phosphate ores from the Upper Cretaceous at Ruseifa, Jordan. Publication Geologie und Palaontologie Institut, Universitat Hamburg 59, 167-188.

18- Bayer, H.-J., Hotzl, H., Jado, A. R., Roscher, B. & Voggenreiter, W. 1988. Sedimentary and structural evolution of the northwest Arabian Red Sea margin. Tectonophysics, 153, 137-152.

19- Bender, F. (1968a): Geologische karte von Jordanian. MaBstab 1: 250,000 (5 Blatter), Hannover.

20- Bender, F. (1968b): Geologie von Jordanian. Beitrage zur regionalen Geologie der Erde. Band 7, Borntraeger. Berlin. 230pp.

21- Bender, F. (1974a): Geologische karte von Jordanian. MaBstab 1: 100,000 (3 Blatter), Hannover.

22- Bender, F. (1974b): Geology of Jordan. Contribution of the Regional Geology of the Earth. Borntraeger. Berlin, 196pp.

23- Bender, F. (1975): Geology of the Arabian Peninsula, Jordan. U. S. Department of the Interior, Geological Survey Professional paper 560-I. Washington.

24- Belbeisi, M. (1992): Jordan's water resources and the expected domistic demand by the years 200 and 2010, detailed according to area. In Jordan's water resources and their future p[potential, Symposium Proceedings, 27-28 Oct. 1991. Friederich Ebert Stiftung, Amman, Jordan.

25- Burdon, D. (1959): Handbook of the Geology of Jordan; to accompany and explain the three sheet of 1:250,000 Geological map, East of the Rift by A. M. Quennell. Govt. Hashemite Kingdom of Jordan, 82pp.

26- Chen, C., Kalbacher, T., Bauer, S. and Kolditz, O. (2003): Integration of GIS in GeoSys and Geometric Unit-GeoLib. ZAG-GHI Annual Report, GeoSys–Preprint [2003-49], Center of Applied Geosciences, University of Tuebingen.

27- Chen, C., Sawarieh, A., Kalbacher, T., Beinhorn, M., Wang, W. and Kolditz, O. (2004): A GIS based Hydro-system Model: Application to the Zarqa Ma'in – Jiza areas in Central Jordan. GeoSys-Preprint [2004-01]. Center of Applied Geosciences, Geohydrology/HydroInformatics, University of Tübingen.

28- Craig, H. (1961): Isotope variation in meteoric waters, Sciences. 133: 1702 –1703.

29- Dansgard, W., Johnson, S. J., Clausen, H. B. and Langway, C.C. (1971): Climatic record revealed by the camp century ice core. In Karl Turekian, ed., The Late Cenozoic Glacial Ages, New Haven: Yale Univ. Press, p. 37-56. 1508.

30- Darling, W. G. (1991): Jordan geothermal consultancy – Hydrogeochemical aspects. BGS. Keyworh, UK. 18pp

31- Dermage, J. and Tournage, D. (1990): Study of the potential and uses of the geothermal resources in Jordan. CFG, France. 70pp.

32- Diabat, A. and Masri, A. (2002): Structural Framework of Central Jordan- Geothermal Project of Central Jordan- Geol. Mapping Div., Geol. Directorate. NRA, Amman.

33- Diabat, A. (2004): Structural map of Jordan, unpublished report.

34- DI Paola, G. (1981): Mission report on visit to the geothermal project JOR/76/004 in the Hashemite Kingdom of Jordan from 30 November to 4 December 1981. UN/DTCD Report, New York.

35- Duffield, W., Edwin, A., McKee, H., Salem, F. and Teimeh, M. (1987): K-AR ages, Chemical Composition, and Geothermal significance of Cenozoic Basalt near the Jordan Rift. Technical report. NRA, Amman.

36- Evans, R. B. and Allen, D. J. (1989): A geophysical visit to Jordan as part of geothermal resources studies. BGS. Keyworh, UK. 59pp.

37- Faraj, B. (1988): Geothermal Gradient Map of Jordan. PetroCanada International assistance corporation, NRA, Amman.

38- Flanigan V. J. and EL Kaysi, Q. (1984): Preliminary interpretation of audio-Magnetotelluric (ATM) sounding in the Zara-Zarqa Ma'in geothermal areas. Kingdom of Jordan. Preliminary report USGS.

39- Fournier, R. O. and Truesdell, A. H. (1974): An empirical Na-K-Ca geothermometer for natural waters. Geochim. Cosmochim. Acta, 37, 1255-1275.

40- Fournier, R. O. (1977): Chemical geothermometers and mixing model for geothermal systems. Geothermics, 5, 41-50.

41- Fournier, R. (1979): Geochemical and hydrologic considerations and the use of enthalpy-chloride diagrams in the prediction of underground conditions in hot spring systems. Journal of Volcanology and Geothermal Research, 5:1-16.

42- Freund, R., Zak, I. & Goldberg, M. 1970. The shear along the Dead Sea Rift. Philosophical Transations of the Royal Society of London, Ser. A267, 107-130.

43- Galanis, S. P., Sass, J. H., Munroe, R. J. and Abu Ajameih, M. (1986): Heat flow at Zarqa Ma'in and Zara and a geothermal reconnaissance of Jordan. U.S. Geol. Survey.

44- Garfunkel, Z., Zak, I. and Freund R. (1981): Active faulting in the Dead Sea Rift. In: Freund R. and Garfunkel I. (ed.) The Dead Sea Rift. Tectonophysics V. 80. 1-26pp.

45- Gass, I. G. 1979. Evolutionary model for the Pan-African crystalline basement. In: Evolution and mineralization of the Arabian-Nubian Shield. Bulletin of the Institute of Applied Geology, Jeddah, 1, 11-20.

46- Giggenbach, W. F. (1988): Geothermal solute equilibria. Derivation of NA-K-Mg-Ca. geoindicators. Geochem, Cosmochem, ACTA, 52:2749-2765.

47- Giggenbach, W.F. (1991): Chemical techniques in geothermal exploration. In: D'Aniore, F. (coordinator), Application of geothermal reservoir development. UNITARI UNDP publication, Rome, 119-142.

48- Girdler, R. W. & Styles, P. 1982. Comments on ' The Gulf of Aden: Structure and evolution of a young ocean basin and continental margin' by J. R. Cochran. Journal of Geophysical Reserch, 87, 6761-6763.

49- Hakki, W. and Teimeh, M. (1981): The geology of Zarqa Ma'in and Zara areas, NRA Amman.

50- Huyakorn, P. S. and Pinder, G. F., (1983): Computational Methods in Subsurface Flow. Academic Press, INC. 111 Fifth Avenue, New York 10003. USA.

51- Istok, J. (1989): Groundwater Modeling by the Finite Element Method. American Geophysical Union, 2000 Florida Avenue, NW, Washington, DC 20009.

52- Jaser, D. (1986): The geology of Khan Ez Zabib. Map sheet no.3253. N.R.A. Amman, Jordan.

53- Jaser, D., and the project staff, 2002. Preliminary results of the geology and structures , geophysics, geochemistry and hydrological works in the course of the NRA-Geothermal project-Central Jordan.

54- JICA, (1987): Hydrogeological and water use study in the Mujib watershed. Amman, Jordan.

55- Jeries, A. (1986): Hydrogeology and Hydrochemistry of the area south of Amman (Palestine grid 100–140 N, 225 – 255 E). MSc. Thesis. Department of Geology and Mineralogy, University of Jordan.

56- Kalbacher, T., Wang, W., McDermott, Ch., Kolditz, O. and Taniguchi, T. (2003): Development and Application of a CAD Interface for Fractured Rock. ROCKFLOW-Preprint [2003-5], Submitted to 12th International Meshing Roundtable, New Mexico, USA, 2003.

57- Kappelmeyer, O. (1985): Report on Exploration for Geothermal Energy in Jordan, Hanover, Germany.

58- Khdeir, K. (1997): An assessment of regional hydrogeological framework of the Mesozoic aquifer system of Jordan. PhD thesis, University of Birmingham, UK.

59- Khoury, H. , Salameh, E. and Udluft, P. (1984): on the Zerka Ma'in(Therma Kallirrhoes) travertine/ Dead Sea (Hydrochemistry, Geochemistry and Isotopic composition). Neues Jahrb. Geol. Paläntol.Monats., 8: 472-484

60- Krenkel, E. (1924): Der Syriasche Bogen. Zentralbulletin fur Mineralogie. Geologie und Palaontologie 9, p. 274-281,10,301-313.

61- Krouse, H. R. (1980): Sulphur isotopes in our environment, In: Fritz, P. and Fontes, J.-Ch., (Eds.) Handbook of Environmental Isotope Geochemistry, Vol. 1, Elsevier Scientific Publishing Company, Amsterdam-Oxford-New York: 227-257.

62- Kolditz, O., Beinhorn, M., Kalbacher, T., Bauer, S., McDermott Ch., Guttmann J., Sawarieh A. and Sauter M. (2003): Software Concepts and Tools for Groundwater Modeling. GeoSys-Preprint[2003-33]. Center of Applied Geosciences, Geohydrology /HydroInformatics, University of Tuebingen. Submitted to 5th International Symposium on the Eastern Mediterranean Geology, Thessaloniki, Greece, 2004.

63- Kolditz, O., De Jonge, J., Beinhorn, M., Xie, M., Kalbacher, T., Wang, W., Bauer, S., McDermott, Ch., Kaiser C. I. and Kohlmeier, R. (2003): ROCKFLOW – Theory and User Manual, release 3.9. Technical Report, Groundwater Modeling Group, Center for Applied Geosciences, University of Tuebingen & Institute of Fluid Mechanics, University of Hannover. GeoSys–Preprint [2003-37], Center of Applied Geosciences, Geohydrology/ HydroInformatics, University of Tuebingen.

64- Kolditz, O., Chen, C., Kalbacher, T., Sawarieh, A. and Beinhorn, M. (2004): A GIS based water resources modelling, Int. Conference of Numerical Methods in Environmental Problems, Okayama, 22-23.12.2004.

65- Lloyd, J. (1969): The Hydrogeology of the southern desert of Jordan. UNDP/FAO Project 212. Tech. Rep. 1.

66- Lloyd, J. W. and Heathcoat, J. A. (1985): Natural inorganic chemistry in relation to groundwater, Clarendon Pres, Oxford.

67- Mabey, R. D. (1980): Recommended program for the Zarqa Ma'in and Zara area, U.S. Geol. Survey.

68- MacDonald, Sir M. and Partners (1965): East Bank Jordan Water Resources. Report to Central Water Authority, Hashemite Kingdom of Jordan.

69- Margane, A., Hobler, M., Al Momani, M. and Subah, A. (2002): Contributions to the hydrogeology of northern and central Jordan. Geologisches Jahrbuch Reihe C, Heft 68.

70- Marinelli, G. (1977): Report on the possibility of developing Geothermal Resources in Jordan. University of Pisa.

71- Masri, A. (2002): Evidences on dextral movement and reactivated along Siwaqa Fault/Central Jordan. Proceedings of the 6th International conference on the geology of the Arab World, Vol.1, pp327-334. Cairo University, Feb. 2002.

72- Masri, M. (1963): Report on the geology of the Amman-Zarqa area. Unpublished report, Central water Authority, Amman-Jordan.

73- Massarweh, R. (1987): Report on GTZ-2D Well, internal report, NRA, Amman.

74- Massarweh, R. and Sawarieh, A. (1995): Uses of Thermal Water in Jordan. The Third Jordanian Scientific Week, The Higher Council for Science and Technology. Amman.

75- Mazor, E., Kuafman, A. and Carmi, I. (1973): Hammat Gader (Israel) Geochemistry of a mixed thermal complex. J. Hydrol., 18: 289-303.

76- Mazor, E., Levitte, D., Truesdell, A. H., Healy, J. and Nissenbaum, A. (1980): Mixing models and ionic geothermometers applied to warm water (up to 60C°) springs: Jordan Rift Valley, Israel. Journal of hydrology 45:1-19.

77- McEwen, R. and Holconmbe, H. (1982): Interpretation of Resistivity Data in Zarqa Ma'in and Zara Hot Springs. Exploration Geothermics. Santiago, California, USA.

78- McNitt, S. (1976): Geothermal Resources In Jordan - Interpretation of data submitted by the Government. UNDP report.

79- Myslil, V. (1988): Report on evaluation of geothermal potential of Jordan. Strojexport prague, Gzechoslovakia, Geological Survey, Prague.

80- Parker, D.H. (1970): The Hydrogeology of the Mesozoic-Cainozoic of the western highlands and east Jordan. UNDP/FAO, AG2, SF/JOR G, Technical Report No. 2, Rome.

81- Pearson, F. J. Jr. and Rightmire, C. T.   (1980): Sulphur and Oxygen isotopes in aqueous Sulphur compounds. In: Fritz, P. and Fontes, J. Ch., Handbook of Environmental isotope Geochemistry, Vol. 1, Elsevier scientific Publishing company, Amsterdam– Oxford – New York: 227- 257.

82- Powell, J.H. (1988): The geology of Karak; Map sheet No. 3152III, Bulletin-8, NRA. Amman.

83- Powell, J.H. (1989): Stratigraphy and sedimentation of the Phanerozoic in central and south Jordan: Part B-Kurnub, Ajlun and Belqa Group. Bulletin-11, NRA. Amman, Jordan.

84- Price, H. S., Cavendish, J.C. and Varga, R. A. (1968): Numerical methods of higher order accuracy for diffusion convection equations. Society of Petroleum Engineers Journal, pp. 293-303.

85- Purser, B. H. and Hoetzl, H. (1988): The sedimentary evolution of the Red Sea rift: A comparison of the northwest (Egyptian) and northeast (Saudi Arabian) margins. Tectonophysics, 153: 193-208.

86- Quennell, A.M. (1951): The geology and mineral resources of former Transjordan. Colon. Geol. Min. Resource. 2. 2.

87- Quennell, A.M. (1956): Tectonics of the Dead Sea Rift. Proc. 20th. Int. Geol. Congress. Mexico, Ass. Deserv. Geol. Afrricanos, 385-403.

88- Remson, I., Appel, C.A. and Webster, R. A. (1965): Groundwater models solved by digital computer. Journal of the hydraulics Division, American Society of Civil Engineers, Vol.91, No. HY3, pp 133-147.

89- Rimawi, O. (2004): Groundwater Flow Modelling of Wadi Waleh Water Resources (Amman-Wadi Sir Aquifer System). Draft Final, University of Jordan , Amman, Feb.2004.

89- Salameh E. and Khudeir, K. (1983): Thermal water system in Jordan, Neues Jahrb. Geol. Paläntol., Monatsch., 4:249-256.

90- Salameh, E. and Rimawi, O. (1984): Isotopic analyses and hydrochemistry of the thermal springs along the eastern side of the Jordan-Dead Sea-Wadi Araba Rift Valley. Journal of hydrology, 73: 129 –145.

91- Salameh, E. (1986): The reason of elevated temperature in the lower aquifer complex in Central Jordan. Ground water in semiarid and arid regions. Proceedings of the international congress, vol.1. Amman, Jordan, May 1986.

93- Salameh, E. and Rimawi, O. (1988): The special features of the ground water flow system in central Jordan. Dirasat, vol. 9, University of Jordan, Amman.

94- Salameh, E. Rimawi, O. and Hamed, KH. (1991): Curative thermal and mineral water in Jordan. Water Resources Center Issue. No.-15. Jordan University-Amman.

95- Salameh, E. and Udluft, P. (1985): The hydrodynamic pattern of the central part of Jordan, Geol. Jahrb, C38, PP. 39-53.

96- Salameh, E. and Bannayan, H. (1993): Water Resources of Jordan- Present Status and Future Potentials. Friedrich Ebert Stiftung, Amman.

97- Salameh, E. (1996): Water Quality in Jordan (impacts on environments and future generations resources base). Friedrich Ebert Stiftung, Royal Society for the conservation of nature.

98- Saudi, A. (1999): The geochemistry of the thermal fluids in the field near Queen Alia Air port in Jordan and Selfoss in Iceland, reports of the United Nation University.

99- Sawarieh, A. (1990): Hydrogeology of the Wadi Waleh Sub-basin and Zarqa Ma'in Hot Springs. MSc thesis, University of London, UK. 60pp.

100- Sawarieh, A. (1992): Thermal Boreholes near Queen Alia Airport. NRA, Amman. 47pp.

101- Sawarieh, A. and Massarweh, R. (1993): Thermal springs in Wadi Ibn Hammad. NRA, Amman. 32pp.

102- Sawarieh, A. and Massarweh, R. (1996): Geothermal Water in Zara and Zarqa Ma'in Area. Report No. 8. NRA, Amman. 36 pp.

103- Sawarieh, A. and Massarweh, R. (1997): Geothermal water in Mukhiebeh and North Shuneh areas. Report No. 9. NRA, Amman. 26pp.

104- Sawarieh, A., Hoetzl, H. and Salameh, E. (2004): Hydrogeology of thermal water from Zara-Zarqa Ma'in and Jiza areas, Jordan. Proceedings of the 5th Int. Symposium on Eastern Mediterranean Geology, Extended abstracts. Vol-3,pp1564-1567. Thessaloniki, Greece. 14-20 April, 2004.

105- Sawarieh, A., Hoetzl, H. and Salameh, E. (2004). Hydrochemistry and origin of thermal water from Zara-Zarqa Ma'in and Jiza areas, Central Jordan. Proceedings of the 5th Int. Symposium on Eastern Mediterranean Geology, Extended abstracts. Vol-3,pp1560-1563. Thessaloniki, Greece. 14-20 April, 2004.

106- Sawarieh, A., Chen, C., Beinhorn, M., Kolditz, O., Salameh, E. and Hoetzl, H. (2004): A GIS based model for groundwater flow and heat transport in Zara-Zarqa Ma'in and Jiza areas, Central Jordan. Proceedings of the 2nd Int. Conference on water for life in the middle east. Turkey, 10-14 October 2004.

107- Shawabkeh, Kh. (1998): The geology of Ma'in Area. Map sheet No. 3153III. NRA, Amman, Jordan.

108- Trimaj, T. (1987): Final report on Borehole GTZ-2D, strojexport and Geological Survey, Ostrava.

109- Truesdell, A. H. and Fournier, R. O. (1977): Procedure for estimating the temperature of a hot water component in a mixed water by using a plot of dissolved silica verses enthalpy. J. Res. U.S. Geol. Survey, 5, 1, 49-52.

110- Truesdell, A. H. (1979): Final report on the chemistry and the geothermal Energy possibilities of Zarqa Ma'in–Zara hot springs, Jordan. USGS, Menlo Park, California, USA(unpuplished Report).

111-Truesdell, A., Duffield, W. and Abu Ajamieh, M. (1983): Origin and heat source of thermal waters at Zarqa Ma'in and Zara, Jordan: extended abstracts of 4th Intl. Symposium on Water-Rock Interactions, Misasa, Japan, Aug. 29-Sep. 3, 1983, pp 508-811.

112- Truesdell, A.H. (1991): Effects of physical processes on geothermal fluids. In: D'Axnore, F. (coordinator), Application of geochemistry in geothermal reservoir development. UYIITAR/UNDP publication, Rome, 7 1-92.

113- Wolfart, R. (1959): Geology and Hydrology of the Irbid district (Hashemite Kingdom of Jordan). Bundesanstalt fur Bodenferschung, Hannover.

114- Zienkiewicz, O. C., Meyer, P., and Cheung, Y. K. (1966): Solution of anisotropic seepage problems by finite elements. Proceedings American Society of Civil Engineers, Vol. 92 EMI, pp. 111-120.

115- Zienkiewicz, O.C. (1971): The finite element method in engineering science, Mc Graw- Hill, London.

APPENDIXES

Well ID	Owner or well Name	Coordinate PG		Annual pumping (m³/y)				
		East	North	1999	2000	2001	2002	2003
CD1016	Waleh-1	224090	106650	636	1512			
CD1019	Waleh-9	219375	108100	1230067	993698			
CD1095	Waleh-6	223380	107250	117504	160008			
CD1099	Waleh-13	224930	106990	336000	347172	336252	350004	384636
CD1100	Waleh-14	223900	107050	106872	149868	127644	150000	110208
CD3386	Waleh-17	226500	108600	16992	95916	156948	105348	
CD3387	Waleh-5	220815	107710	25320	120		104604	
CD3131	Haidan-1	219813	107757		993698	837098		
CD3132	Haidan-2	219802	107865	321977	295234	234994	280006	213592
CD3135	Haidan-3	219460	108108	1230067				
CD3136	Haidan-5	219675	108061		993698	837098	1044236	1252722
CD3137	Haidan-6	219757	107992		993698	837098	1044236	1252722
CD3138	Haidan-7	219280	108159	1230067	993698	837098	1044236	1252722
CD3139	Haidan-8	219330	108303	1230067		837098		
CD3141	Haidan-10	219491	108388	321977	295234	234994	280006	213592
CD3143	Haidan-12	219606	108507	1230067	993698	837098	1044236	1252722
CD3144	Haidan-13	219682	108628	1230067	993698	837098	1044236	1252722
CD3243	Haidan-15	219742	108628	1230067	993698	837098	1044236	1252722
CD3364	Haidan-16	219560	108680	1230067	993698	837098	1044236	1252722
CD3437	Haidan deep-2	219680	108685		993698	837098	1044236	1252722
CD1032	D. EL Mour	240120	100120	284400	384768			
CD3277	Musaitbeh-3	246870	101550	205950	303883	179963	180975	17715

CD3278	Musaitbeh-2	247850	99950	205950	303883	179963	180975	238826
CD3279	Musaitbeh-1	246900	101200	205950	303883	179963	180975	238826
CD3328	Musaitbeh-5	248000	101500	205950	303883	179963	180975	238826
CD3179	Muleih	232000	111000	23911	18283	27394	21218	17805
CD1074	Qastel-6	242750	131700		92604			
CD1080	Qastel-12	238950	125850	6108	2436			
CD1082	Qastel-14	239000	131560	205653				
CD1083	Qastel-15	239050	132000	205653	337755			300841
CD1084	Qastel-16	239650	132150	205653	337755			102412
CD1085	Qastel-17	239150	132590	205653	337755			300841
CD1086	Qastel-18	239200	132000	205653	337755			33060
CD3283	Qastel-5A	239750	128710	205653			215926	300841
CD3324	Qastel-11A	239300	130750	205653	337755	316463	215926	300841
CD1200	Erainbeh-1	243518	117749	325012	370424	410315	342030	302044
CD3232	Q.A.Port-4	243750	125000	294732	424512		341352	296076
CD3365	Yadudeh-2	234600	138600	21500	267111	465180	378795	474726
CD1134	Tunaib-1(pp87)	242550	131710		249996	394560	200004	256116
CD3348	Traffic Inst-1	257810	121330					17796
CD1027	SULEIMAN M. BARBAKH	251490	114875	208788	91932	71496	65448	13584
CD1033	HALEEM SALFITI	232700	137840	444420	190308	262908	296916	285852
CD1035	U'KASH HATMAL EL ZABIN NO 1	233680	123670	45672	20076	9588		42312
CD1036	ABDALLAH NASIR SALMAN	232580	109700	65004	54996	39504	45000	3072
CD1040	SUBHI TA'AMSEH	252025	121900	168000	157332	49524	51996	69864
CD1043	SAMI EL FAYEZ / JIZA	244480	123920	114000				
CD1044	HAKEM SULTAN EL FAYEZ	241950	121255	108000	43740	103260	53904	79680
CD1045	YAZEED ABU JABIR	235260	136720	78504	47724	45432	44172	40140

CD1047	MAHMOUD MOHAMMAD HAMED	249350	116600	85428	120360	45288	66696	38004
CD1049	CHIKEN GREAT FARMS CO.	233970	129600	44592	8352	1980	3852	2268
CD1051	KHALAF MNAIZEL EL MAHAKEEM	241500	116550	360000	192456	150732	151704	161904
CD1052	MASHHOUR EL FAYEZ	244020	123090	92496	94128	85992	13140	22728
CD1053	MAJID EL FAYEZ	237731	130155	280500	314784	178812	85800	110868
CD1054	FAHED ABU JABER /YADOUDEH	235600	139510	72000	12000	14196	35004	43200
CD1055	RAKAN EL FAYEZ NO 1	244150	120000	41040	24636	216276	5004	
CD1057	TRAD EL FAYEZ / ZIZIA	240935	119965	64800	141996	111576	101220	133128
CD1060	ALI EL FAYEZ NO 3	234275	134260	144000	48144	47352	42132	46776
CD1061	RAKAN EL FAYEZ NO 3	237200	131645	50952	83232	40068	1428	
CD1062	SAMI EL FAYEZ NO 3	233185	131050	336000	172800	49500	55500	154200
CD1064	FAWWAZ ABU JABER	235670	135670	75648	71208	75156	62712	54432
CD1065	MOUNIRA EL FAYEZ	235260	130850	66000	5004			
CD1066	MOHAMMAD DARWEESH EL SATEL	246365	114000		39996	72504	50004	108000
CD1067	MASOUD MOHAMMAD EL RUQOUB	246430	97720		105000	18396	7560	0
CD1068	A'KEF EL FAYEZ 2/ZIZYA(PP82)	239440	129880	406704	298056	249024	294444	216000
CD1070	TALAL MITHQAL EL FAYEZ	241550	119850	92496	45000	0	0	73632
CD1230	TAYEL MITHQAL EL FAYEZ	235335	131600	54000	9600	4524	65424	165372
CD1233	HANI MISHAEL ELSAYEGH	256470	120100	10680	4752	30528	30072	21324
CD1234	MOHAMMAD ADLI DALAL	253795	117865	13860	10356	10536	10200	25896
CD1235	ISSA AHMAD ABDELHAFEEDH	256100	121770	156936	40824	26244	33540	18516
CD1240	FAYEZ SHARARI ALKNEIA'N	256450	116000	74520	33936	23496	44628	23592
CD1242	SHAMS EDDIN HILAL KHALIL	258825	118800	29520	10488	6588	5004	
CD1243	HANI MISHAEL ELSAYEGH	257225	121275	13488	14184	5496	3108	
CD1244	MOHAMMAD JAMEEL KHAMEES	262250	101000	81708	58356	22620	75168	48996
CD1246	SULTAN MAHMOUD AL KHLAIFAT	267634	104285	25596	38472	24576	48144	44496

CD1252	MOHAMMAD A. KAREEM ELZUBEIDI	236090	126170	218076	213552	235512	150984	92688
CD1253	TRAD SHAHER EL FAYEZ	232590	128265	984	1152	1200	1152	5064
CD1255	ABDELRUHMAN EL U'DWAN & CO.	231470	131690	25116	30396	25296	35952	37368
CD1256	ABDELHADI ABU HAMMAD	246300	135900	65772	45492	39924	48300	17628
CD1260	ABDELHAFEEDH I ELKHANNAN 1	236850	104000	103284	68136			
CD1261	H.R.H.MOHAMMAD BEN TALAL	241250	130300	233748	150228	144756	103788	185928
CD1262	ABDALLAH RADY ESSATEL	248100	113100		53712	48300	50004	72000
CD1263	BADER BATHI ELZIBEN	247720	115150	38544	53712	102888	65496	141924
CD1264	HMAIDY MOHAMMAD EL FAYEZ	239460	129210	306000	19044			
CD1265	MISH'AL ELAHMAD ELSABBAH	236940	132520	47340	55500	48816	19368	18012
CD1266	ALI ABDALLAH ABU RBAIHA	224600	108620	108000	129252	143280	75516	67500
CD1267	JORDAN IRON BARS CO.	242100	130600	8484				
CD1268	DUGHEIM FARHAN ELHAMID	236700	113210		61716	36756		
CD1269	MINWER OBEID FALAH ELNOUFAL	231700	122380				45108	45000
CD1270	MOHAMMAD ABD ELA'MMOURI	248900	107340	44172	48996	29424	11160	15096
CD1271	KAMAL SULEIMAN EL DARDISI	245350	101520	71196	154068	57936	25356	49080
CD1273	DALMEH KAYED MOHAMMAD	243890	98270	205296	185496	220380	280848	317388
CD1274	A'WAD FANATEL ELZAIDAN	236320	98300	50004	65388	25404	33396	40500
CD1276	ABD RABBO GHADBAN ELSHNOUN	247150	100060	381360	300384	441816	399996	99000
CD1277	HASHEM KHALEEL EL QEISI	234800	99065	93936	60720	6024	33828	35712
CD1278	MAHMOUD ABD ABU OBEID	239980	112960	82980	155376	86736	92340	64800
CD1279	DARWEESH SALEM A'RAR	241780	100350		35256			
CD1280	RAGHDA HAMDI MANGO	238410	134260	27228	20808			
CD1281	LEFI KASEB AL NEIF	239270	102750	79632	73212	39504		
CD1282	OBEID HTAILAN SALAMEH	247630	103320	120000	400644	195528	174996	230640
CD1283	JAMAL BSHARA AL BSHARAT	232580	141680	26844	25740	23220	18120	22824

CD1284	AHMAD SALAMEH SULEIMAN	244120	102990	64392	24996	26496	75348	95112
CD1285	MOHAMMAD SHAHER EL FAYEZ	246900	107060	279048	417660	179724	248844	190572
CD1288	A'YED SAHL ELMUE'SH	238500	98400	16008	156156	59028	110328	103080
CD1291	SHEIMAN JADA'N ALI SHTAIWI	243420	101300		5736			
CD1292	GHASSAB SA'UD EL QADI	247525	109077	14880	12072	12276	4848	15528
CD1294	MOHAMMAD SALEEM IQBEIL	240120	104430	577476	320004	325548	300000	354660
CD1295	FAHED TAWFEEQ ZAYID	239115	104500	28800	35676	40152	37836	36708
CD1299	E'ID A'TWI SALAMEH	250625	123150	12504	147588	91908	50112	
CD1300	MOHAMMAD SHAHER ELFAYEZ	245360	99650	240000	165816	104568	190512	169284
CD1301	BANDAR DHAHER MOHAMMAD	234400	126900	996	49920			
CD1302	DHAIFALLAH MUTLAQ ADDUREIBI	253105	108390	48000	45780	22572		51540
CD1303	HAMMAD SALEM EL SAHEEM	232750	111150	15600	80316	22308	32304	97368
CD1305	SALEM A'YED SAMARA	243278	117065		278088	15000	150540	121836
CD1306	ABDELAZEEZ A'WWAD ELMOUR	237000	100000	108000	90000	109872	148860	58308
CD1307	FAYSAL DAIFALLAH EL DURAIBY	254315	106805	16332	18648	13188		
CD1308	IBRAHEEM MOHAMMAD EL LOUZI	231200	131640	266664	199152	111612	48588	279528
CD1310	NASHMI MITHQAL EL FAYEZ	233700	131850	4308				
CD1313	SHAHAR ZEID ELFAYEZ	234300	131175	36000	43584	20496	43572	44964
CD1315	DAHHAM DERDAH EL FAYEZ	239420	135230					4500
CD1316	HIJAB FAHD K.EL FAYEZ	246050	119380	120000	85500	225504	233760	240216
CD1317	HARRAN BEN KHAZAR EL BAKHEET	238760	136940	90000	40500	39372	50004	54000
CD1318	LAMYA BENT MAJEED EL SHAIKH	252150	115381	95292				
CD1319	JADALLAH IBRAHEEM NAJI	249695	117535	124464	86856	89988	55236	29340
CD1327	MOHAMMAD MINWER ELNOUFAL	250135	114980				17388	50520
CD1328	SALEM KHLEIF E'YADEH	234080	109440	120600	141552	42672	70104	23988
CD1329	KHALED MINWER EL NOUFAL	250330	113950	35004	996			

CD1331	KHLEIF ALI HUSAIN	245240	118345					119556
CD1332	RASHAD AMEEN SALEH	245970	105300	19200	18744	8592	35496	178224
CD1333	ALI MITHQAL EL FAYEZ	237970	130940	459000	375000	285000	300000	243840
CD1334	A'YYASH SALMAN ELKEDRAWI	251490	119700	140448	219312	80496	179148	147372
CD1335	ABDALLAH AHMAD YOUSEF	236035	123550	177780	138192	120504	65532	212004
CD1336	SAMI MITHQAL EL FAYEZ	243180	123650	110004	50004	45216	69996	35772
CD1337	FAHMI YOUSEF SHAM	245675	104830	253656	192276	105216	201000	120948
CD1338	FALEH ZA'AL EL FAYEZ	247278	119185	222000	268800	172500	200004	216000
CD1339	A'WAD HAMDAN EL RSHOUD	242850	117530	279996	372300	52380	175500	153432
CD1341	MOHAMMAD AHMAD HAMED	246830	116615	180000	288984	360060	141276	174300
CD1342	MAHMOUD MOHAMMAD HAMED	251116	116660	207504				
CD1343	SULEIMAN DAMEN ELNOFAL	251710	115860	14868	2748	4896	9756	6768
CD1344	MUSALLAM E'ID BAKHEET	243925	118325	212892	790476	479820	324624	341376
CD1346	A'DEL MOHAMMAD SULEIMAN	231570	110470	47820	26784	42120	32436	54000
CD1347	E'ID BEN NA'UR (TUNAIB)	240220	134070	270000	446604	507864	350004	198780
CD1349	GHALEB ABU JABER	236145	136365	82896	43824	46320	52860	64104
CD1350	FAWZIYYEH BINT M.ELHUSAIN	250295	116600	89004	56400	35856	30936	45000
CD1351	IRSHAID NADA KHUDEIR	240940	114040	95484				
CD1354	FARHAN SA'D ABU JABER	236930	138270	37212	15372	15468	14208	20172
CD1355	MIT'EB ZA'AL AL KNEI'AN	247900	119720			9144	10248	32400
CD1356	YOUSEF ABDELFATTAH	245455	103870	243300	290388	129864	84828	272436
CD1358	MOHAMMAD BAD'I ABDELHAFEETH	246550	104550	79296	71892	77016	44496	564
CD1359	SAMEEH ISHAQ ELFARAH	239550	120380	14328	14808	12588	13740	20796
CD1360	JAMAL BSHARA AL BSHARAT	234100	138505	360000	285024	375816	324888	429660
CD1363	BADI A'WWAD HAMDAN	239990	117575	93804	77856	32976	33252	75228
CD1365	MUTELLEH S.ELSATEL	244340	116010	196956	57924	56520	69996	81000

CD1372	MANSOUR ABDI BEN TAREEF	226800	106945	270000	181824	45324	43356	152424
CD1385	A'KEF EL FAYEZ 3(PP480)ZIZYA 2	239900	129715			28896	46296	3912
CD1401	SHAHER F.EL FAYEZ	240670	126710	188316	193068	128784	90576	135000
CD1403	GHALEB ABU JABER	237360	137210	120000	30084	52344	84996	156912
CD1404	JAMAL BSHARA AL BSHARAT	234620	138920	279792	705852	486684	402072	424080
CD1407	SULEIMAN HARB ELE'ID	242200	141950	6108	7200	8016	10500	4896
CD1409	MOHAMMAD ALI ELNABILSI	230270	131890	287040	382056	344376	355032	332616
CD3000	RAKAN MITHGAL ELFAYEZ	237050	131240	84000	62448	88752	100872	9348
CD3001	MUSA IBRAHEEM EL SA'DI	255000	120800	93144	132888	24324	36564	31308
CD3003	AHMAD MOHAMMAD ABU HAIDH	255120	118480	99000	71220	82464	88728	
CD3005	MOHAMMAD A. BAYER MUSA	258275	107410	162000	183072	165696	235932	204132
CD3010	A'WWAD ABD ELSHAWABKEH	268400	98350	30048	17496	16956	16776	10740
CD3011	HAMDA HAMADEH AL ZAIDAN	263190	103360	1200		45840	130500	170712
CD3012	SALMA D. KHADER EL NAIF	271900	90800	10548	67308	170328		
CD3013	MAHMOUD SALAMEH ABU JADDO'U	268700	100600	8004	3336	3252	12000	8520
CD3015	HUSAIN KAMEL HUSAIN A'NAN	262350	107630	45312	53688	52236	51300	73836
CD3016	AHMAD MOHAMMAD ABU HAIDH	263800	107240	216000	163332	129504	69996	92316
CD3017	MOHAMMAD ALI AHMAD AL RUQUB	263000	104950	106380	106200	86532	85524	49164
CD3018	YOUSEF HASAN H. HASANAIN	265150	105100	24720	17760	15252	35244	90192
CD3019	FUAD SA'AD FARHAN ABU JABER	270000	106000	176448	187584	116556	112524	249000
CD3020	FAHED S. F. ABU JABER	234570	139700	125952	84288	85320	145476	147864
CD3023	KHADER M. ABU SA'DA & PART.	264770	101330	45456	23940	75504	45228	20004
CD3025	U'WAITHER A. T. EL ZIBEN	254800	105300	28800			12000	
CD3026	JAYEZ THOUQAN EL BAKHEET	254265	114420	30144	82992	185496	0	203940
CD3027	MOHAMMAD ALI QAWOOQ	255900	114350	64776	42144	32904	45504	41928
CD3029	E'ID MUSALLAM SULEIMAN	258720	101650	94392	46368	41172	42396	32520

CD3032	SA'UD RAKHEES EL ZIBEN	256150	101925	96000		25380	215028	57600
CD3034	ABDELRUHMAN EL U'DWAN	231400	131700	288000	440148	350496	365520	382908
CD3035	HMAIDY MOHAMMAD ELFAYEZ	239800	129150	62676	69996	45000	99996	4164
CD3036	HMAIDY MOHAMMAD ELFAYEZ	238520	129945	72000	35004	9996	50004	20424
CD3037	MOHAMMAD GH. T. EL ZIBEN	253200	105600	20004	50004	58500	150000	108000
CD3039	NAWAL ABDELRUHMAN IBRAHEEM	270700	104725	129600	48264	39576	36012	
CD3040	FAHED RAJA A'WWAD EL WTHEIRI	268830	102640	77496	54996	45504		
CD3041	SALEH AYYASH S. EL KADRAWI	270420	101670	38892	40200		62136	
CD3046	MOHAMMAD A. JABER DARAWEESH	270245	108210	188496	185040	130572	181668	89100
CD3048	SALEH MOHAMMAD RADI EL SATEL	256880	105380	144000	79308	35796	43212	41724
CD3049	PRINCE ALI BIN NAYEF/MUSHATTA	252780	129570	90000	45000	40500	37908	43500
CD3051	GHAZI M. EL USTAH & PART	247080	135530	25812	32892	37176	33168	16656
CD3054	JALAL SAMI MUSHARBASH	250700	126350	46980	28872	19536	18480	34608
CD3055	HARRAN BEN KHAZAR EL BAKHEET	250050	129240	103512	31020			10800
CD3056	HUSAIN S. FARAJALLAH AHMAD	259800	125670	135468	101616	36768	120000	101016
CD3058	ALI A'TWA Q. EL A'ZAZMEH	266010	107840		158196	90564	80448	64680
CD3059	FUAD T. QATTAN	233610	130210	108000	103584	72708	78072	79212
CD3060	ALI DHAIL A. EL DAHHALEEN	255450	102700	177504	141192	118404	8460	27444
CD3061	MAHMOUD M. IRSHAID EL TAYYEB	257885	100750	164148	136800	150504	15000	9720
CD3062	HLALAH SALAMEH M. EL ZIBEN	256515	103385	247128	265164	273768	243252	137928
CD3063	BADER HWAILEH EL ZIBEN	255500	105000				67764	130440
CD3064	E'ID S. S. ABU JKHAIDIM	260920	100990	71640	86208	69936	138576	17016
CD3066	DHAIFALLAH S. EL ZIBEN & PART.	255425	101180	32004	74928	36204	40464	20856
CD3067	JAWAHER M. EL FAYEZ	252000	101750	350364	310836	396096	432408	326868
CD3069	SALEEM LAFI S. EL RAHEELEH	255920	105980	222660	146976	51636		132252
CD3071	KHALED J. M. ADDURAIBI	256670	109460				75984	114708

CD3072	AHMAD MATHHOUR ALDURAIBY	248475	108355	129480	60144	78468	7944	48600
CD3073	SHTAIWY A. S. AL JAM'ANY	257200	95980	57312	115536	45024	48612	83352
CD3077	IBRAHEEM K. A. EL I'TER	262060	108550				129996	108000
CD3081	SIHAIWI JAZA'A TRAD NAWARSEH	266000	99800	21000				120000
CD3090	YAHYA A. EL MUSALI	270885	110950	4836	720	2376	5880	2004
CD3098	MOHAMMAD KAREEM EL ZBAIDY	260450	104490	90000	50892	103992	115740	92232
CD3099	AHMAD DHAHER EL DAHAMSHEH	269420	101580	5400	23388	22380	21672	14364
CD3102	MOHAMMAD SULEIMAN BARBAKH	264540	108000			28500	37956	30828
CD3113	KHALED A. K. AL ZUBAIDI	258000	106450				22668	66156
CD3121	QUEEN ALIA INTERNAT.AIRPORT 3	243000	124400	14736	4680		190140	126240
CD3127	I'NAD MOHAMMAD EL FAYEZ 1	237080	127380	0	29412	59880	47316	28404
CD3161	HAMER SHAHER EL FAYEZ	236750	129850	59196	118404	120012	76260	18156
CD3167	I'NAD MOHAMMAD EL FAYEZ 3	240650	127850	177924	2004	2004	1500	
CD3168	ZEID BIN SHAKER	233100	134100			10200	32484	35712
CD3170	MOHAMMAD YOUSEF EL WREIKAT	271000	108950	71964	22296	8004	20736	66408
CD3177	MISBAH ZAKI MOHAMMAD EL SOUS	254865	121845	27888	29844	30264	34824	24912
CD3183	KAREEM NAWWASH EL ZIBEN	250850	101530	273132	271452	335304	177084	214272
CD3185	MOHAMMAD SH. H. ABU RAQIQ	256935	102550	162000	9372	19200	115920	48264
CD3186	ISSA M. EL JILANI	266200	102810	31080				
CD3192	HWAILEH E'ID Q. EL ZIBEN	259970	101810	84180	96324	69504	103308	81468
CD3193	SALAMEH MIFLEH EL ZIBEN	251045	103330	173700	130836	30312	47688	318552
CD3195	JLAYYEL SARSAK SHINWAN ALZIBEN	264495	98940	2376				
CD3196	JABIR H. M. SULEIMAN	252300	100750	206304	159504	220500	249996	37920
CD3198	MOHAMMAD HWAILEH EL ZIBEN	251830	102730	208068	329268	243600	307620	181164
CD3200	FANKHAIR A. T. EL ZIBEN	253490	105220	44760	137568	65868	75324	61212
CD3204	A'KEF EL FAYEZ 5	239280	129885	450000	694860	765564	776736	611676

CD3212	MAHMOUD A. ABU MATAR	252900	103450	13800	15504	18576	54420	52728
CD3213	MOHAMMAD A. TH. MSHAQI	246125	103650	31980	30396	18516	25500	119832
CD3214	SULTAN M. H. AL KHLAIFAT	265055	108405	0	0	0	0	65796
CD3215	IRON & STEEL UNITED MFG.CO.1	240060	121470	3144	72	144	0	0
CD3217	RFAIFAN KHALED AL KHRAISHA	253700	129070	30000	48000	18504	20496	4836
CD3218	ISSA W. IBRAHEEM QA'WAR	259380	124170	128820	144264	32544	54996	128952
CD3236	PRINCESS BASMA	248850	128220	150000	99996	99996	99996	99996
CD3237	PRINCESS BASMA	248210	128840	150000	99996	99996	99996	99996
CD3238	I'NAD MOHAMMAD EL FAYEZ 2	240550	128700	57900	9996	2040	2004	45000
CD3239	ABDELHAFEDH MAR'I ELKHANNAN	233170	103570	10884	9204	9504	27036	11412
CD3240	TAWFEEQ FARES SALMAN	237420	122850	104664	91860	77892	70668	74244
CD3242	RAGHDA MANGO /TUNAIB	238600	134500	32988	37920	25920	14988	4320
CD3246	NAWAL ABD. EL A'QIRBAWY	255195	105905					151956
CD3251	MOHAMMAD H. AL MUBARAK	258710	128860	112500	120000	39468	195456	97776
CD3253	FAHED M. SULEIMAN AL GHUBAIN	257420	128350	89604	81036	45708	92148	103884
CD3258	I'NAD MOHAMMED ELFAYEZ 4	240458	128502	393996	360576	372480	107616	398580
CD3261	MOHAMMAD S. M. BARBAKH	254380	113425	253740	243744	100920	270000	252864
CD3262	ZEID BEN SHAKER	244900	98450	168240	145488	292692	160536	198000
CD3264	ALHIKMA INVESTMENT CO.	244100	129730	2280	1020	6084	240732	1416
CD3267	MUNEERA MITHGAL ELFAYEZ	235830	131050	94284	60816	4416	10512	19356
CD3268	MIT'EB ZA'AL ELFAYEZ	247900	119720	225000	101820	160500	24984	216000
CD3269	HMAIDY ZA'AL EL FAYEZ	248365	118850	129600	249996	190500	309996	78276
CD3271	MAMDOUH SULTAN ELFAYEZ	241600	120850	252504	403620	562836	200004	268668
CD3272	I'MAD KHALEEF ABU SHIHAB	253900	116200	411996	378120	198504	205716	268164
CD3273	KINA CO. FOR SANITARY PAPER	244725	117135	514560	365616	409644	314172	284448
CD3274	GHAZI M.NABHAN AL JABALI	234210	133220	39252	10800	13572	22764	39792

CD3275	RASHED BEN KHALFAN EL DHAHIRI	236670	103850	230400	409944	413316	469956	326988
CD3280	RAZI PHARMACEUTICAL INDUSTRY	234975	132850	20820	18180	18708	13032	14400
CD3285	GENERAL SPECIALIZED STEEL	252420	133860	2544	6000	5508	3312	4500
CD3288	U'KASH HATMAL ELZIBEN	234600	122160	13152	24			72420
CD3289	MOHAMMAD H. M.ALMASHAYEKH	235300	105350	112500	450000	399996	350004	424728
CD3290	RAJA'EE MOHAMMAD GHANEM	238100	101900	62496	51132	12888	14592	8676
CD3291	HINNAH SULEIMAN MATALGA	224565	106345	41676	35112	28872	74328	45804
CD3293	SABRI M. AHMAD MUSTAFA	249600	117040	2544	2376	2856	2148	1536
CD3294	GHZAYYEL MOHAMMAD EL FAYEZ	242070	123320	81600	38892	21396	204	0
CD3295	THAMER ZEID ELFAYEZ	242865	120910	53148	36732	15840	35820	20796
CD3296	SAMI MITHGAL ELFAYEZ	233000	131100	13164	28800	25500	18000	
CD3298	MOHAMMAD BARAKAT E'LAYYAN	250840	115825	132276	101604	89952	71904	104328
CD3299	RASHED BEN KHALFAN EL DHAHIRI	246860	106750	253212	228768	126228	242664	230508
CD3315	NA'IL SALEEM KHAIR	236360	132755	15072	3540	4992		
CD3316	SA'UD FAHED TALAL ALTHIYAB	244240	128910	107472	24000	53064	46452	42204
CD3322	GULF INDUST. DEVELOPMENT CO	244710	114495	1908	2664	4068	17016	37488
CD3323	ZAYTOUNEH UNIVERSITY	234975	137780	25308	8664	22608	8400	32748
CD3326	QUEEN ALIA INTERNAT.AIRPORT 6	241937	124542	245688	166860	0	163380	150084
CD3330	ATALLA SAYYAH MIRSAL ELNIMER	262500	118400	79248	92328	140304	140004	0
CD3331	ISA'AF ELHAJ SA'UD ELNABILSI	226930	133960	172656	190704	48096	13248	22908
CD3334	UNIVERSAL IRON & STEEL INDUSTR	252900	134635	4728	4380	5016	4284	4824
CD3344	NA'IL SALEEM KHAIR	236280	133000	46488	49680	33288	37128	24012
CD3345	PRINCE ALI BEN NAYEF	252400	128400	16236	43200	30504	39312	36912
CD3346	GHALEB SALEH ABU JABER	235050	142320	15204	22188	16656	23916	13752
CD3349	ALI ADEL ODEH AND PARTNER	241210	123850	21024	17976	10428	15984	8040
CD3350	AL ISRAA UNIVERSITY 2	238210	133230	13488	57024	57300	62172	68652

CD3375	SAKHER MOHAMMAD D. ELMOUR	258450	96240	0	195996	98496	150000	70128
CD3376	FAYSAL A'KEF EL FAYEZ	262950	112100	14496	73104	65304	90840	52716
CD3377	SHEHADEH SALAMEH AL AQTASH	230955	111310	7032	7368	8364	9180	8736
CD3378	INT. CO. FOR MEDICAL INDUSTRIES	240775	129535	540	11784	14232	7836	7032
CD3379	DAHHAM DERDAH EL FAYEZ	242730	132025		30000	111276	200004	198852
CD3381	LATIN PATRIARCHATE	231950	141530		192	2256	10212	8796
CD3382	FAWWAZ HUWAIMIL ELZIBEN	231000	126400			54912	84504	57528
CD3383	MIT'EB NASER AKHU SUHAINEH	251450	93950			68508	95100	21540
CD3384	MOHAMMAD N. S. AKHU SUHAINEH	241000	102020		19740			
CD3398	NABEEL ABDELLATEEF SAKKIJHA	241115	116660		237468	102120	165000	233784
CD3400	ABDELHAFEEDH EL KA'ABNEH	236980	104070		64824	225384	208980	271608
CD3401	HARRAN KHAZAR EL BAKHEET	238575	136950		14736	92424	100008	144000
CD3421	ZIAD KHALAF EL MANASEER	236750	135200				62844	75048
CD3443	MUNIRAH MITHQAL EL FAYEZ	235260	130850					26988
CD3444	HUSAM SA'EED AL NIMER	236090	126170					101376

Well ID	Well Owner or well name	Coordinates PG		Elev. (m)	Well Depth (m)	SWL (m)	Yield (m³/h)	Draw Dwn. (m)	S.C. m³/h/m	T (m2/d)	S.TH. (m)	K (m/d)
		North	East									
CD1016	WALA NO 1	106650	224090	458	77	8.9	47	14.55	3.2	109	68.1	2.2 E-5
CD1019	WALA NO 9	108100	219375	350	106	10.15	134	0.58	231	7854	155.9	4.4 E-4
CD1095	WALA NO 6	107250	223380	454	218	25.68	140	14.78	9.6	326	191.3	6.9 E-6
CD1099	WALA NO 13	106990	224930	496	177	36.8	124.5	3.6	35	1190	129.2	6.1 E-5
CD1100	WALA NO 14	107050	223900	476	244	26.22	77	73.35	1.1	37	214.8	2 E-6
CD3386	WALA NO 17	108600	226500	500	155							
CD3387	WALA 5A	107710	220815	425	161	37.1	88	45.4	1.9	65	193	2.7 E-6
CD3131	HEEDAN NO 1	107757	219813	320	197	3.1	28	82	0.3	10		
CD3132	HEEDAN NO 2	107865	219802	339	148	0	184	32.64	5.6	190		
CD3135	HEEDAN NO 4	108108	219460	360	108	5.4	226	0.75	301.3	10244		
CD3136	HEEDAN NO 5	108061	219675	350	137	1.25	205	1	205	6970		
CD3137	HEEDAN NO 6	107992	219757	340	86	2.1	225	13.15	17.1	581		
CD3138	HEEDAN NO 7	108159	219280	360	56	1.2	325	3.55	91.5	3111		
CD3139	HEEDAN NO 8	108303	219330	360	108	0	388	0.9	431.1	14657		
CD3141	HEEDAN NO 10	108388	219491	350	81	2.63	207	15.88	13	442		
CD3143	HEEDAN NO 12	108507	219606	351	31							
CD3144	HEEDAN NO 13	108628	219682	355	126	6.6	220	0.9	244.4	8310		
CD3243	HEEDAN NO 15	108628	219742	355	130	5.3	231	1.35	171.1	5817		
CD3364	HEEDAN NO.16	108680	219560	360	30	22.1	100	0.5	200	6800		
CD3437	HEEDAN DEEP 2	108685	219680	356	250	42.6	142	0.47	302.1	10271		
CD1032	DAB'AN KH. EL MOUR	100120	240120	750	316	188	88	12	7.3	248	128	2.3 E-5
CD3277	MUSAITBEH NO 3	101550	246870	720	298	159.8		3.3				
CD3278	MUSAITBEH NO 2	99950	247850	718	296	160	44	13.3	3.3	112		
CD3279	MUSAITBEH NO 1	101200	246900	720	282	167.7	64	23.92	2.7	92		
CD3328	MUSAITBEH NO 5	101500	248000	724	300	149.5	81	5.18	15.6	530		
CD3179	MULEIH	111000	232000	650	198	137.6	57	7.13	8	272		
CD3174	QASTAL NO 6	131700	242750	740	363	151.7	30	4.5	6.7	228	211.3	1.4 E-5
CD1080	QASTAL NO 12	125850	238950	720	343	146.6	39	61.8	0.6	20	194.4	1.6 E-6
CD1082	QASTAL NO 14	131560	239000	750	188	166.5	67	1.2	55.8	1897	33.5	6.5 E-4

CD1083	QASTAL NO 15	132000	239050	745	224	167	55	33	1.7	58	57	1.1 E-5
CD1084	QASTAL NO 16	132150	239650	735	202	163.1	65	9.75	6.7	228	37.85	6 E-5
CD1085	QASTAL NO 17	132590	239150	742	204	165.6	75	2.35	31.9	1085	38.4	3.3 E-4
CD1086	QASTAL NO 18	132000	239200	740	204	171.2	70	5.6	12.5	425	32.8	1.5 E-4
CD3283	QASTAL NO 5A	128710	239750	740	440	164.7	35	193.55	0.2	7		1.35 E-6
CD3324	QASTAL NO 11A	130750	239300	748	361	173.7	60	0.35	171.4	5828		1.9 E-3
CD1200	ARAINBEH NO 1	117749	243518	699	292	144.5	87	1.17	74.4	2530	141.1	2.1 E-4
CD3232	Q.A.I..AIRPORT 4	125000	243750	710	400	154.2	32	44.18	0.7	24		
CD1134	TUNAIB 1 (PP 87)	131710	242550	730	162	152					10	
CD3348	TRAFFIC INST.1	121330	257.81	850	415	250.5	65	7.09	9.2	313	68	5.3 E-5
CD1027	S. M. BARBAKH	114875	251490	716	290	156.9	80	0.35	229	7786	133	6.8 E-4
CD1033	HALEEM SALFITI	137927	233340	825	248	110.4	53	34.2	1.55	53	138	4.4 E-6
CD1035	U'KASH ZABIN - 1	123670	233680	730	352	176	40	59	0.7	24	176	1.5 E-6
CD1036	ABDALLAH N. SALMAN	109700	232580	560	152	82.8	50	44.7	1.1	37	69	6.2 E-6
CD1040	SUBHI TA'AMSEH	121900	252025	720	225	164.1	50	28.5	1.75	60		1.1 E-5
CD1043	SAMI EL FAYEZ / JIZA	123920	244480	710	280	143.5	45	75.7	0.6	20		1.85 E-6
CD1044	HAKEM S. EL FAYEZ	121255	241950	716	283	159.7	65	17.5	3.7	126		1.2 E-5
CD1045	YAZEED ABU JABIR	136720	235260	789	230	119	30	69.1	0.43	15		8.1 E-7
CD1047	MAHMOUD M. HAMED	116600	249350	690	210	136	60	0.12	500	17000		2.7 E-3
CD1049	CHIKEN FARMS CO.	129600	233970	744	261	164.2	10	61.68	0.16	5		6.6 E-7
CD1051	KHALAFM.EL AHAKEEM	116550	241500	710	265	151.6	75	0.05	1500	51000		
CD1052	MASHHOUR EL FAYEZ	123090	244020	715	266	151.5	55	1.9	28.9	983		9.9 E-5
CD1053	MAJID EL FAYEZ	130155	237731	737	264	162.3	50	0.8	62.5	2125		2.4 E-4
CD1054	FAHED ABU JABER	139510	235600	820	180	72.75	63	30.75	2	68		7.5 E-6
CD1055	RAKAN EL FAYEZ NO 1	120000	244150	710	230	161.1	62	1.18	52.5	1785		7.8 E-4
CD1057	TRAD EL FAYEZ / ZIZIA	119965	240935	710	370	152.5	50	82.7	0.6	20		1.2 E-6
CD1060	ALI EL FAYEZ NO 3	134260	234275	775	250	148.4	46	39.9	1.2	41		4.37 E-6
CD1061	RAKAN EL FAYEZ NO 3	131645	237200	745	285	169.1	25	53.3	0.47	16		1.6 E-6
CD1062	SAMI EL FAYEZ NO 3	131050	233185	755	270	190.7	82	0.4	205	6970		1 E-3
CD1064	FAWWAZ ABU JABER	135670	235670	780	263	146	35	96	0.37	13		1.3 E-6
CD1065	MOUNIRA EL FAYEZ	130865	235220	758	236	182.4	60	0.95	63.2	2149		4.6 E-4
CD1066	M. DARWEESH EL SATEL	114000	246365	702	323	152.9	50	22.1	2.3	78		5.2 E-6
CD1067	MASOUD M. EL RUQOUB	97720	246430	741	320	169.4	52	111.8	0.5	17		1.3 E-6
CD1068	A'KEF EL FAYEZ (PP82)	129960	239490	746	209	168	8	35	0.23	8		2.2 E-6

CD1070	TALAL M. EL FAYEZ	119850	241550	708.6	248	145.7	79	32.3	2.5	85		9.5 E-6
CD1230	TAYEL M. EL FAYEZ	131600	235335	769	271	194.4	60	0.5	120	4080		6.2 E-4
CD1233	HANI ELSAYEGH	120100	256470	742	305	198	77	51.2	1.5	51		9 E-6
CD1234	M. ADLI DALAL	117365	253795	716	275	159.3	60	60	1.2	41		3.3 E-6
CD1235	ISSA A. ABDELHAFEEDH	121800	256600	768	280	211.6	72	33	2.2	75		1.3 E-5
CD1240	FAYEZ SH. ALKNEIA'N	116000	256450	719	275	163	65	9	7.2	245		2.5 E-5
CD1242	SHAMS EDDIN KHALIL	118800	258825	742	350	190.6	35	63	0.55	19		2 E-6
CD1243	HANI ELSAYEGH	121275	257225	770	300	212.2	45	45	1	34		5.9 E-7
CD1244	M. JAMEEL KHAMEES	101000	262250	830	430	250	40	17	2.35	80		
CD1246	SULTAN AL KHLAIFAT	104285	267634	797	377	210	60	18.3	3.28	112		
CD1252	MOHAMMAD ELZUBEIDI	126170	236090	749	344	176.4	60	38.5	1.56	53	140	4.4 E-6
CD1253	TRAD SH. EL FAYEZ	128265	232590	780	370	222	50	67	0.75	26		
CD1255	ABDRUHMANELU'DWAN	131690	231470	760	365	183.4	18	159	0.11	4	150	3.1 E-7
CD1256	ABDELHADIA. HAMMAD	135900	246300	762	420	185.6	44	22.5	1.95	66		
CD1260	A. ELKHANNAN 1	104000	236850	700	344	136.6	40	39.2	1	34		
CD1261	H.R.H.M. BEN TALAL	130300	241250	732	323	161.7	55	7	7.9	269	174	1.8 E-5
CD1262	ABDALLAH R. ESSATEL	113100	248100	740	330	165	45	62	0.73	25	170	1.7 E-6
CD1263	BADER BATHI ELZIBEN	115150	247720	705	240	156.1	91	4.4	20.7	704		9.7 E-5
CD1264	HMAIDY M. EL FAYEZ	129350	239350	732	335	160.6	55	7	7.9	269		1.8 E-5
CD1265	MISH'AL ELSABBAH	132270	236640	760	395	191	25	89	0.28	10		5.8 E-7
CD1266	ALI ABU RBAIHA	108620	224600	580	200	113.6	50	6.87	7.28	248		
CD1267	JORDAN IRON BARS CO.	130600	242100	730	300	158.5	48	0.35	137.1	4661		
CD1268	DUGHEIM F. ELHAMID	113210	236700	682	255	141.6	60	31.15	1.94	66		6.7 E-6
CD1269	MINWER O. ELNOUFAL	122380	231700	763	334	205	35	68	0.52	18		1.6 E-6
CD1270	MOHAMMAD A'MMOURI	107325	248870	758	282	190.6	60	26	2.3	78		1 E-5
CD1271	KAMAL EL DARDISI	101520	245350	700	251	137.8	100	4	25	850		
CD1273	DALMEH MOHAMMAD	98260	243900	741	262	169.2	75	0.7	107	3638		4.5 E-4
CD1274	A'WAD ELZAIDAN	98345	236255	768	328	206.1	50	41.25	1.2	41		3.9 E-6
CD1276	ABD RABBO ELSHNOUN	100090	247120	720	260	147.8	70	2.3	30.4	1034		1 E-4
CD1277	HASHEM EL QEISI	99040	234785	746	322	183.7	61	27.66	2.2	75		4.7 E-6
CD1278	MAHMOUD ABU OBEID	112965	239995	693	304	143.9	70	0.05	1400	47600		3.4 E-3
CD1279	DARWEESH S. A'RAR	100350	241780	720	304	156.5	65	15.2	4.27	145	147.5	1.1 E-5
CD1280	RAGHDA H. MANGO	134330	234390	789	305	181.6	32	48	0.7	24		6.6 E-5
CD1281	LEFI KASEB AL NEIF	102750	239270	717	323	158.7	75	0.85	88.2	2999		2.1 E-4

CD1282	OBEID H. SALAMEH	103320	247630	716	297	142.3	85	12.55	6.8	231		1.7 E-5
CD1283	JAMAL B. AL BSHARAT	141680	232580	920	349	116	15	33	0.45	15		
CD1284	AHMAD S. SULEIMAN	103000	244140	694	255	123.7	62	1.27	48.8	1659		1.5 E-4
CD1285	MOHAMMAD EL FAYEZ	107060	246900	753	369	185.7	70	43	1.6	54		3.5 E-6
CD1288	A'YED SAHL ELMUE'SH	98400	238500	760	290	196.6	54	52.6	1	34		
CD1291	SULIMAN J. SHTAIWI	101300	243420	720	297	142.1	81	16	5.1	173		
CD1292	GHASSAB EL QADI	109077	247525	701	340	133.6	20	70	0.3	10		1.2 E-5
CD1294	MOHAMMAD S. IQBEIL	104430	240150	708	322	148.4	76	0.6	126.7	4308		2.9 E-4
CD1295	FAHED TAWFEEQ ZAYID	104500	239115	695	303	139.9	50	59.2	0.85	29		2.1 E-4
CD1299	E'ID A'TWI SALAMEH	123150	250625	720	328	162.6	40	62.95	0.6	20		
CD1300	MOHAMMAD ELFAYEZ	99650	245360	740	314	177.2	50	36	1.39	47		
CD1301	BANDAR H.MOHAMMAD	126900	234400	725	350	170	32	90	0.4	14		
CD1302	DH. ADDUREIBI	108390	253105	763	350	196.2	55	52	1.1	37		2.7 E-6
CD1303	HAMMAD EL SAHEEM	111060	232830	590	255	89.66	45	8	5.6	190		1 E-5
CD1305	SALEM A'YED SAMARA	117065	243740	696	241	138.1	65	2.8	23.2	789		8.9 E-5
CD1306	ABDELAZEEZ ELMOUR	99415	239275	763	350	199	70	25.75	2.71	92		
CD1307	FAYSAL EL DURAIBY	106805	254315	779	350	225.9	32	46.78	0.68	23		
CD1308	IBRAHEEM EL LOUZI	131605	232190	757	305	192.5	60	0.7	85.7	2914		3 E-4
CD1310	NASHMI EL FAYEZ	131800	233805	756	227	189.1	70	71.7	0.98	33		1 E-5
CD1313	SAHAR ZEID ELFAYEZ	131140	234290	762	385	196	32	44	0.73	25		1.5 E-6
CD1315	DAHHAM EL FAYEZ	135230	239420	786	310	213	60	17.28	3.5	119		1.4 E-5
CD1316	HIJAB FAHD K.EL FAYEZ	119380	246050	690	247	134.9	75	20.7	3.62	123		
CD1317	HARRAN EL BAKHEET	136940	238760	785	213	184	65	4	16.25	553		
CD1318	LAMYA BENTEL SHAIKH	115390	252625	710	275	155.7	60	1.95	30.8	1047		1 E-4
CD1319	JADALLAH NAJI	117530	249720	699	245	142.8	65	31.95	2	68		1.7 E-5
CD1327	MOHAMMAD ELNOUFAL	115075	250175	710	304	155	71	0.81	87.6	2978		2.3 E-4
CD1328	SALEM KHLEIF E'YADEH	109440	234080	580	267	93	60	40	1.5	51		
CD1329	KHALED EL NOUFAL	113935	250340	742	326	192.3	60	53.18	1.13	38		3.2 E-6
CD1331	KHLEIF ALI HUSAIN	118265	245255	689	267	130.5	70	3.6	19.4	660		5.6 E-5
CD1332	RASHAD AMEEN SALEH	105300	245990	707	315	133.2	72	38.54	1.9	65		4.1 E-6
CD1333	ALI MITHQAL EL FAYEZ	130925	238000	737	260	161.9	45	0.15	300	10200		1.2 E-3
CD1334	A'YYASH ELKEDRAWI	119700	251490	713	250	155.9	55	38.8	1.42	48		5.9 E-6
CD1335	ABDALLAH YOUSEF	123550	236030	725	370	152.5	50	82.7	0.6	20		1.2 E-7
CD1336	SAMI EL FAYEZ	123655	243055	716	265	153.3	59	0.58	101.7	3458		3.6 E-4

CD1337	FAHMI YOUSEF SHAM	104830	245675	700	322	135.5	70	1.9	36.85	1253		
CD1338	FALEH ZA'AL EL FAYEZ	118920	247325	706	297	150.8	76	16.6	4.6	156		1.3 E-5
CD1339	A'WAD EL RSHOUD	117530	242850	706	265	159	120	0.5	240	8160		
CD1341	MOHAMMAD HAMED	116615	246830	680	210	128.7	75	19.05	3.94	134		
CD1342	MAHMOUD HAMED	116640	251072	698	225	143.3	80	2.27	35	1190		1.7 E-4
CD1343	SULEIMAN ELNOFAL	115815	251690	703	273	148.3	60	28.8	2.1	71		6.6 E-6
CD1344	MUSALLAM BAKHEET	118260	243950	718	257	158.9	62	0.53	117	3978		
CD1346	A'DEL SULEIMAN	110300	231560	638	250	144.6	25	76.4	0.3	10		1.3 E-6
CD1347	E'ID BEN NA'UR	133970	240300	754	215	179.1	50	0.3	166.7	5668		1.8 E-3
CD1349	GHALEB ABU JABER	136365	236100	786	303	144.3	35	49.6	0.71	24		1.7 E-6
CD1350	FAWZIYYEH ELHUSAIN	116540	250300	696	220	140.9	50	48.9	1	34		4.6 E-6
CD1351	IRSHAID KHUDEIR	114040	240940	700	292	146	50	64	0.78	27		
CD1354	FARHAN ABU JABER	138150	237160	808	180	152.4	50	10.9	4.59	156		6.5 E-5
CD1355	MIT'EB Z. AL KNEI'AN	117950	247920	691	200	139	60	0.18	333	11322		2.2 E-3
CD1356	YOUSEF ABDELFATTAH	104010	245385	719	301	147.6	70	2.8	25	850		6.5 E-5
CD1358	M. ABDELHAFEETH	104550	246550	720	228	147	55	24.65	2.23	76		
CD1359	SAMEEH ELFARAH	120110	239175	685	270	121.3	90	46.2	1.95	66		5.2 E-6
CD1360	JAMAL AL BSHARAT	138490	234135	843	213	109.6	57	17.6	3.23	110		1.2 E-5
CD1363	BADI A'WWAD HAMDAN	117649	239926	680	270	136.5	60	54.5	1.1	37		3.2 E-6
CD1365	MUTELLEH S.ELSATEL	116010	244340	670	305	147.1	52	42	1.24	42		
CD1372	MANSOUR BEN TAREEF	106945	226800	682	390	204	75	17.3	4.33	147		
CD1385	A'KEF EL FAYEZ (PP480)	129710	239890	737	300	166	80	8	10	340		
CD1401	SHAHER F.EL FAYEZ	126980	240150	726	245	155.7	44	22.3	1.97	67		8.7 E-6
CD1403	GHALEB ABU JABER	137110	237110	793	202	145.6	53	4.28	12.4	422		3.6 E-5
CD1404	JAMAL AL BSHARAT	138730	234590	821	225	95	62	1.88	33	1122		1 E-4
CD1407	SULEIMAN HARB ELE'ID	141950	242200	840	365	162.8	18	64.2	0.28	10		
CD1409	M. ALI ELNABILSI	131880	230260	774	308	219.1	80	3.25	24.6	836		1.1 E-4
CD3000	RAKAN ELFAYEZ	131645	237200	745	285	169.1	25	53.3	0.47	16		1.6 E-6
CD3001	MUSA EL SA'DI	120800	255000	734	325	183.3	45	70	0.64	22		
CD3003	AHMAD ABU HAIDH	118480	255120	720	370	168.4	50	17	2.94	100		
CD3005	M. A. BAYER MUSA	107410	258275	810	319	202	60	23	2.6	88		
CD3010	A'WWAD SHAWABKEH	98350	268400	860	344	271.6	50	5	10	340		
CD3011	HAMDA AL ZAIDAN	103360	263190	810	330	222	50	18	2.78	95		
CD3012	SALMA EL NAIF	90800	271900	930	385	321.6	60	5.65	10.62	361		

CD3013	M. ABU JADDO'U	100600	268700	840	360	250.5	33	26	1.27	43		
CD3015	HUSAIN KAMEL A'NAN	107630	262350	760	364	189.3	50	7	7.14	243		
CD3016	AHMAD ABU HAIDH	107240	263800	780		201.9	60	33.6	1.78	61		
CD3017	MOHAMMAD AL RUQUB	104950	263000	790	390	198.5	60	7	8.57	291		
CD3018	YOUSEF HASANAIN	105100	265150	815	310	228.3	60	6.7	8.95	304		
CD3019	FUAD ABU JABER	106000	270000	800	375	223	50	17	2.94	100		
CD3020	FAHED S. F. ABU JABER	139860	234550	820	201	91.9	20	27.53	0.73	25		2.7 E-6
CD3023	KHADER ABU SA'DA	101330	264770	842	380	253	45	22.5	2	68		
CD3025	U'WAITHER EL ZIBEN	105300	254800	765	343	214.5	55	41.45	1.32	45		
CD3026	JAYEZ EL BAKHEET	114420	254265	720	358	172.4	45	41.8	1.07	36		
CD3027	M. ALI QAWOOQ	114350	255900	720	450	174.7	60	11.5	5.22	177		
CD3029	E'ID SULEIMAN	101650	258720	810	400	217.1	50	26	1.92	65		
CD3032	SA'UD R. EL ZIBEN	101925	256150	775	300	200.8	53	34	1.56	53		
CD3034	ABDRUHMAN EL'DWAN	131700	231400	762	265	205.2	60	0.7	85.7	2914		2.25 E-4
CD3035	HMAIDY M. ELFAYEZ	129150	239800	730	347	163.1	60	47	1.27	43		7.9 E-5
CD3036	HMAIDY M. ELFAYEZ	129945	238520	730	350	172.1	50	24	2.08	71		
CD3037	MOHAMMAD EL ZIBEN	105600	253200	760	403	215	60	19	3.16	107		
CD3039	NAWAL IBRAHEEM	104725	270700	790	380	234	45	42.5	1.06	36		
CD3040	FAHED EL WTHEIRI	102640	268830	820	365	226	45	53	0.85	29		
CD3041	SALEH EL KADRAWI	101670	270420	835	370	245.2	50	0.4	125	4250		
CD3046	M. A. DARAWEESH	108210	270245	840	430	283.3	40	27	1.48	50		
CD3048	SALEH M. EL SATEL	105380	256880	800	320	237.5	45	24.5	1.84	63		
CD3049	P. ALI BIN NAYEF	129570	252780	768	445	208	30	71	0.42	14		
CD3051	GHAZI M. EL USTAH	135530	247080	770	370	192.5	15	155	0.1	3		
CD3054	JALAL MUSHARBASH	126350	250700	738	475	174.5	25	61	0.41	14		
CD3055	HARRAN ELBAKHEET	129240	250050	760	354	192.4	60	24.1	2.49	85		
CD3056	HUSAIN S. F. AHMAD	125670	259800	870	421	273.3	60	1.5	40	1360		
CD3058	ALI EL A'ZAZMEH	107840	266010		365	208.3	60	11.5	5.22	177		
CD3059	FUAD T. QATTAN	130210	233610	755	327	194.4	36	48.6	0.74	25		2.1 E-6
CD3060	ALI EL DAHHALEEN	102700	255450	770	400	193	55	38.5	1.43	49		
CD3061	MAHMOUD EL TAYYEB	100750	257885	780	450	192	52	120	0.43	15		
CD3062	HLALAH EL ZIBEN	103385	256515	775	392	208.5	60	5.9	10.17	346		
CD3063	BADER H. EL ZIBEN	105000	255500	780	400	211.1	60	8.5	7.06	240		
CD3064	E'ID S. S. ABU JKHAIDIM	100990	260920	840	390	230	55	17	3.23	110		

CD3066	DHAIFALLAH EL ZIBEN	101180	255425	765	302	183.5	60	5.5	10.9	371		
CD3067	JAWAHER M. EL FAYEZ	101750	252000	740	350	168.3	60	0.5	120	4080		
CD3069	SALEEM EL RAHEELEH	105980	255920	790	322	222.2	50	7.5	6.66	226		
CD3071	KHALED ADDURAIBI	109460	256670	770	300	204.5	60	11.5	5.22	177		
CD3072	AHMAD M. ALDURAIBY	108355	248475	720	326	158.2	60	17	3.53	120		
CD3073	SHTAIWY AL JAM'ANY	95980	257200	790	276	190.4	60	19.5	3.07	104		
CD3077	IBRAHEEM K. A. EL I'TER	108550	262060	770	355	200	50	18	2.78	95		
CD3081	SIHAIWI JAZA'A TRAD	99800	266000	860	374	256.6	60	12	5	170		
CD3090	YAHYA A. EL MUSALI	110950	270885	850	420	277.7	60	5	12	408		
CD3098	MOHAMMAD EL ZBAIDY	104490	260450	810	377	220.5	60	18	3.33	113		
CD3099	AHMAD ELDAHAMSHEH	101580	269420	830	372	237.8	50	47.6	1.05	36		
CD3102	M. SULEIMAN BARBAKH	108000	264540	806	392	205.3	40	66.2	0.6	20		
CD3113	KHALED AL ZUBAIDI	106450	258000	780	337	204.7	60	4.5	13.33	453		
CD3121	QUEEN ALIA AIRPORT-3	124400	243000	705	325	153.8	45	0.85	52.94	1800		
CD3127	I'NAD M. EL FAYEZ -1	127380	237080	715	405							
CD3161	HAMER SH. EL FAYEZ	129880	236800	757	306	184	40	35.6	1.12	38		2.6 E-6
CD3167	I'NAD M. EL FAYEZ 3	127850	240650	720	320	148.9	68	0.85	80	2720		
CD3168	ZEID BIN SHAKER	134100	233100	820	420							
CD3170	M. Y. EL WREIKAT	108950	271000	845	370							
CD3177	MISBAH ZAKI EL SOUS	121845	254865	740	352	190.9	42	121	0.35	12		
CD3183	KAREEM N. EL ZIBEN	101530	250850	735	350	164.2	60	13.95	4.3	146		
CD3185	MOHAMAD ABU RAQIQ	102550	256935	790	370	209	47	37.5	1.25	43		
CD3186	ISSA M. EL JILANI	102810	266200	814								
CD3192	HWAILEH EL ZIBEN	101810	259970	820	400	223.2	55	32	1.7	58		
CD3193	SALAMEH EL ZIBEN	103330	251045	750	300	160.8	60	10	6	204		
CD3195	JLAYYEL S. ALZIBEN	98940	264495	858	320	251.5	60	15	4	136		
CD3196	JABIR H. M. SULEIMAN	100750	252300	740	352	171.3	60	28	2.14	73		
CD3198	MOHAMMAD EL ZIBEN	102730	251830	737	311	169	60	7	8.57	291		
CD3200	FANKHAIR EL ZIBEN	105220	253490	765	338	201.6	60	12	5	170		
CD3204	A'KEF EL FAYEZ 5	129885	239280	734	270	171.3	80	1.6	50	1700		
CD3212	MAHMOUD ABU MATAR	103450	252900	745	290	172	60	4	15	510		
CD3213	MOHAMMAD MSHAQI	103650	246125	710	286	148	60	1.25	48	1632		1.17 E-4
CD3214	SULTAN KHLAIFAT	108405	265055	780	305	205	60	9.5	6.13	208		
CD3215	IRON & STEEL UNITED	121470	240060	690	405							

CD3217	RFAIFAN AL KHRAISHA	129070	253700	780	400	217.3	60	36	1.66	56		
CD3218	ISSA QA'WAR	124170	259380	860	403	304.3	35	3.5	10	340		
CD3236	PRINCESS BASMA	128220	248850	730	343	170.5	67	8.4	8	272		
CD3237	PRINCESS BASMA	128840	248210	735								
CD3238	I'NAD M. EL FAYEZ 2	128700	240550	720	330	151.2	15	99.58	0.15	5		
CD3239	ABDHAFEDHELKHANAN	103570	233170	730	450	219.8	12	108	0.11	4		
CD3240	TAWFEEQ SALMAN	122850	237420	715	420	181.8	50	98	0.51	17		9.8 E-7
CD3242	RAGHDA MANGO	134500	238600	775	392	148	12	103	0.116	4		9 E-6
CD3246	NAWAL EL A'QIRBAWY	105905	255195	800	370	233	60	22.5	2.66	90		
CD3251	M. H. AL MUBARAK	128860	258710	420								
CD3253	FAHED M. AL GHUBAIN	128350	257420	800	450	245.7	52	58	0.9	31		
CD3258	I'NAD M..ELFAYEZ 4	128502	240458	721								
CD3261	M. S. M. BARBAKH	113425	254380	740	340	198.8	60	0.4	150	5100		
CD3262	ZEID BEN SHAKER	98450	244900	738	310	180.5	60	8	7.5	255		1.95 E-5
CD3264	ALHIKMA INVESTMENT	129730	244100	740	344	171.1	37	37.5	1	34		2.2 E-6
CD3267	MUNEERA M . ELFAYEZ	131050	235830	749	335	182.7	25	100.4	0.25	9		
CD3269	HMAIDY Z. EL FAYEZ	118875	248265	696	305	139.6	72	18.6	3.9	133		9.3 E-6
CD3270	RAKAN M. ELFAYEZ	119500	245940	694	370							
CD3271	MAMDOUH ELFAYEZ	120810	241550	718	243	155.5	50	9.45	5.3	180		2.4 E-5
CD3272	I'MAD ABU SHIHAB	116200	253900	705								
CD3273	KINA CO.	117135	244725	700	341	164.4	60	9.05	6.63	225		2 E-5
CD3274	GHAZI M. AL JABALI	133220	234210	761	470	164.2	35	237	0.148	5		
CD3275	RASHED EL DHAHIRI	103850	236670	690								
CD3280	RAZI PHARMACEUTICAL	132850	234975	785	450	248	23	52	0.44	15		
CD3285	G. SPECIALIZED STEEL	133860	252420	800	451	205.4	55	90.1	0.61	21		
CD3288	U'KASH ELZIBEN	122160	234600	715	390							
CD3289	M.H.ALMASHAYEKH	105350	235300	698	322	210	35	42	0.83	28		1 E-7
CD3290	RAJA'EE M. GHANEM	101900	238100	730	324	170.6	90	69	1.3	44		
CD3291	HINNAH MATALGA	106345	224565	640	130	16	60	51	1.2	41		
CD3293	SABRI M. MUSTAFA	117040	249600	708	355	171.4	60	156.6	0.38	13		
CD3294	GHZAYYEL EL FAYEZ	123320	242070	711	400	173	37	134	0.3	10		
CD3295	THAMER ZEID ELFAYEZ	120910	242865	721	410	197.4	55	108	0.51	17		
CD3296	SAMI M. ELFAYEZ	131100	233000	750								
CD3298	MOHAMMAD E'LAYYAN	115825	250840	700	310	146.2	45	62.1	0.7	24		1.7 E-6

CD3299	RASHED EL DHAHIRI	106750	246860	742	369	185	70	43	1.63	55		3.5 E-6
CD3315	NA'IL SALEEM KHAIR	132755	236360	761	370	196.4	20	52.55	0.38	13		7.4 E-7
CD3316	SA'UD FAHED ALTHIYAB	128910	244240	740	300	171.2	30	83.05	0.36	12		1.15 E-6
CD3322	GULF INDUST. CO.	114495	244710	625	396	180.3	60	14.4	4.2	143		
CD3323	ZAYTOUNEH UNI.	137780	234975	810	440	121	10	129	0.08	3		
CD3326	QUEEN ALIA.AIRPORT- 6	124542	241937	712	391	158	70	6	11.7	398		
CD3330	ATALLA S. ELNIMER	118400	262500	769	320	218	55	25.5	2.2	75		
CD3331	ISA'AF ELHAJ ELNABILSI	133960	226930	870	278	147.2	50	17.92	2.8	95		
CD3334	UNI. IRON & STEEL IND.	134635	252900	822	463	252.5	30	97.5	0.3	10		
CD3344	NA'IL SALEEM KHAIR	133000	236280	780	357	203.5	7	141.5	0.05	2		1.7 E-7
CD3345	PRINCE ALI BEN NAYEF	128400	252400	800	400	250.5	25	63	0.4	14		
CD3346	GHALEB S. ABU JABER	142320	235050	900	310	179.7	6	81	0.17	6		
CD3349	ALI ODEH & PARTNER	123850	241210	710	327	188	60	66	0.91	31		2 E-6
CD3350	AL ISRAA UNIVERSITY 2	133230	238210	770	350	222.8	50	62	0.8	27		
CD3375	SAKHER M. ELMOUR	96240	258450	803	300	207	60	21	2.86	97		
CD3376	FAYSAL A'KEF EL FAYEZ	112100	262950	790	390	203.7	60	4.3	13.95	474		
CD3377	SHEHADEH AL AQTASH	111310	230955	660	270	137	15					
CD3378	INT. CO. MEDICAL IND.	129535	240775	730	350	181	15	143	0.1	3		
CD3379	DAHHAM EL FAYEZ	132070	242870	734	310	158	108	2.75	39.3	1336		1 E-4
CD3381	LATIN PATRIARCHATE	141530	231950	900	325	189.7	20	42	0.48	16		
CD3382	FAWWAZ H.ELZIBEN	126400	231000	770	420							
CD3383	MIT'EB AKHU SUHAINEH	93950	251450	770	350	192.5	35	111	0.31	11		
CD3384	M. AKHU SUHAINEH	102020	241000	720	360	174.7	60	2	30	1020		1 E-4
CD3398	NABEEL SAKKIJHA	116660	241115	700	316	151.6	75	0.05	1400	47600		4.8 E-3
CD3400	ABD. EL KA'ABNEH	104070	236980	700	290	172.5	50	4	12.5	425		3.1 E-5
CD3401	HARRAN EL BAKHEET	136950	238575	780								
CD3421	ZIAD EL MANASEER	135200	236750	790	350	239	20	71	0.28	10		
CD3443	MUNIRAH EL FAYEZ	130850	235260	735	335	196	25	15	1.66	56		1.2 E-5
CD3444	HUSAM S. AL NIMER	126170	236090	730	340	280	30	40	0.75	26		